Carbon Dynamics on Floodplains of the Yangtze and Mekong Rivers

Benjamin L. Miller

A dissertation

submitted in partial fulfillment of the

requirements for the degree of

Doctor of Philosophy

University of Washington

2020

Reading Committee:

Gordon W. Holtgrieve, Chair

Daniel E. Schindler

Jeffrey E. Richey

Program Authorized to Offer Degree:

Aquatic and Fishery Sciences

University of Washington

Abstract

Carbon Dynamics on Floodplains of the Yangtze and Mekong Rivers

Benjamin L. Miller

Chair of the Supervisory Committee:

Gordon W. Holtgrieve

School of Aquatic and Fishery Sciences

The lateral expansion and contraction of rivers across their floodplains inextricably links aquatic and terrestrial ecosystem processes for part of each year, yet our understanding of the ecological responses to this seasonal hydrologic forcing is distinctly incomplete. The Flood Pulse Concept (FPC) predicts how *in-situ* primary production and respiration respond to this forcing. Although many of its predictions remain untested, the FPC is highly-cited and continues to guide hypotheses of ecosystem studies in tropical and subtropical flood-pulse rivers.

In Chapter 1 of this dissertation, I reviewed the literature published from 1989 to 2019 on tropical rivers to provide an updated narrative of how primary production and respiration change in response to the seasonal flood-pulse. The literature shows that the *in-situ* respiration of a combination of aquatic and terrestrial organic carbon (C) exceeds primary production in tropical and subtropical flood-pulse rivers (i.e.,ecosystems are net heterotrophic). For the remainder of

the dissertation, I propose that this net heterotrophy changes in response to flood-pulse hydrology and is sustained by both aerobic and anaerobic metabolism, contributing to the composition of dissolved C gases in water, atmospheric emissions of C gases, and the energetic base of aquatic food webs. I further propose that such cycling of C in flood-pulse rivers is fundamentally changed by hydropower development, which alters the magnitude and timing of the seasonal flood-pulse.

Net heterotrophy within inland waters sustained by terrestrial-aquatic transfers of organic C and its subsequent, *in-situ* aerobic respiration constitutes one of the most significant findings by aquatic ecologists over the past thirty years (Cole et al., 1994; del Giorgio and Peters, 1994). One of the defining features of net heterotrophy within rivers and lakes is the oversaturation of dissolved carbon dioxide (CO_2) relative to atmospheric levels as a byproduct of aerobic respiration. When "plumbing" the global C cycle, Cole et al. (2007) posited a unidirectional transfer of organic C from terrestrial to aquatic ecosystems, and assigned only three fates to this C: burial within sediments, aerobic respiration and diffusive loss of CO_2 to the atmosphere, and export to the oceans. Recently, Abril and Borges (2019) proposed the bidirectional expansion and contraction of floodwaters over the terrestrial landscape as a major revision to the model presented by Cole et al. (2007).

In Chapter 2, I hypothesized that the bidirectional expansion and contraction of rivers and lakes over the terrestrial landscape for months each year during the flood-pulse would create anaerobic floodplain habitat conducive to a fourth fate for organic C and additional cause of CO_2 oversaturation within inland waters: methane (CH_4) production and oxidation. I further hypothesized that net heterotrophy, dissolved CO_2 and CH_4, and their diffusive fluxes to the atmosphere would increase with water levels and floodplain inundation. I tested these

hypotheses in Tonle Sap Lake (TSL), on a tributary of the Lower Mekong River in Southeast Asia. Each June through September, monsoonal rains in this river basin increase TSL levels by up to 7 m and lake surface area by up to 12,000 km^2 (Holtgrieve et al., 2013). I measured the concentrations of respiratory gases (O_2, CO_2, CH_4) and isotopic composition of CO_2 and CH_4 during different flood stages in the TSL and used these data to model aerobic ecosystem metabolism and diffusive fluxes of CO_2 and CH_4 from TSL to the atmosphere. Stable C isotopes demonstrate that 67-97 % of dissolved CO_2 was derived from CH_4 oxidation. Dissolved CO_2 and CH_4 were unrelated to aerobic respiration and inundation time, which shared a strong, negative relationship. The flood-pulse increased net heterotrophy and diffusion, from 3,700 ±500 mg C-CO_2 m^{-2} d^{-1} and 0.5 ±0.2 mg C-CH_4 m^{-2} d^{-1} during the rising-water stage to 10,000 ±1,000 mg C-CO_2 m^{-2} d^{-1} and 110 ±40 mg C-CH_4 m^{-2} d^{-1} during the high-water stage. These data highlight that anaerobic metabolism can play a key role in the oversaturation and diffusive flux of CO_2 within rivers and lakes, particularly when these waters expand and contract across the terrestrial landscape.

The apparent magnitude of CH_4 production and oxidation in TSL suggested that this anaerobic energetic pathway may—at the same time—sustain net heterotrophy and introduce significant amounts of C to the base of the lake's food web. Traces of methane-derived C within the biomass of chironomids (Jones et al., 1999; Bunn and Boon, 2003), zooplankton (Bastviken et al., 2003; Kankaala et al., 2006), and fish (Sanseverino et al., 2013) have been detected in other lake food webs using stable C isotopes. Yet, metabolism measured at the base of lake food webs has traditionally focused on photosynthesis and whole-ecosystem aerobic respiration (*ER*). In Chapter 3, I hypothesized that CH_4 production would introduce C to the TSL food web at rates comparable to photosynthetic gross primary production (*GPP*), and that CH_4 oxidation would

transfer this C to higher trophic levels at rates comparable to net ecosystem production (*NPP*) until it was detectable in the food web using stable isotopes. I further hypothesized that rates of CH_4 production, oxidation, and their contribution to ecosystem metabolism in TSL would increase with lake level and floodplain duration. CH_4 production comprised up to 36 ±7 % of C introduced to the TSL food web through *GPP* and CH_4 oxidation comprised up to 11 ±3 % of *NPP*. Rates of both CH_4 production and oxidation were small compared to *ER*, suggesting that net heterotrophy in TSL is sustained by *ER*, despite sizeable contributions from CH_4. CH_4 production and oxidation were greatest during full flooding, but neither were correlated with floodplain duration as expected. Certain invertebrates and fish showed unambiguous methane-derived C within their biomass. Collectively, these results demonstrate that CH_4 production and oxidation contribute to the overall energetic base of TSL.

Flood-pulse rivers like the Lower Mekong are being altered by hydropower development at rates higher than anywhere else (Arias et al., 2013; Zarfl et al., 2015). Some of the highest rates of impoundment (>100 dams currently planned) are in China's Yangtze River basin (Zarfl et al., 2015). The Three Gorges Reservoir (TGR) has notably altered the Yangtze River flood-pulse; water levels on the TGR floodplain now fluctuate by up to 30 m annually (Chen et al., 2009). During low reservoir storage, water levels near Kai Xian are much as they were before the TGR, presenting a proxy for pre-dam C cycling on the TGR floodplain. In Chapter 4, I measured this C cycling in terms of atmospheric CO_2 and CH_4 fluxes from aquatic environments (i.e., ponds) on the TGR floodplain during low reservoir storage, and from the reservoir, itself, following inundation and high reservoir storage. I hypothesized that the magnitudes and ecosystem drivers of these fluxes would change with hydrology between low reservoir storage and high reservoir storage. Like other studies (Del Sontro et al., 2016), we found that CH_4

ebullition comprised a majority of CH_4 fluxes (60-68 %) during low reservoir storage, but was two orders of magnitude lower during high reservoir storage. We also found that floodplain inundation by the TGR significantly moderated areal atmospheric CO_2 and CH_4 fluxes (diffusion and ebullition). Linear mixed effects modeling indicated that *in-situ* respiration was the dominant ecosystem driver of fluxes during both low and high reservoir storage. Thus, these data show that the magnitudes, but not the drivers, of atmospheric CO_2 and CH_4 fluxes have been altered along with Yangtze River flood-pulse hydrology by the TGR.

A central theme that has emerged from the dissertation research presented here is the importance of anaerobic metabolism, specifically CH_4 production and oxidation, within inland waters. Anaerobic metabolism has been largely ignored in studies of aquatic C cycling and ecosystem metabolism, with implications for C accounting in other flood-pulse and anaerobic ecosystems, worldwide. Collectively, this work demonstrates that CH_4 production and oxidation contribute significantly to CO_2 oversaturation, atmospheric C fluxes, and aquatic biota, challenging existing assumptions about terrestrial-aquatic transfers, net heterotrophy, and food web support within flood-pulse rivers and lakes.

Chapter 1

Primary production and respiration on the floodplains of large, tropical rivers—A review of predictions by the flood-pulse concept

Benjamin L. Miller[1]

Thomas K. Pool[1,2]

Gordon W. Holtgrieve[1]

1. School of Aquatic and Fishery Sciences, University of Washington
2. Department of Biology, Seattle University

1.0 Abstract

The Flood-pulse Concept (FPC; 1989) describes the lateral expansion and contraction of tropical rivers across their floodplains following annual monsoonal precipitation, and how these hydrologic changes affect *in-situ* primary production and respiration. Although predictions by the FPC are speculative or based largely on observations in a single river, the Amazon, the FPC is highly-cited and continues to guide hypotheses of ecosystem studies in tropical flood-pulse rivers. We comprehensively reviewed the literature published from 1989 to 2019 in flood-pulse rivers to provide an updated narrative on primary production and respiration in these ecosystems. The FPC predicts that the flood-pulse will drive community composition of primary producers on the floodplain. The FPC also predicts that primary production will exceed respiration on the floodplain throughout flood pulse. The FPC further predicts the floodplain will contribute more organic carbon (C) to respiration at the base of flood-pulse ecosystems than the "pulsing" river, and that this organic carbon will be mobilized by flood waters and respired within microbial and benthic food webs under progressively anoxic conditions on the floodplain. Our literature review confirms that the community composition of primary producers on tropical river floodplains is driven by flood-pulse hydrology. In contrast to the predictions by the FPC, the literature shows that respiration far exceeds primary production in high-order tropical rivers and their floodplains. The literature also shows that upstream *in-situ* primary producers are important to secondary production and respiration at the base of heterotrophic food webs in flood-pulse ecosystems, which also contradicts the FPC. As the flood-pulse progresses, we show that photomineralization—in addition to methanogenesis—becomes an increasingly important fate for organic C on tropical river floodplains. We hypothesize that ecosystem parameters in flood-pulse rivers and their floodplains can be described using a hysteresis, in which parameter

response—such as phytoplankton abundance—differs along a rising or falling hydrograph. We speculate how the FPC might be further modified under global change. This review corrects inaccuracies of the FPC, improving theoretical bases for future studies in this globally-important class of rivers.

2.0 Introduction

Many of the world's earliest civilizations occurred on the floodplains of large tropical and subtropical rivers, such as the Nile, Indus, and Yangtze. The annual flooding of these rivers and resulting agricultural productivity underlaying early Egyptian, Indian, and Chinese societies have long been recognized by their inhabitants and archaeologists. However, the importance of floodplain ecosystem dynamics has only recently received attention by ecologists. All ecosystems experience regular pulses of abiotic physical forcing, including temperature, solar irradiance, and precipitation (Winemiller et al., 2014). Temperature and solar irradiance are relatively constant in tropical and subtropical ecosystems at annual time scales. This leaves precipitation as the primary physical forcing mechanism affecting tropical and subtropical watersheds on an annual basis. Along the Intertropical Convergence Zone, precipitation is often monsoonal and highly predictable, causing similarly predictable annual flooding. This annual predictability, or "rhythmicity," of floods has been shown to underlay common metrics of productivity from one flood stage to another within tropical rivers, such as organic C export and fish species richness (Jardine et al., 2015; Sabo et al., 2017).

Junk et al. (1989) first characterized the annual flooding of the Amazon River across its floodplains and the blurring of classical aquatic and terrestrial boundaries as the Flood-pulse Concept (FPC). There were a number of conceptual precursors to the FPC that attempted to describe large scale ecological patterns in rivers. These overwhelmingly focused on spatial

variation based on the unidirectional flow of water in temperate rivers. As early as 1945, the Fish Zones Concept predicted a change in the spatial distribution of fishes from high gradient, fast-moving waters upstream to low gradient, slow-moving waters downstream, according to their life histories and morphological traits (Gerking, 1945). The River Continuum Concept (RCC) also operates on a longitudinal basis, but includes predictions about the energetic base of the food web (Vannote et al., 1980). Vannote et al. (1980) were fundamentally concerned with inputs of terrestrial organic carbon (C) from upstream to downstream, and the implications this has for the balance of primary production and respiration and community composition of benthic insects. The RCC predicted that respiration would exceed production in mid-order rivers due to riparian shading and terrestrial organic C inputs, but that rivers would become increasingly net autotrophic (i.e., primary production will exceed respiration) as they broadened at high orders (Vannote et al., 1980).

The FPC was proposed as an alternative to the RCC nine years later (Junk et al., 1989). The major departure of the FPC from the RCC is the integration of space and time as a river overflows its banks on an annual basis, creating lateral connectivity between the main channel and floodplain. The FPC makes several predictions about *in-situ* primary production and respiration at the base of "pulsing" tropical river ecosystems. Notably, the FPC predicts that (i) the flood-pulse will drive community composition of primary producers on floodplains. The FPC also predicts that (ii) primary production will exceed respiration on the floodplain throughout the annual flood pulse. The FPC further predicts (iii) the floodplain will contribute more organic carbon (C) to respiration at the base of flood-pulse ecosystems than the "pulsing" river, and that (iv) this organic carbon will be mobilized by the flood waters and respired within microbial and benthic food webs under progressively anoxic conditions on the floodplain.

However, many of these predictions are speculative or based largely on observations in a single river, the Amazon. Others have reviewed the applicability of the FPC to modified river-floodplain ecosystems (Bayley, 1995), fisheries (Junk and Bayley, 2007), and floodplain lakes (Wantzen et al., 2008), but none have synthesized recent findings in the tropical flood-pulse rivers that first inspired the FPC.

Predictions by the original FPC have been cited over 6,500 times, yet primary production and respiration in tropical and subtropical rivers remains significantly understudied relative to temperate rivers (Raymond et al., 2013). Tropical flood-pulse rivers are responsible for up to 48 % of mean annual riverine discharge, and their ecosystem dynamics collectively describe over half of the freshwater resources on Earth. Updating predictions made by the original FPC about these ecosystem dynamics is critical to guiding future, much-needed research in tropical and sub-tropical rivers.

We comprehensively reviewed the literature on primary production and respiration in flood-pulse rivers from 1989 to 2019. From this, we provide an updated narrative on primary production and respiration in these ecosystems with reference to predictions by the original FPC. Like Junk et al. (1989), this review focuses on tropical flood-pulse watersheds, though information from temperate flood-pulse watersheds is included where potentially useful, or where information from the tropics is scarce. We confirm that (i) the community composition of primary producers is driven by flood-pulse hydrology. We hypothesize that these and other ecosystem dynamics can be succinctly described a hysteresis, in which rising- and falling-water dynamics differ. In contrast to the predictions by both the FPC and RCC, the literature shows (ii) consistent net heterotrophy (i.e., respiration exceeding primary production) in high-order tropical rivers and their floodplains, but (iii) highlights the importance of upstream *in-situ*

primary producers to respiration at the base of heterotrophic food webs. (iv) Photomineralization, unrecognized by the original FPC, and methanogenesis become increasingly important fates for organic C on the floodplain during later stages of the flood-pulse. An updated understanding of flood-pulse ecosystem dynamics will aid in (v) predicting the effects of rapidly changing land use and climate on tropical flood-pulse hydrology, and the numerous ecosystems services humans have long relied on from the world's largest rivers.

(i) As predicted by the FPC, flood-pulse hydrology drives community composition of primary producers on the floodplain.

During the rising-water stage of the flood pulse, riverine discharge increases dramatically (Figure 1). In low-gradient tropical flood-pulse rivers, this water rapidly exceeds bank-full in the main channel and expands laterally over adjacent floodplains (Figures 2a and 2b). At the same time, mean water depth decreases as it incorporates the shallows of inundated floodplains.

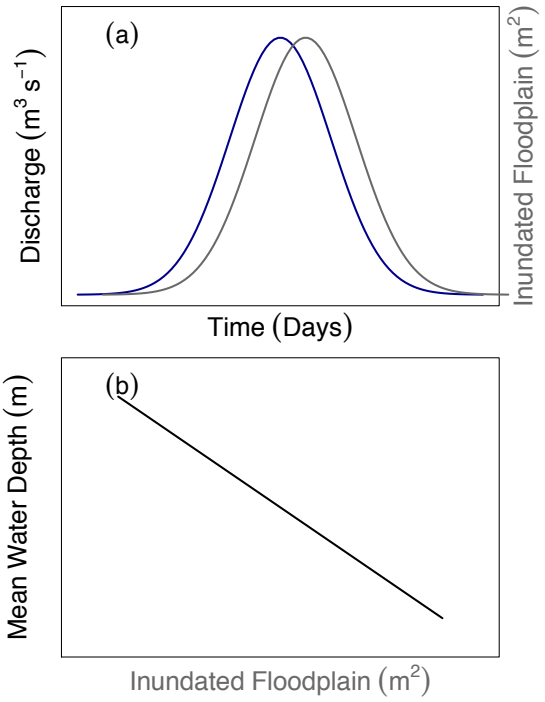

Figure 1. An increase in riverine discharge, in m^3 s^{-1}, during the rising-water stage of the flood-pulse (blue line) results in a lagged increase in the area of inundated floodplain, in m^2 (grey line). As discharge and water level exceeds bank-full in the main channel and expands laterally over adjacent floodplains, the area of inundated floodplain increases. As the area of inundated floodplain increases, mean water depth-in m—decreases.

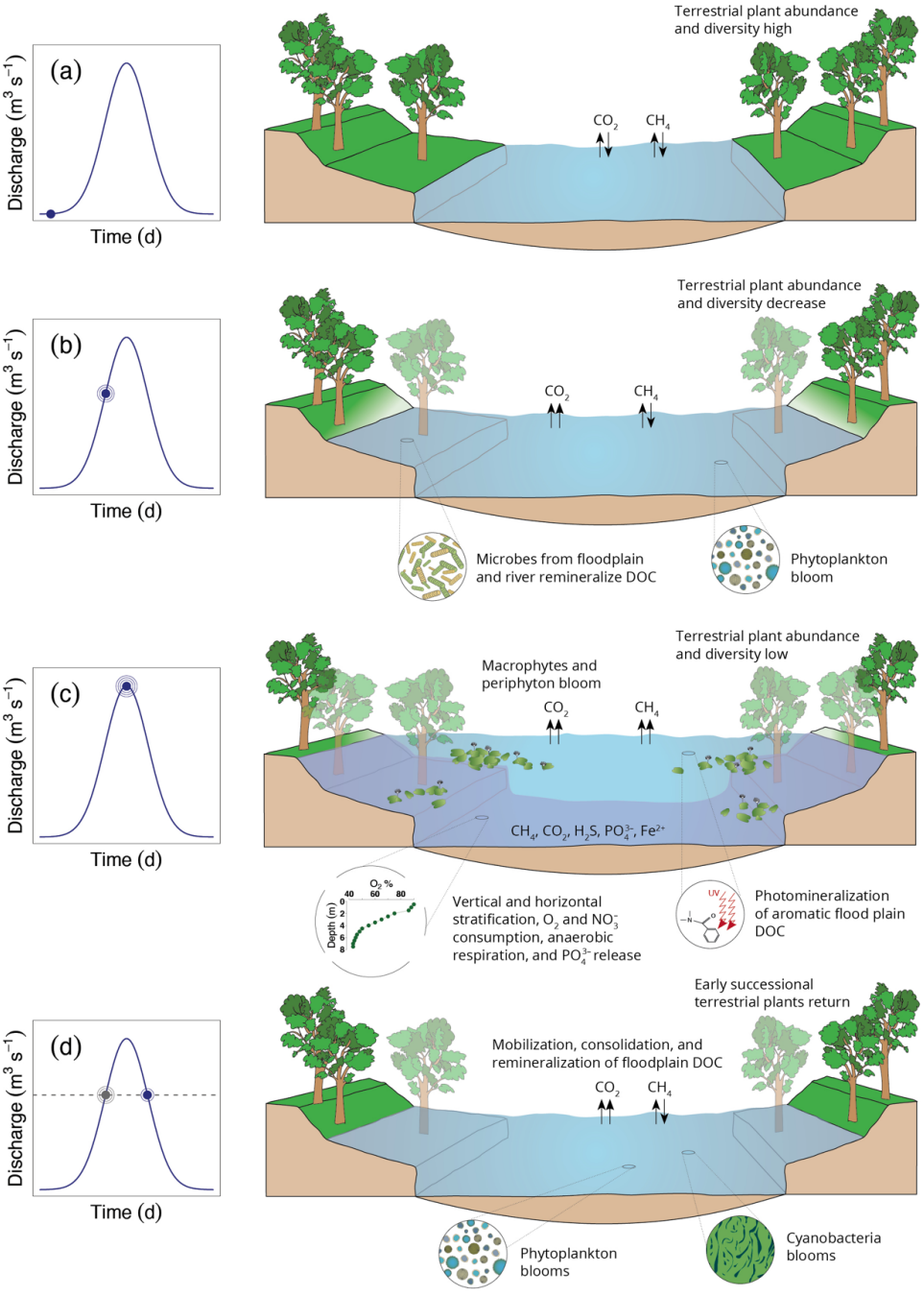

Figure 2. The low-water (a), rising-water (b), high-water (c), and falling-water (d) stages of the flood-pulse in tropical rivers. A discharge relationship is included for each flood stage panel. During the falling-water stage, two discharges are included to emphasize the return of falling-water discharge to a level last seen during the rising-water stage. Arrows represent net diffusion of carbon dioxide (CO_2) and methane (CH_4) between the "pulsing" water body and the atmosphere.

The FPC predicts that the rising-water stage of the flood-pulse will lead to blooms of phytoplankton on the floodplain (Junk et al., 1989). The FPC attributes these blooms to the mobilization of riverine and floodplain organic C by advancing floodwaters, and the subsequent release of limiting nutrients within organic C compounds as they are respired by the microbial community (Junk et al., 1989). Such increases in phytoplankton biomass have since been observed on the Orinoco (Venezuela; Montoya et al., 2006), Amazon (Brazil; Oliveira and Calheiros, 2000), Murray (Australia; Cook et al., 2015), and Ayapel floodplains (Montoya et al., 2010) during the rising-water stage of the flood-pulse (Figure 2b). Microbial respiration of suspended organic C during the rising-water stage of the flood pulse (McClain et al., 2003; Mladenov et al., 2005) has been shown to stimulate primary production by 1) releasing inorganic nutrients (Jones et al., 1988; Klug, 2002; Kinsman-Costello et al., 2014), 2) providing respiratory as well as atmospheric DIC for photosynthesis (Jansson et al., 2012; Lapierre and del Giorgio, 2012), and 3) attenuating ultraviolet radiation harmful to primary producers at shallow depths (Maloney et al., 2005). Mladenov et al. (2005) and Oliveira et al. (2010) observed sharp increases in dissolved organic C (DOC), phytoplankton, nitrogen, and phosphorus as the tropical Okavango and Amazon rivers expanded onto their respective floodplains. Additionally, Kobayashi et al. (2013) found that organic C was the best predictor of phytoplankton production on a temperate Australian floodplain. Overall, there is strong literature support for the FPC's predicted mobilization of organic C, nutrient release, and resulting increase in phytoplankton production during the rising-water stage of the flood-pulse.

During the high-water stage of the flood-pulse, the FPC predicts that that low water velocity and depositional environments on the floodplain would allow for a deeper euphotic zone, greater macrophyte and periphyton abundance, and less rooted terrestrial vegetation (Junk

et al., 1989). Studies have shown an increase in floating, submerged, and emergent macrophytes during the high-water stage on temperate (Keruzore et al., 2013) and tropical (Sousa et al., 2011; Gomes et al., 2012; Chapparo et al., 2014; Ward et al., 2016) floodplains. Others have verified that the composition and succession of certain primary producers varies with inundation time, or the amount of time river waters have submerged the floodplain. Sousa et al. (2011) showed a positive relationship between inundation time and macrophyte abundance. Arias et al. (2013; 2018) showed a negative relationship between inundation time and terrestrial plant diversity on floodplains of the Lower Mekong (Figures 2b and 2c); up to 11 terrestrial plant species per 100 m^2 grew in areas flooded for 1-5 months, compared with just 3-5 species in areas flooded for 8-10 months. In the Brazilian Pantanal, Ferreira-Junior et al. (2016) further documented a small fraction (8 %) of local tree species in areas of the floodplain experiencing the longest inundation times. Among the trees that grow in these areas of the floodplain, annual growth rings indicate a physiological winter when inundation deprives roots of oxygen (Gottsberger, 1978). The flood-pulse may therefore be viewed as a disturbance regime that simplifies the terrestrial plant community, facilitating the invasion of floating and submerged macrophytes and the establishment of early successional terrestrial species, such as shrubs (Dorado-Rodrigues et al., 2015; Toth, 2015).

Until recently, few have investigated the relative contribution of periphyton to primary production on the floodplain, though periphyton production was long ago estimated to equal phytoplankton production on the floodplain by Junk et al. (1989) and Bayley et al. (1989). Ample surface area on macrophytes, trees, and on the shallow benthos may provide extensive habitat for epiphytic periphyton during the high-water stage of the flood-pulse. Additionally, settling of suspended organic C as water residence time increases on the floodplain, due in part

to flow resistance by emergent macrophytes and other vegetation (Vastila et al., 2016), may support expansion of the euphotic zone for periphyton production (Junk et al., 1989; Tockner et al., 1999). Accordingly, Dunck et al. (2015) showed development of a more abundant and diverse community of periphyton on the Parana floodplain (Brazil) following 18 days of flooding. Working on the Kakadu (Australia) floodplain, Ward et al. (2016) and Pettit et al. (2016) presented the more nuanced findings that emergent macrophytes and those with floating leaves, such as grasses and lotuses, both shade the water column provide a less structurally complex surface for development of epiphytic periphyton communities during the high-water stage. By contrast, greater structural complexity of submerged macrophytes within the euphotic zone allowed for denser coverings of periphyton than could be found on emergent macrophytes (Pettit et al., 2016). This may also explain why areas of the Amazon floodplain (Brazil) with dense tree cover were shown to have low periphyton production, compared to other study sites (Bleich et al., 2015). Thus, growth of periphyton and primary producers as a whole may be patchy on the floodplain (Montoya et al., 2006).

The FPC includes few predictions about primary or secondary production during the falling-water stage of the flood-pulse (Junk et al., 1989). Increases in both phytoplankton production and respiration have been observed from the high- to falling-water stage on Columbian and Australian floodplains (Figure 3d; Montoya et al., 2010; Wallace and Furst, 2016)). Phytoplankton, floating and submerged macrophytes, seeds and propagules of floodplain plants (Boedeltje et al., 2004), fish (Teixeira-de Mello et al., 2016), and other floodplain organisms have been shown to be mobilized by receding floodwaters. Suspension, consolidation, and respiration of this and other organic C in progressively smaller aquatic

floodplain environments (Yurek et al., 2016) likely results in the same nutrient release described previously for the rising-water stage of the flood pulse, stimulating phytoplankton production.

Increases in blue-green algae, or cyanobacteria from the high- to falling-water stage have also been observed on the tropical Tonle Sap (Holtgrieve, *pers. comm.*) and temperate Danube (Mihaljevic et al., 2011) floodplains during the falling-water stage of the flood pulse (Figure 2d). Cyanobacteria are competitive in ecological niches that have low light and are nitrogen limited. Water on the floodplain during this flood stage can become light-limited due to mobilization of organic C (see above). At the same time, dynamic water levels can create alternately aerobic to anaerobic sediment redox conditions and increased phosphorus release (Keitel et al., 2016). This may change nutrient stoichiometry, lead to nitrogen limitation, and facilitate growth of cyanobacteria as floodwaters recede during this stage.

The trajectories of primary producer abundance over the course of the flood-pulse can be hypothesized based on the literature reviewed using a hysteresis. A hysteresis is a well-known description in hydrology of nonlinear parameter response to an increase and subsequent decrease in discharge (Caleta et al., 1991). In the case of the flood-pulse, the response trajectory of an ecosystem parameter to the disturbance represented by the rising-water stage may be different than its recovery trajectory during the falling-water stage. Accordingly, the literature reviewed shows different abundances of the same primary producers during the rising-, and falling-water stages of the flood-pulse. Differences occur even when discharge in the central, "pulsing" water returns to a similar or identical magnitude during these flood stages (Figure 2d). For example, phytoplankton blooms during the rising-water stage (Figure 3a). Phytoplankton then declines with the mobilization of floodplain organic C and development of macrophyte communities during the high-water stage, blooming again—to a lesser extent—during the falling-water stage.

Terrestrial plant abundance and diversity are greatest during the low-water stage of the flood pulse, but decline with inundation during subsequent flood stages (Figure 3b). Macrophytes and periphyton bloom during the high-water stage (Figure 3c and Figure 3d), but are low during the subsequent falling- and low-water stages. Blue-green algae blooms during the falling-water stage (Figure 3e).

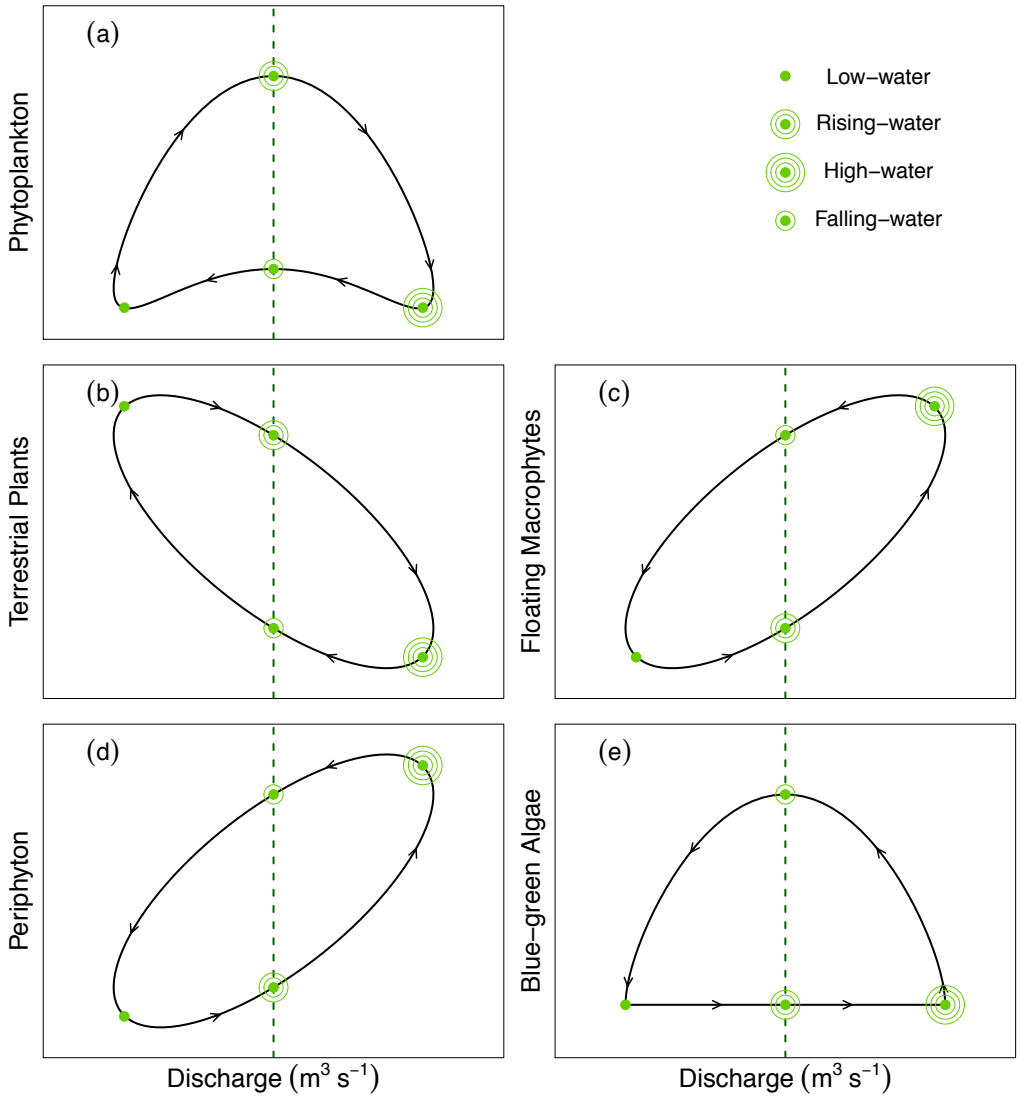

Figure 3. Hypothesized trajectories of primary producer abundance using a hysteresis, based on the literature reviewed. Green dashed lines indicate different primary producer abundances at the same level of discharge during different flood stages.

(ii) Respiration exceeds *in-situ* primary production on the floodplains of tropical rivers, in contrast to predictions by the original FPC.

The FPC posits that seasonal increases in different primary producers on the floodplain will result in "high P / R ratios for large river-floodplain systems," meaning that primary production will exceed respiration (Junk et al., 1989). Data on these metabolic ratios are scarce in flood-pulse ecosystems, but consistently show the opposite of what the FPC predicts. Cook et al. (2015) showed that gross primary production (*GPP*) in the subtropical Murray River basin increased two-fold during the flood pulse relative to low-water or base flow, consistent with predictions by the FPC; however, ecosystem respiration (*ER*) increased five-fold during the same period, leading to net heterotrophy ($GPP < ER$). As shown in Table 1, *ER* also consistently exceeded *GPP* during the flood-pulse when measured on floodplains of the San Francisco (temperate United States; Lehman et al., 2008), the Mekong (tropical Cambodia; Holtgrieve et al., 2013), Yellow (temperate China; Sun et al., 2016), and Mitchell Rivers (tropical Australia; Hunt et al., 2012). In some areas of the Mekong, Yellow, and Mitchell Rivers, E_R was an order of magnitude greater than *GPP*.

Table 1. Comparison of mean *GPP* and *ER* rates measured in main channel, lake, and floodplain environments of the San Francisco, Mekong, Yellow, and Mitchell Rivers during the flood-pulse. Units vary; ecosystem metabolism measured within aquatic environments and expressed in terms of m^2 has been multiplied by mixing depth (Winslow et al., 2016).

Study	Continent	Watershed	Environment	GPP	ER	Units
Lehman et al., 2008	North America	San Francisco River	Main Channel	0.11 ±0.03	-0.5 ±0.1	g C m^{-2} d^{-1}
			Floodplain	0.4 ±0.1	-0.5 ±0.1	
Holtgrieve et al., 2013	Asia	Mekong River	Lake-1	4 ±3	-30 ±20	g O_2 m^{-3} d^{-1}
			Floodplain-1	4 ±1	-4 ±1	
			Lake-2	3 ±1	-4 ±1	
			Floodplain-2	30 ±10	-4 ±1	
Sun et al., 2016	Asia	Yellow River	Floodplain-1	2 ±1	-9 ±4	g O_2 m^{-3} d^{-1}
			Floodplain-2	3 ±2	-10 ±3	g O_2 m^{-3} d^{-1}
Hunt et al., 2012	Australia	Mitchell River	Main Channel-1	2.1 ±0.6	-5 ±1	g O_2 m^{-2} d^{-1}
			Main Channel-2	2.3 ±0.5	-4.4 ±0.8	
			Main Channel-3	4 ±2	-17 ±7	

Each of these studies measures the balance of *GPP* and *ER* using fluctuations in dissolved oxygen (O_2) over a discrete time period (usually a daily cycle). However, there are a suite of respiratory pathways that do not involve the consumption of dissolved O_2 and occur in the absence of O_2. These include denitrification, the reduction of iron, manganese, and sulfate, and methanogenesis. Thus, the high rates of *ER* relative to *GPP* measured by the studies, above, actually represent a minimum estimate of *ER*. There are no studies within inland waters that incorporate the full suite of anaerobic respiratory pathways into estimates of *ER*.

Widespread CO_2 supersaturation and atmospheric emissions from inland waters, globally, and tropical rivers, particularly, further indicate net heterotrophy. CO_2 supersaturation typically occurs when *ER* exceeds *GPP*, leading to diffusive emissions of CO_2 across the air-water interface to the atmosphere. This is considered a strong indicator of net heterotrophy within an ecosystem (Cole and Caraco, 2001). Measured PCO_2 in rivers typically ranges from 1,000 μatm

to almost 17,000 μatm, compared to an atmospheric equilibrium value of roughly 370 to 410 μatm depending on local atmospheric pressure, temperature, and when the sampling occurred (Cole and Caraco, 2001; Richey et al., 2002; Johnson et al., 2008; Humborg et al., 2010; Borges et al., 2015). The tropics, alone, are responsible for 80 % of global riverine CO_2 emissions (Raymond et al., 2013; Hartmann et al., 2014; Lauerwald et al., 2015; Abril and Borges, 2019). In the Amazon River, CO_2-C emissions have been shown to be 13-fold higher than other organic and inorganic C export mechanisms (Richey et al., 2002). Junk et al. (1989) briefly acknowledged atmospheric C emissions as a fate for floodplain organic C by citing work by Melack and Fisher (1983) in the Amazon, but included no predictions about how C emissions might be driven by flood-pulse hydrology, or its relationship to net metabolic balance. As Abril and Borges (2019) highlighted in a recent review, it is unclear whether a majority of C emissions originate from the main channel of rivers or from their floodplains. Raymond et al. (2013) identified "fringing wetlands" in Amazonia and Southeast Asia as major sources of uncertainty for global C emissions from inland waters to the atmosphere. Abril et al. (2014) and Borges et al. (2015) have since shown that riverine C emissions increase with areal coverage of the "fringing wetlands" described by Raymond et al. (2013) on floodplains of the Amazon and Congo Rivers. Such wetlands are estimated to occupy between 60 % and 75 % of tropical watersheds (Abril and Borges et al., 2019), necessitating further study on how C emissions may be driven by flood-pulse hydrology.

(iii) Contrary to predictions by the FPC, upstream *in-situ* primary production can be important to secondary production in tropical rivers and their floodplains as it is respired at the base of heterotrophic food webs.

The FPC predicts that high water velocity and suspended solids will limit *in-situ* primary production by phytoplankton, macrophytes, and periphyton in the main channel of high-order tropical rivers, rendering these relatively unimportant to heterotrophic food webs on the floodplain (Junk et al., 1989). Thus, the FPC discounts the importance of this *in-situ* primary production in favor of pre-flood, "antecedent" terrestrial primary production. The FPC predicts that antecedent terrestrial organic C will be mobilized by advancing flood waters, reaching the greatest concentrations during the rising-water stage of the flood-pulse (Junk et al., 1989; Bayley, 1995). Despite these predictions, there are few data on "partitioning respiration between a river or its floodplain (Battin et al. 2009)."

In contrast to predictions by the original FPC, evidence suggests organic C originating from aquatic primary production in the main channel of tropical rivers may fuel the high rates of respiration and net heterotrophy observed on the floodplains of tropical flood-pulse rivers. River waters tend to carry more particulate organic C (POC) and DOC than has been shown to leach from floodplain sediments during the rising-water stage of the flood-pulse in the tropical Mekong (Cambodia), Fitzroy (Australia), and Amazon Rivers (Ellis et al., 2012; Fellman et al., 2013; Moreira-Turq et al., 2013). Based on a combination of C/N, elemental, and carbon stable isotope analyses, POC and DOC sampled on the floodplain was shown to originate primarily from phytoplankton in the main channel (Thorp, 2002; Ellis et al., 2011; Moreira-Turcq et al., 2013). Another study by Fellman et al. (2013) concluded that the $^{13}C/^{12}C$ of DOC was indistinguishable between a tropical Australian river and its floodplain following bankfull, emphasizing the connectivity of these environments during the rising-water stage.

The source of organic C influences its susceptibility to microbial respiration, or "lability." Floodplain POC and DOC originating from lignin-rich formerly terrestrial plant tissues has a higher ratio of C to nitrogen than POC and DOC derived from *in-situ* primary production. In the original FPC paper, itself, Junk et al. (1989) cited low biological oxygen demand (a proxy for microbial respiration rates) at their sampling sites in the Amazon as evidence for the presence of relatively recalcitrant humic organic C. Humic organic C results from the incomplete respiration of lignin-rich plants. It is aromatic in structure (Weishaar et al., 2003), characterized by stable conjugated rings of unsaturated bonds, and relatively recalcitrant to further microbial respiration. This means that organic C derived from *in-situ* production by phytoplankton, periphyton, or even macrophytes the main channel is likely to be more labile than floodplain POC and DOC.

DOC concentrations have been shown to spike immediately following inundation during the rising-water stage of the flood-pulse in subtropical, tropical, and Mediterranean floodplains (Burns and Ryder, 2001; Wainright et al., 1992; Vasquez et al., 2015; Zuijdgeest et al., 2016). None of these studies explicitly compared DOC concentrations measured during the low-water stage, in the main channel, to DOC concentrations measured during the rising-water stage, on the floodplain. We made this comparison for four, high-order tropical rivers (Table 2). Assuming DOC concentrations in the main channel remain the same during the rising-water stage from constant upstream inflow and resupply, the main channel tended to introduce more DOC to the water column than the floodplain (Castillo, 2000; Carvahlo et al., 2003; Mladenov et al., 2005; Amado et al., 2006; Farjalla et al., 2006; Mackay et al., 2011). This was represented by a <100 % change in DOC concentrations from the low-water stage, in the main channel, to the rising-water stage, on the floodplain. A notable exception was the Oubangui River (Bouillon et al., 2012; Mann et al., 2014), which receives not just one peak in precipitation but at least two per

year (Alsdorf et al., 2016). Collectively, these studies suggest that riverine inputs of DOC could be a more important driver of floodplain respiration than previously acknowledged by the FPC.

Table 2. Comparison of mean DOC concentrations measured in the main channel of the large, tropical Okavango, Oubangui, Amazon, and Orinoco Rivers during the low-water stage of the flood-pulse, and mean DOC concentrations measured on the floodplain during the rising-water stage.

Study	Continent	Watershed	Environment	mg DOC L^{-1}
Mackay et al., 2014	Africa	Okavango	Main Channel	8.1
			Floodplain	9.1
			Percent Change	***12 %***
Mann et al., 2014	Africa	Oubangui	Main Channel	6.3
			Floodplain	10.1
			Percent Change	***60 %***
Mann et al., 2014	Africa	Oubangui	Main Channel	4.3
			Floodplain	9.2
			Percent Change	***114 %***
Mann et al., 2014	Africa	Oubangui	Main Channel	12.7
			Floodplain	42.2
			Percent Change	***232 %***
Bouillion et al., 2012	Africa	Oubangui	Main Channel	2.5
			Floodplain	11.0
			Percent Change	***340 %***
Mladenov et al., 2005	Africa	Okavango	Main Channel	5.0
			Floodplain	6.5
			Percent Change	***30 %***
Mladenov et al., 2005	Africa	Okavango	Main Channel	6.0
			Floodplain	8.0
			Percent Change	***33 %***
Mladenov et al., 2005	Africa	Okavango	Main Channel	9.0
			Floodplain	9.5
			Percent Change	***6 %***
Mladenov et al., 2005	Africa	Okavango	Main Channel	9.0
			Floodplain	13.5
			Percent Change	***50 %***
Mladenov et al., 2005	Africa	Okavango	Main Channel	11.0
			Floodplain	13.0
			Percent Change	***18 %***
Farjalla et al., 2006	South America	Amazon	Main Channel	18.5
			Floodplain	31.2
			Percent Change	***69 %***
Amado et al., 2006	South America	Amazon	Main Channel	4.1
			Floodplain	5.5
			Percent Change	***36 %***
de Melo et al., 2020	South America	Amazon	Main Channel	3.7
			Floodplain	4.5
			Percent Change	***22 %***
Carvahlo et al., 2003	South America	Amazon	Main Channel	3.5
			Floodplain	7.0
			Percent Change	***97 %***
Castillo et al., 2005	South America	Orinoco	Main Channel	6.6
			Floodplain	8.7
			Percent Change	***32 %***
Castillo et al., 2000	South America	Orinoco	Main Channel	8.1
			Floodplain	9.6
			Percent Change	***19 %***

The introduction of relatively labile riverine DOC and the mobilization of relatively recalcitrant floodplain (i.e., formerly terrestrial) DOC is likely to lead to greater diversity and respiration rates among microbial community members adapted to metabolize both (Adams et al., 2014). Members of the riverine microbial community have been shown to increase on the floodplain during the rising-water stage of the flood-pulse (de Melo et al., 2019). Burns and Ryder (2001) show that the "activity" of extracellular enzymes secreted by that microbial community is highest during the first 7 days of inundation on a tropical Australian floodplain, dropping from Day 7 to Day 21. Microbial community composition was also found to consist of fast growing, abundant R-strategists during the rising water stage, which rapidly metabolized DOC (Schutz et al., 2010). Microbial diversity is subject environmental heterogeneity on the floodplain, and few studies have combined microbial community metrics with respiration measurements. However, Bodmer et al. (2016) indicates that introductions of labile riverine DOC and increased microbial diversity stimulate respiration, possibly priming recalcitrant terrestrial organic C compounds to undergo further breakdown during the rising-stage.

The FPC anticipates respiration of *in-situ* (e.g., algal) primary production on the floodplain at the base of localized heterotrophic food webs, and export within the biomass of mobile higher-trophic level consumers such as fish and invertebrates (Junk et al., 1989). However, phytoplankton exported from the floodplain in contracting flood waters may also be an important C source to riverine food webs downstream. Elemental analyses by Ellis et al. (2011) and Moreira-Turq et al. (2013) have indicated sizeable exports of phytoplankton cells from the floodplain to the main channel during this flood stage in the Mekong and Amazon Rivers, respectively. In the San Francisco River, up to 37 % of floodplain phytoplankton cells were exported downstream (Lehman et al., 2008). A recent review of 26 studies of high-order river

food webs by Roach et al. (2013) suggested that phytoplankton and periphyton contribute more C to upper trophic levels when compared to terrestrial plants. Accordingly, another review of several studies conducted in the Orinoco River and its floodplain showed that phytoplankton and periphyton were the predominant C sources for fish and invertebrates, even though macrophytes and terrestrial organic C comprised 98 % of available C (Lewis et al., 2001). These studies support predictions by the FPC that made about respiration of *in-situ* primary production at the base of heterotrophic food webs, albeit downstream of the floodplain and in the main channel of tropical rivers.

The literature supports a synthesis of the FPC and Thorp and Delong's Riverine Productivity Model (RPM; 1994), which acknowledges the importance of upstream *in-situ* primary production in supporting respiration at the base of heterotrophic food webs downstream. The most recent iteration of the RPM states that "the primary annual energy source supporting overall metazoan production and species diversity in mid-to higher-trophic levels of most rivers (>4th order) is [*in-situ*] primary production entering food webs via algal-grazer and decomposer pathways" (Thorp, 2002). Thus, 1) upstream, *in-situ* primary production from the main channel is important to respiration on the floodplain during the rising-water stage of the flood-pulse, and 2) later blooms of *in-situ* primary producers on the floodplain during the falling-water stage is likewise important to respiration in the main channel following downstream export.

(iv) Photomineralization, unrecognized by the FPC, and methanogenesis become increasingly important fates for organic C on the floodplain during later stages of the flood-pulse.

The literature also shows that the source, structure, and size of dominant fractions of organic C may change over the course of the flood-pulse. During the high-water stage of the

flood pulse, respiration may stabilize or even decline as labile organic carbon is depleted and more recalcitrant terrestrial POC and DOC remains in the water column (Moreira-Turq et al., 2013; de Melo et al., 2020). There is ample evidence in the literature for the limited utilization of this terrestrial POC and DOC by the microbial community. On the Amazon floodplain, an increase in fatty acids associated with relatively recalcitrant, terrestrial DOC and POC was documented by Mortillaro et al. (2012) during the high-water stage of the flood pulse, with fatty acids associated with more labile organic C decreasing proportionately throughout the flood pulse. Increasing recalcitrance of organic C has been shown to limit both denitrification (Fellows et al., 2011) and other respiratory pathways (Amon and Benner, 1996; de Melo et al., 2020). A lack of labile organic C, progressively unfavorable redox conditions (Junk et al., 1989), and low pH resulting from the buildup of organic acids (Abril et al., 2014) may limit microbial respiration during the high-water stage.

Studies of floodplain lakes in the Amazon comparing rates of microbial respiration and photomineralization illustrate the relative importance of the photomineralization as an oxidative pathway for organic C. Photomineralization was entirely unrecognized by the original FPC (Junk et al., 1989). Floodplain lakes are unconnected to the main channel during low-water, but become connected during the rising- and high-water stages of the flood-pulse. During the low-water stage, *in-situ* primary production by macrophytes and phytoplankton contribute more labile DOC to the water column (Moreira-Turq et al., 2013), allowing for higher rates of microbial respiration (Waichmann et al., 1996; Castillo et al., 2000; Amado et al., 2006; Farjalla et al., 2006). During later stages of the flood-pulse, more floodplain POC and DOC are mobilized and lability decreases (Amon and Benner, 1996; Amado et al., 2006; Farjalla et al., 2006). As microbial respiration decreases, photomineralization becomes an increasingly important

oxidative pathway for organic C (Amado et al., 2006). In a study by Amado et al. (2006), CO_2 production by microbial respiration and photomineralization were roughly equal during the low-water stage of the flood-pulse (54 % and 46 %, respectively). During the subsequent high-water stage, microbial respiration accounted for just 10 % of CO_2 production, while photomineralization accounted for 90 % and led to an 18 % increase in total CO_2 produced (Amado et al., 2006). An earlier study by Amon and Benner (1996) demonstrated that photomineralization consumed seven times more oxygen in surface waters than microbial respiration during the high-water stage, with the important caveat that light attenuation limited photomineralization, though not microbial respiration, at greater depths. As a result, microbial respiration was responsible for most oxygen and DOC consumption when this consumption was integrated throughout the water column (Amon and Benner, 2006). Furthermore, incomplete photo-oxidation can make relatively recalcitrant floodplain POC and DOC more labile (David et al., 2018; Haywood et al., 2018), enhancing microbial respiration via both aerobic (Amado et al., 2006) and anaerobic pathways (Bianchi et al., 1996). These studies of floodplain lakes collectively highlight that photomineralization is an important oxidative pathway for organic C during the high-water stage of the flood-pulse.

The FPC predicts that increasing water residence time on the floodplain during the high-water stage of the flood-pulse will result in aerobic microbial respiration and dissolved O_2 depletion, which has since been shown empirically (Mann et al., 2014; Kaller et al., 2015). As water depth increases during the high-water stage, oxygen depletion and vertical stratification can evolve, particularly as suspended sediments and DOC attenuate light in the water column. This has led to dramatic vertical and horizontal redox gradients in the Amazon (Richey et al., 1988), Pantanal (Devol et al., 1996; Hamilton et al., 1997), Mekong (Holtgrieve et al., 2013;

Arias et al., 2014), and other tropical rivers, and with them different oxidative pathways for organic C.

The FPC predicts that methanogenesis, specifically, will become a thermodynamically favorable oxidative pathway for organic C on the floodplain during the high-water stage of the flood-pulse. In temperate lakes, methanogenesis has been estimated to represent 0.5 % to 17 % of heterotrophic bacterial production, measured using incorporation of labelled organic C into bacterial biomass (Bastviken and Tranvik, 2001; Bastviken et al., 2003). The thousands of km^2 over which the Amazon, Oubangui, Mekong, and other flood-pulses occur makes even greater contributions by methanogenesis to microbial production likely in these ecosystems. Richey et al. (1988) estimated that 50 % of respiration on the Amazon floodplain is anaerobic. Since, measurements of anaerobic respiration relative to aerobic respiration within inland waters and the floodplains of tropical rivers have been sparse or non-existent.

Like primary production, we hypothesize the trajectories of ecosystem parameters related to respiration over the course of the flood-pulse using a hysteresis, based on the literature reviewed. The balance of *GPP* and *ER*, or *NEP*, reaches its maximum during the rising-water stage of the flood-pulse, tracking phytoplankton blooms (Figure 5a). Riverine DOC is introduced to the floodplain throughout the rising- and early high-water stages (Figure 5b). Floodplain DOC, by contrast, is mobilized primarily during the rising- and falling-water stages by expanding and contracting flood waters (Figure 5c). A combination of labile riverine organic C and mobilized floodplain organic C lead to increased microbial respiration and PCO_2 during the rising-water stages, peaking during the falling-water stage as floodplain waters are again mixed and consolidated (Figure 5d). During the rising- and high-water stage, methanogenesis becomes an increasingly favorable oxidative pathway as dissolved O_2 is depleted (Figure 5e).

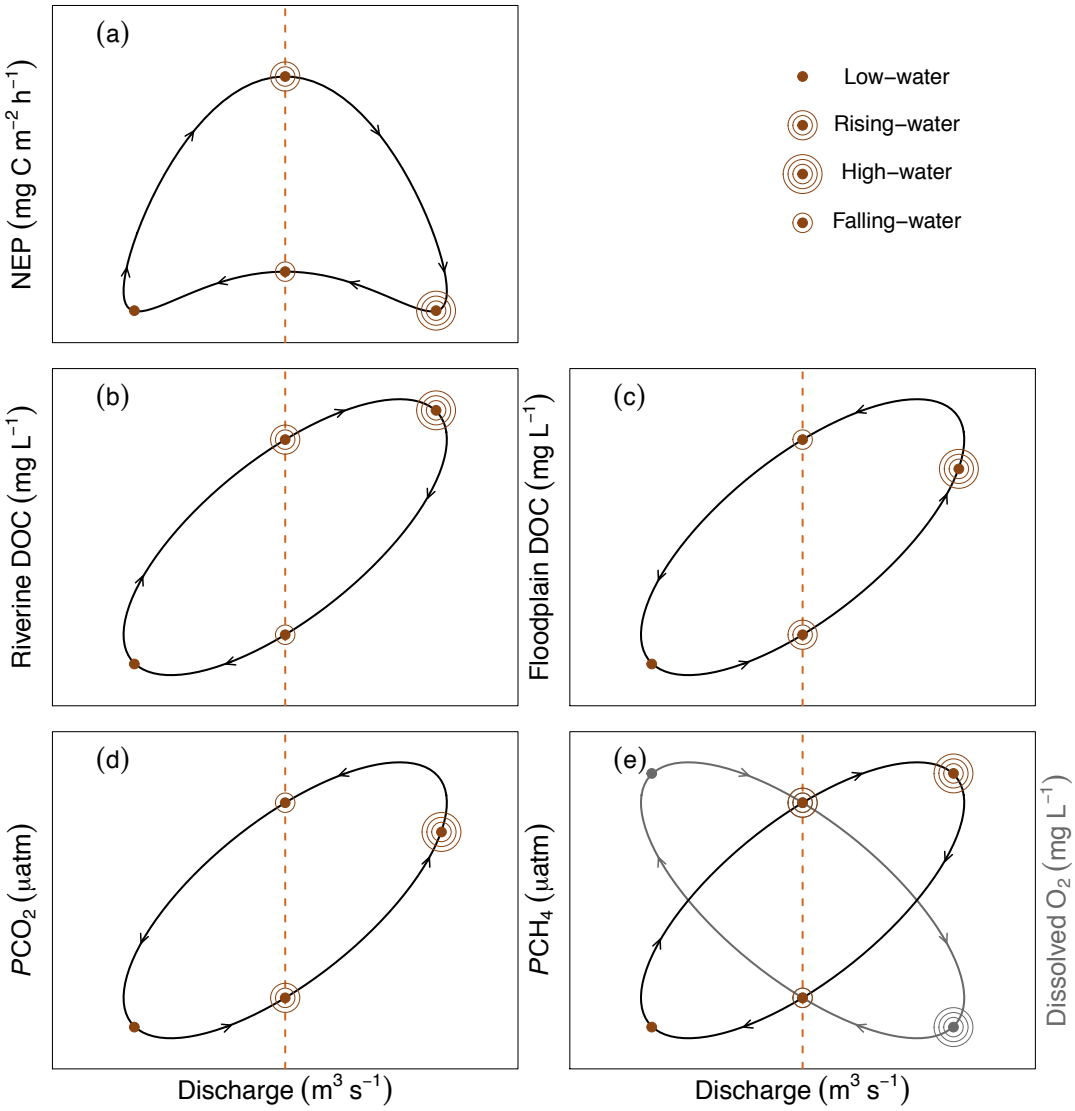

Figure 4. Hypothesized trajectories of ecosystem parameters related to the respiration of organic C using a hysteresis, based on the literature reviewed. Orange dashed lines indicate different rates or concentrations at the same level of discharge during different flood stages.

Notably, dissolved O_2, PCO_2, and DOC have been shown to follow a hysteresis through deployment of continuous sensors by Zuijdgeest et al. (2016). However, the trajectories measured by Zuijdgeest et al. (2016) varied slightly from those we hypothesized, based on the literature. In Zuijdgeest et al. (2016) and the Upper Zambezi River, dissolved O_2 was higher during the falling-water stage, rather than during the rising-water stage as we expected. Riverine

DOC followed the same trajectory we expected (Zuigdgeest et al., 2016). PCO_2 reached its maximum in the Upper Zambezi River during the rising-water stage, rather than during the falling-water stage as we hypothesized. These data confirm that ecosystem parameters related to the respiration of organic C follow a hysteresis during the flood-pulse, though trajectories may be watershed-specific.

(v) The FPC can be further modified to reflect rapidly changing land use and climate in the tropics.

The subtropics and tropics between 35 degrees north and 35 degrees south are home to many high-order flood-pulse rivers, such as the Amazon, Orinoco, Parana, Nile, Okavango, Zambezi, Oubangui, Ganges, Indus, Yangtze, Irrawady, and Mekong, which are collectively responsible for much of global, mean annual discharge (Figure 6). In addition, the tropics are home to 54% of the world's renewable water resources, 40% of its population, and accelerating land-use change (*State of the Tropics*, 2019), including floodplain modification (Hamilton, 2010).

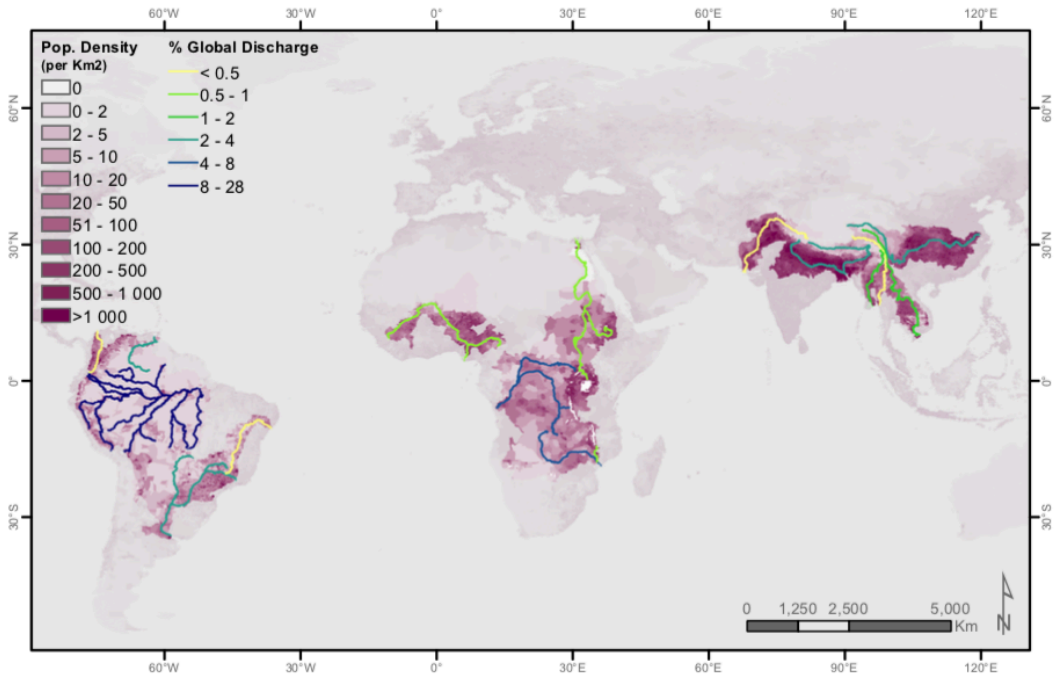

Figure 5. Subtropical and tropical rivers between 35 degrees north and 35 degrees south, by contribution to global, mean annual riverine discharge. Population density, per km^2, is also shown to highlight that many tropical rivers are adjacent to densely-populated areas.

Most of the literature available for our review has been conducted in Australian rivers and the Okavango, Oubangui, Orinoco, and Amazon watersheds. These watersheds are relatively undisturbed compared to the world's other, great flood-pulse rivers, such as the Yangtze, Mekong, Irrawaddy, Ganges, Indus, and Brahmaputra. These rivers have some of the oldest continuous human habitation and highest population densities on the planet, yet the mechanisms for their productivity, on which billions of people have relied, have not been distinguished from the Amazon, for example. The ways in which large numbers of people have altered these watersheds and manipulated their productivity for thousands of years is beyond the scope of this review. We can, however, speculate on how hydropower development and other land use changes could impact C cycling within flood-pulse watersheds.

One significant way that contemporary populations are altering flood pulse rivers is hydropower development. The rate of hydropower development is greatest in tropical flood-

pulse rivers (Zarfl et al., 2015). The highest rates of impoundment (>100 dams currently planned) are in the Amazon-La Plata River basins of Brazil, the Ganges-Bramaputra River basins of India and Nepal, and the Yangzte River basin of China (Zarfl et al., 2015). Hydropower development on the lower Mekong is predicted to change the extent and duration of the lower Mekong flood-pulse (Arias et al., 2014), increasing water levels over a longer low-water stage and decreasing water levels over a shorter high-water stage (Sabo et al., 2017; Dang et al., 2018). According to this review, a shorter and less extensive high-water stage may decrease seasonal maxima in macrophytes and periphyton. This may be offset slightly by fewer losses in terrestrial plants on the floodplain, though—as the literature shows—terrestrial organic C is less labile that *in-situ* aquatic primary production. The effects on phytoplankton production are less clear; blooms of this primary producer, which appear to be important to respiration, occur during the rising- and falling-water stages. If the extent and duration of the flood-pulse is abbreviated with hydropower development, these flood stages will presumably be shortened, as well. However, apart from rising- and falling-water dynamics, reservoirs also slow riverine flow, leading to sediment and organic C deposition and perhaps greater phytoplankton production (Jacinthe et al. 2012). For the respiration of C, a smaller floodplain area may decrease the area over which aerobic and anaerobic respiration (e.g., methanogenesis) can occur. The connectivity of these environments is crucial to the high rates of respiration observed in flood-pulse ecosystems; without it, respiration at the base of the heterotrophic food web is likely to decrease.

Changes in precipitation patterns and land use have implications for how water flows across and is filtered through landscapes after it falls as rain, further affecting organic C transport and transformation. Monsoonal precipitation is projected to increase in magnitude by 2 % by 2020, 4 % by 2050, and 8 % by 2020, as well as in intensity (i.e., magnitude per time) (Costa-

Cabral et al., 2008). Land use change in the tropical Southeast Asia and the tropics, more generally, can be characterized by deforestation, peatland degradation, agricultural and pastoral expansion and contraction, and urbanization. Throughout the 1990s, Southeast Asia experienced the highest level of deforestation of any tropical region (Meittenen et al., 2011). Zhang et al. (2017) show that increases in annual runoff associated with deforestation are statistically significant, and Sanders et al. (2018) show peaks in organic C burial within Amazonian floodplain lakes during periods of deforestation. Runoff from deforested land may increase organic C transport overall, but decrease its transformation, resulting in the delivery of greater quantities of less labile, more recalcitrant terrestrial organic C to flood-pulse watersheds. At the same time, runoff from urban areas and wastewater treatment effluent may become sources of labile organic C (Hosen et al., 2014; Kaushal et al., 2014) and dissolved CO_2 and CH_4 (Wang et al., 2017; Yoon et al., 2017). The FPC should be modified along with other paradigms of large river ecology to reflect impoundment and other land use changes in increasingly densely-populated regions (Park et al., 2018).

3.0 Conclusion

Using the literature on tropical flood-pulse rivers published since 1989, we can begin to modify the predictions of the FPC (Junk et al., 1989). Several of the FPC's highly cited predictions have been borne out by subsequent studies that we reviewed (Table 3). These include the structuring of floodplain vegetation by the flood-pulse, the mobilization and respiration of floodplain organic C by the flood-pulse, the subsequent transfer of this organic C into the heterotrophic food web, and the development of anaerobic conditions and CH_4 production on the floodplain as the flood-pulse progresses (Table 3). Importantly, this review demonstrates that—in contrast to the original FPC—respiration far exceeds production on the

floodplains of tropical rivers. The FPC also underestimated the importance of *in-situ* primary production to respiration at the base of heterotrophic food webs, both on the floodplain during the rising-water stage and in the main channel during the falling-water stage. The FPC correctly identified methanogenesis as an increasingly important oxidative pathway for organic C during the high-water stage, but did not account for photomineralization (Junk et al., 1989). We hypothesize the trajectories of ecosystem parameters related to primary production and respiration over the course of the flood-pulse using a hysteresis, based on the literature reviewed; however, more directed field studies are necessary to confirm these hypotheses. The modification of predictions by the FPC updates this seminal paradigm in aquatic ecology and points to important future research directions, including how hydropower development affects primary production and respiration in a modified flood-pulse ecosystem.

Table 3. Junk et al. (1989)'s predictions for primary production and respiration during the flood-pulse, compared with the more recent findings published by the literature reviewed.

Junk et al., 1989	This synthesis
Flood-pulse drives vegetative composition on floodplain	☒
Phytoplankton blooms throughout flood-pulse	Phytoplankton blooms during rising- & falling-water, macrophytes & periphyton blooms during high-water stage
Photosynthesis > respiration on floodplain throughout flood-pulse	Photosynthesis < respiration on the floodplain throughout flood-pulse
In-situ production in main channel unimportant to heterotrophic food webs relative to antecedent floodplain DOC during rising-water stage	Labile DOC from i*n-situ* production in main channel exceeds more recalcitrant antecedent floodplain DOC during rising-water stage
Both riverine and floodplain organic C mobilized during rising- & falling-water stages	☒
Progressively anaerobic conditions develop during high-water	☒
Microbial respiration of floodplain organic C	Microbial respiration and photomineralization of floodplain organic C
Export of organic C from floodplain within biomass of fish & invertebrates	Export of organic C from floodplain via atmospheric emissions of CO_2 & CH_4 and phytoplankton, in addition to fish & invertebrates

4.0 Acknowledgements

This work was partially supported by the National Science Foundation through a Graduate Research Fellowship (DGE1256260) and Innovations at the Nexus of Food Energy and Water (EAR 1740042) award. Additional funding was provided by the Margaret A. Cargill Philanthropies. We thank Heidi Roop, Catherine Schwartz, and David French for assistance with maps and graphic design. All data and data products presented in figures and analyses are available by following the link: https://github.com/blm8/Flood-Pulse-Review.git.

5.0 Literature Cited

Abril, G. and A.V. Borges (2019), Ideas and perspectives—Carbon leaks from flooded land—Do we need to replumb the inland water active pipe?, *Biogeosciences*, 16, 769-784, 769-784. http://doi.org/10.5194/bg-16-769-2019

Abril, G., J.M. Martinez, L.F. Artigas, P. Moreira-Turcq, M.F. Benedetti, L. Vidal, T. Meziane, J.H. Kim, M.C. Bernardes, N. Savoye, J. Deborde, E.L. Souza, P. Alberic, M.F.L. de Souza, and F. Roland (2014), Amazon River carbon dioxide outgassing fueled by wetlands. *Nature*, 505(7483), 395–398. http://doi.org/10.1038/nature12797

Adams, H.E., B.C. Crump, and G.W. Kling (2014), Metacommunity dynamics of bacteria in an arctic lake: The impact of species sorting and mass effects on bacterial production and biogeography, *Frontiers in Microbiology*, 82(5), 1-10. http://doi.org/10.3389/fmicb.2014.00082

Aitkenhead, J. A., and W.H. McDowell (2000), Soil C:N ratio as a predictor of annual riverine DOC flux at local and global scales, *Global Biogeochemical Cycles*, 14(1), 127–138. http://doi.org/10.1029/1999GB900083

Alsdorf, D., E. Beighley, Al Laraque, H. Lee, R. Tshimanga, F. O'Loughlin, G. Mahe, B. Dingha, G. Moukandi, and R.G.M. Spencer (2016), Opportunities for hydrologic research in the Congo Basin. *Reviews of Geophysics*, 54, 378-409. http://doi.org/10.1002/2016RG000517

Amado, A. M., V.F. Farjalla, F.D.A. Esteves, R.L. Bozelli, F. Roland, and A. Enrich-Prast (2006), Complementary pathways of dissolved organic carbon removal pathways in clear-water Amazonian ecosystems: Photochemical degradation and bacterial uptake, *FEMS Microbiology Ecology*, 56(1), 8–17. http://doi.org/10.1111/j.1574-6941.2006.00028.x

Amon, R.M.W. and R. Benner (1996), Photochemical and microbial consumption of dissolved organic carbon and dissolved oxygen in the Amazon River system, *Geochemica et Cosmochimica Acta*, 60(10), 1783-1792. http://doi.org/10.1016/0016-7037(96)00055-5

Arias, M.E., F. Wittmann, P. Parolin, M. Murray-Hudson, and T.A. Cochrane (2018), Interactions between flooding and upland disturbance drives species diversity in large river floodplains, *Hydrobiologia*, 814, 5-17. http://doi.org/10.1007/s10750-016-2664-3

Arias, M.E., T.A. Cochrane, M. Kummu, H. Lauri, G.W. Holtgrieve, J. Koponen, and T. Piman (2014), Impacts of hydropower and climate change on drivers of ecological productivity of Southeast Asia's most important wetland, *Ecological Modelling*, 272, 252-263. http://doi.org/10.1016/j.ecolmodel.2013.10.015

Arias, M.E., T.A. Cochrane, D. Norton, T.J. Killeen, and P. Khon (2013), The flood pulse as the

underlying driver of vegetation in the largest wetland and fishery of the Mekong Basin, *AMBIO*, 42(7), 864-876. http://doi.org/10.1007/s13280-013-0424-4

Aufdenkampe, A. K., E. Mayorga, P.A. Raymond, J.M. Melack, S.C. Doney, S.R. Alin, R.E. Aalto, and K. Yoo (2011), Riverine coupling of biogeochemical cycles between land, oceans, and atmosphere, *Frontiers in Ecology and the Environment*, 9(1), 53–60. http://doi.org/10.1890/100014

Bass, A. M., N.C. Munksgaard, M. Leblanc, S. Tweed, and M.I. Bird (2014), Contrasting carbon export dynamics of human impacted and pristine tropical catchments in response to a short-lived discharge event, *Hydrological Processes*, 28(4), 1835–1843. http://doi.org/10.1002/hyp.9716

Bastviken, D., J. Ejlertsson, I. Sundh, and L. Tranvik (2003), Methane as a source of carbon and energy for lake pelagic foodwebs, *Ecology*, 84(4), 969-981. http://doi.org/10.1890/0012-9658(2003)084[0969:MAASOC]2.0.CO;2

Bastviken, D. and L. Tranvik (2001), The leucine incorporation method estimates bacterial growth equally well in both oxic and anoxic lake water, *Applied and Environmental Microbiology*, 67, 2916-2921. http://10.1128/AEM.67.7.2916-2921.2001

Battin, T. J., L.A. Kaplan, S. Findlay, C.S. Hopkinson, E. Marti, A.I. Packman, J.D. Newbold, and F. Sabater (2009), Biophysical controls on organic carbon fluxes in fluvial networks, *Nature Geoscience*, 2(8), 595–595. http://doi.org/10.1038/ngeo602

Battin, T. J. (1998), Dissolved organic matter and its optical properties in a blackwater tributary of the upper Orinoco river, Venezuela, *Organic Geochemistry*, 28(9–10), 561–569. http://doi.org/10.1016/S0146-6380(98)00028-X

Bayley, P.B. (1995), Understanding large river-floodplain ecosystems, *BioScience*, 45(3), 153-158. http://doi.org/10.2307/1312554

Beal, E.J., C.H. House, and V.J. Orphan (2009), Manganese- and iron-dependent marine methane oxidation, *Science*, 325(5937), 184-187. http://doi.org/10.1126/science.1169984

Bianchi, T.S., M.E. Freer, R.G. Wetzl (1996), Temporal and spatial variability, and the role of dissolved organic carbon (DOC) in methane fluxes from the Sabine River floodplain (southeast Texas, USA), *Archiv Fur Hydrobiologie*, 136(2), 261-287.

Bleich, M.E., M.T.F. Piedade, A.F. Mortati, and T. Andre (2015), Autochthonous primary production in southern Amazon headwater streams: Novel indicators of altered environmental integrity, *Ecological Indicators*, 53, 154-161. http://doi.org/10.1016/j.ecolind.2015.01.040

Bodmer, P., M. Heinz, M. Pusch, G. Singer, and K. Premke (2016), Carbon dynamics and their link to dissolved organic matter quality across contrasting stream ecosystems, *Science of the*

Total Environment, 553, 574-586. http://doi.org/10.1016/j.scitotenv.2016.02.095

Boedeltje, G., J.P. Baker, A.T. Brinke, J.M. van Groenendael, and M. Soesbergen (2004), Dispersal phenology of hydrochorous plants in relation to discharge, seed release time and buoyancy of seeds: The flood pulse concept supported, *Journal of Ecology*, 92(5), 786-796. http://doi.org/10.1111/j.0022-0477.2004.00906.x

Borges, A.V., G. Abril, F. Darchambeau, C.R. Teodoru, J. Deborde, L.O. Vidal, T. Lamber, and S. Bouillion (2015), Divergent biophysical controls of aquatic CO2 and CH4 in the world's two largest rivers, *Scientific Reports*, 5, 15614. http://doi.org/doi:10.1038/srep15614

Bouillon, S., A. Yambélé, R.G.M. Spencer, D.P. Gillikin, P.J. Hernes, J. Six, R. Merckx, and A.V. Borges (2012), Organic matter sources, fluxes and greenhouse gas exchange in the Oubangui River (Congo River basin), *Biogeosciences*, 9(6), 2045–2062. http://doi.org/10.5194/bg-9-2045-2012

Burns, A. and D.S. Ryder (2001), Response of bacterial extracellular enzymes to inundation of floodplain sediments, *Freshwater Biology*, 46, 1299–1307. http://doi.org/10.1046/j.1365-2427.2001.00750.x

Caleta, G.P., M. Cumo, G.E. Farello, and T. Setaro (1991), Hysteresis effect in flooding, International Journal of Multiphase Flow, 17(2), 283-289. Http://doi.org/10.1016/0301-9322(91)90021-T

Carvalho, P., S.M. Thomaz, and L.M. Bini (2003), Effects of water level, abiotic and biotic factors on bacterioplankton abundance in lagoons of a tropical floodplain (Parana River, Brazil), *Hydrobiologia*, 510, 67–74. http://doi.org/10.1023/B:HYDR.0000008532.71152.38

Castillo, M. M., J.D. Allan, R.L. Sinsabaugh, and G.W. Kling (2004), Seasonal and interannual variation of bacterial production in lowland rivers of the Orinoco basin, *Freshwater Biology*, 49(11), 1400–1414. http://doi.org/10.1111/j.1365-2427.2004.01277.x

Castillo, M.M., G.W. Kling, and J.D. Allan (2003), Bottom-up controls on bacterial production in tropical lowland rivers, *Limnology and Oceanography*, 48(4), 1466-1475. http://doi.org/10.4319/lo.2003.48.4.1466

Castillo, M. M. (2000). Influence of hydrological seasonality on bacterioplankton in two neotropical floodplain lakes, *Hydrobiologia*, 437, 57–69. http://doi.org/10.1023/A:1026598123694

Chaparro, G., M.S. Fontanarrosa, M.R. Schiaffino, P. de Tezanos-Pinto, and I. O'Farrell (2014). Seasonal-dependence in the responses of biological communities to flood pulses in warm temperate floodplain lakes: Implications for the "alternative stable states" model, *Aquatic Sciences*, 76, 579–594. http://doi.org/10.1007/s00027-014-0356-5

Chen, H., Y. Wu, X. Yuan, Y. Gao, N. Wu, and D. Zhu (2009), Methane emissions from newly created marshes in the drawdown area of the Three Gorges Reservoir, *Journal of Geophysical Research*, 114, D18301. http://doi.org/10.1029/2009JD012410

Cole, J.J. and N.F. Caracao (2001), Carbon in catchments: Connecting terrestrial carbon losses with aquatic metabolism, *Marine and Freshwater Research*, 52, 101-110.

Cook, R.A., B. Gawne, R. Petrie, D.S. Baldwin, G.N. Rees, D.L. Nielsen, and N.S.P. Ning (2015), River metabolism and carbon dynamics in response to flooding in a lowland river, *Marine and Freshwater Research*, 66, 919-927. http://doi.org/10.1071/MF14199

Costa-Cabral, M. C., J.E. Richey, G. Goteti, D.P. Lettenmaier, C. Feldkotter, and A. Snidvongs (2008), Landscape structure and use, climate, and water movement in the Mekong River basin, *Hydrological Processes*, 22, 1731-1746. http://doi.org/10.1002/hyp.6740

Dai, M., Z. Yin, F. Meng, Q. Liu, and W.J. Cai (2012), Spatial distribution of riverine DOC inputs to the ocean—An updated global synthesis, *Current Opinions in Environmental Sustainability*, 4, 170–178. http://doi.org/10.1016/j.cosust.2012.03.003

Dalzell, B. J., T.R. Filley, and J.M. Harbor (2005), Flood pulse influences on terrestrial organic matter export from an agricultural watershed, *Journal of Geophysical Research*, 110, 1–14. http://doi.org/10.1029/2005JG000043

Dang, T.D., T.A. Cochrane, M.E. Arias, and V.P.D. Tri (2018), Future hydrological alterations in the Mekong Delta under the impact of water resources development, land subsidence, and sea level rise, Journal of Hydrology—Regional Studies, 15, 119-133. http://doi.org/10.1016/j.ejrh.2017.12.002

Darby, S.E., C.R. Hackney, J. Leyland, M. Kummu, H. Lauri, D.R. Parsons, J.L. Best, A.P. Nicholas, and R. Aalto (2016), Fluvial sediment supply to a mega-delta reduced by shifting tropical cyclone activity, *Nature*, 539, 276-279. http://doi.org/10.1038/nature19809

David, F., C. Marchand, P. Taillardat, T.N. Nguyen, T. Meziane (2018), Nutritional composition of suspended particulate matter in a tropical mangrove creek during a tidal cycle (Can Gio, Vietnam), Estuarine, Coastal and Shelf Science, 200, 126-130. http://doi.org/10.1016/j.ecss.2017.10.017

Deemer, B.R. J.A. Harrison, S. Li, J.J. Beaulieu, T. DelSontro, N. Barros, J.F. Bezerra-Neto, S.M. Powers, M.A. do Santos, and J.A. Vonk (2016), Greenhouse gas emissions from reservoir water surfaces: A new global synthesis, *BioScience*, 66(11), 949-964. http://doi.org/10.1093/biosci/biw117

Del Giorgio, P.A., J.J. Cole, and A. Cimbleris (1997), Respiration rates in bacteria exceed phytoplankton production in unproductive aquatic systems, *Nature*, 385, 148-151. http://doi.org/10.1038/385148a0

De Melo, M., D.N. Kothawala, S. Bertilsson, J.H. Amaral, B. Forsberg, and H. Sarmiento (2020), Linking dissolved organic matter composition and bacterioplankton communities in an Amazon floodplain system, Limnology and Oceanography, 65(1), 63-76. http://doi.org/10.1002/lno.11250

De Melo, M. L., S. Bertilsson, J.H.F. Amaral, P.M. Barbose, B.R. Forsberg, and H. Sarmento (2019), Flood pulse regulation of bacterioplankton community composition in an Amazonian floodplain lake, *Freshwater Biology*, 64(1), 108-120. http://doi.org/10.1111/fwb.13198

De Oliveira, M.D. and D.F. Calheiros (2000), Flood pulse influence on phytoplankton communities of the south Pantanal floodplain, Brazil, *Hydrobiologia*, 427, 101-112. http://doi.org/10.1023/A:1003951930525

Devol, A., J. Richey, S.L. King, J. Lansdown, and L.A. Martinelli (1996), Seasonal variations in the 13C-CH4 of Amazon floodplain waters, *Mitteilungen Internationale Vereinigung Für Theoretische Und Angewandte Limnologie*, 25, 173-178.

Dorado-Rodrigues, T.F., V.M.G. Layme, F.H.B. Silva, and C.N. da Cunha (2015), Effects of shrub encroachment on the anuran community in periodically flooded grasslands of the largest Neotropical wetland, *Austral Ecology*, 40(5), 547-557. http://doi.org/10.1111/aec.12222

Dunck, B., L. Rodrigues, and D.C. Bicudo (2015), Functional diversity and functional traits of periphytic algae during a short-term successional process in a Neotropical floodplain lake, *Brazilian Journal of Biology*, 75(3). http://doi.org/10.1590/1519-6984.17813

Ellis, E. E., R.G. Keil, A.E. Ingalls, J.E. Richey, and S.R. Alin (2012), Seasonal variability in the sources of particulate organic matter of the Mekong River as discerned by elemental and lignin analyses, *Journal of Geophysical Research: Biogeosciences*, 117(1), 1–16. http://doi.org/10.1029/2011JG001816

Farjalla, V. F., D.A. Azevedo, F.A. Esteves, R.L. Bozelli, F. Roland, and A. Enrich-Prast (2006), Influence of hydrological pulse on bacterial growth and DOC uptake in a clear-water Amazonian lake, *Microbial Ecology*, 52(2), 334–344. http://doi.org/10.1007/s00248-006-9021-4

Ferreira-Junior, W.G., C.E.G.R. Shaefer, C.N. Cunha, T.G. Duarte, L.C. Chieregatto, and F.M.S. Carmo (2016), Flood regime and water table determines tree distribution in a forest-savanna gradient in the Brazilian Pantanal, *Anais da Academia Brasileira de Ciencias*, 88(1). http://doi.org/10.1590/0001-3765201620150341

Fellman, J. B., N.E. Pettit, J. Kalic, and P.F. Grierson (2013), Influence of stream-floodplain biogeochemical linkages on aquatic foodweb structure along a gradient of stream size in a tropical catchment, *Freshwater Science*, 32(1), 217–229. http://doi.org/10.1899/11-117.1

Fellows, C. S., H.M. Hunter, C.E.A. Eccleston, R.W. De Hayr, D.W. Rassam, N.J. Beard, and P.M. Bloesch (2011), Denitrification potential of intermittently saturated floodplain soils from a subtropical perennial stream and an ephemeral tributary, *Soil Biology and Biochemistry*, 43(2), 324–332. http://doi.org/10.1016/j.soilbio.2010.10.019

Fisher, T.R. (1979), Plankton and primary production in aquatic systems of the central Amazon Basin, *Comparative Biochemistry and Physiology*, 62a, 31-38. http://doi.org/10.1016/0300-9629(79)90739-4

Foti, R., M. del Jesus, A. Rinaldo, and I. Rodriguez-Iturbe (2012), Hydroperiod regime controls the organization of plant species in wetlands, *Proceedings of the National Academy of Sciences*, 109, 19596–600. http://doi.org/10.1073/pnas.1218056109

Gerking, S.D. (1945), The distribution of the fishes of Indiana, *In* Frey, D.G., ed., *Investigations of Indiana Lakes and Streams*, 3, 1-137.

Gomes, L. C., C.K. Bulla, A.A. Agostinho, L.P. Vasconcelos, and L.E. Miranda (2012), Fish assemblage dynamics in a Neotropical floodplain relative to aquatic macrophytes and the homogenizing effect of a flood pulse, *Hydrobiologia*, 685(1), 97–107. http://doi.org/10.1007/s10750-011-0870-6

Gottsberger, G. (1978), Seed dispersal by fish in inundated regions of Humaita, Amazonia, *Biotropica*, 10(3), 170-183. http://doi.org/10.2307/2387903

Gu, B., C.L. Schelske, and D.A. Hodell (2004), Extreme ^{13}C enrichments in a shallow hypereutrophic lake—Implications for carbon cycling, *Limnology and Oceanography*, 49(4), 1152-1159. http://doi.org/10.4319/lo.2004.49.4.1152

Hamilton, S.K. (2010), Biogeochemical implications of climate change for tropical rivers and floodplains, *In*: Stevenson, R.J. and S. Sabater (eds) *Global Change and River Ecosystems—Implications for Structure, Function and Ecosystem Services*, *Developments in Hydrobiology*, 215, Springer, Dordrecht, The Netherlands.

Hamilton, S. K., S.J. Sippel, D.F. Calheiros, and J.M. Melack (1997), An anoxic event and other biogeochemical effects of the Pantanal wetland on the Paraguay River, *Limnology and Oceanography*, 42(2), 257–272. http://doi.org/10.4319/lo.1997.42.2.0257

Hartmann, J. R. Lauerwald, and N. Moosdorf (2014), A brief overview of the GLObal RIver CHemistry database GLORICH, *Procedia Earth and Planetary Sciences*, 10, 23-27. http://doi.org/10.1016/j.proeps.2014.08.005

Haywood, B.J., J.R. White, R.L. Cook (2018), Investigation of an early season river flood pulse: Carbon cycling in a subtropical estuary, Science of the Total Environment, 635, 867-877. http://doi.org/10.1016/j.scitotenv.2018.03.379

Hosen, J.D., O.T. McDonough, C.M. Febria, M.A. Palmer (2014), Dissolved organic matter quality and bioavailability changes across an urbanization gradient in headwater streams, Environmental Science and Technology, 48, 7817-7824. http://doi.org/10.1021/es501422z

Hotchkiss, E. R., R.O. Hall, M.A. Baker, E.J. Rosi-Marshall, and J.L. Tank, J. L. (2014). Modeling priming effects on microbial consumption of dissolved organic carbon in rivers. *Journal of Geophysical Research: Biogeosciences*, 119(5), 982–995. http://doi.org/10.1002/2013JG002599

Holtgrieve, G.W., M.E. Arias, K.N. Irvine, D. Lamberts, E.J. Ward, M. Kummu, J. Koponen, J. Sarkkula, and J.E. Richey, (2013), Patterns of ecosystem metabolism in the Tonle Sap Lake, Cambodia with links to capture fisheries, *PLoS ONE*, 8(8), e71395. http://doi.org/10.1371/journal.pone.0071395

Humborg, C., C.M. Moerth, M. Sundbom, H. Borg, T. Blenchner, R. Giesler, and V. Ittekkot (2010), CO2 supersaturation along the aquatic conduit in Swedish watersheds as constrained by terrestrial respiration, aquatic respiration and weathering, *Global Change Biology*, 16, 404-428. http://doi.org/10.1111/j.1365-2486.2009.02092.x

Hunt, R.J., T.D. Jardine, S.K. Hamilton, and S.E. Bunn (2012), Temporal and spatial variation in ecosystem metabolism and food web carbon transfer in a wet-dry tropical river, *Freshwater Biology*, 57(3), 435-450. http://doi.org/10.1111/j.1365-2427.2011.02708.x

Intergovernmental Panel on Climate Change (IPCC) (2007), Climate change 2007: The physical science basis, *In* S. Solomon, D. Qin, M. Manning, Z. Chen, M. Marquis, K.B. Averyt, M.Tignor and H.L. Miller (eds.), Contribution of Working Group I to the Fourth Assessment Report of the Intergovernmental Panel on Climate Change, Cambridge University Press, Cambridge, United Kingdom.

Jacinthe, P.A., G.M. Filippelli, L.P. Tedesco, and R. Raftis (2012), Carbon storage and greenhouse gases emission from a fluvial reservoir in an agricultural landscape, *Catena*, 94, 53-63. http://doi.org/10.1016/j.catena.2011.03.012

Jansson, M., J. Karlsson, and A. Jonsson (2012), Carbon dioxide supersaturation promotes primary production in lakes, *Ecology Letters*, 15(6), 527-532. http://doi.org/10.1111/j.1461-0248.2012.01762.x

Jardine, T.D., B.J. Pusey, S.K. Hamilton, N.E. Pettit, P.M. Davies, M.M. Douglas, V. Sinnamon, I.A. Halliday, and S.E. Bunn (2012), Fish mediate high food web connectivity in the lower reaches of a tropical floodplain river, *Oecologia*, 168(3), 829-838. http://doi.org/10.1007/s00442-011-2148-0

Jansson, M., J. Karlsson, and A. Jonsson (2012), Carbon dioxide supersaturation promotes primary production in lakes. *Ecology Letters*, 15(6), 527–532. http://doi.org/10.1111/j.1461-0248.2012.01762.x

Johnson et al., M.S., J. Lehmann, S.J. Riha (2008), CO2 efflux from Amazonian headwater respresents a significant fate for deep soil respiration, *Geophysical Research Letters*, 35, L17401. http://doi.org/10.1029/2008gl034619

Jones, N.J., D.T. Scott, B.L. Edwards, and R.F. Keim (2014), Perirheic mixing and biogeochemical processing in flow-through and backwater floodplain wetlands, *Water Resources Research*, 50(9), 7394–7405. http://doi.org/10.1002/2014WR015647

Jones, S.H. and M. Alexander (1988), Effect of inorganic nutrients on the acclimation period preceding mineralization of organic chemical in lake water, *Applied and Environmental Microbiology*, 54(12), 3177-3179.

Junk, W.J. and P.B. Bayley (2007), The scope of the flood pulse concept regarding riverine fish and fisheries, given geographic and man-made differences between systems, *American Fisheries Society Symposium*, 49, 1907–1923.

Junk, W.J. and M.T.F. Piedade (1997), Plant life in the floodplains with special reference to herbaceous plants, 147-185, *In* W.J. Junk (ed.), The Central Amazon Floodplain—Ecology of a Pulsing System, *Ecological Studies*, 126.

Junk, W.J., P.B. Bayley, and R.E. Sparks (1989), The flood pulse concept in river-floodplain systems, 110-127, *In* D.P. Dodge (ed.), Proceedings of the International Large River Symposium, *Canadian Special Publication of Fisheries and Aquatic Sciences*, 106.

Kaller, M. D., R.F. Keim, B.L. Edwards, A.R. Harlan, T.E. Pasco, W.E. Kelso, A.D. Rutherford (2015), Aquatic vegetation mediates the relationship between hydrologic connectivity and water quality in a managed floodplain, *Hydrobiologia*, 760(1), 29–41. http://doi.org/10.1007/s10750-015-2300-7

Kaushal, S.S., W.H. McDowell, and W.M. Wollheim (2014), Tracking evolution of urban biogeochemical cycles—Past, present, and future, *Biogeochemistry*, 121, 1-21. http://doi.org/10.1007/s10533-014-0014-y

Keitel, J. D. Zak, and M. Hupfer (2016), Water level fluctuations in a tropical reservoir: The impact of sediment drying, aquatic macrophyte dieback, and oxygen availability on phosphorus mobilization, *Environmental Science and Pollution Research*, 23(7), 6883-6894. http://doi.org/10.1007/s11356-015-5915-3

Keruzore, A.A., N.J. Willby, D.J. Gilvear (2013) The role of lateral connectivity in the meintenance of macrophyte diversity and production in large rivers, *Aquatic Conservation*, 23(2), 301-315. http://doi.org/10.1002/aqc.228

Kinsman-Costello, L.E., J. O'Brien, and S.K. Hamilton (2014), Re-flooding of historically drained wetland leads to rapid sediment phosphorus release, *Ecosystems*, 17, 641-656. http://doi.org/10.1007/s10021-014-9748-6

Kiss, K.T. (1987), Phytoplankton studies in the Szigetkoz section of the Danube during 1981-1982, *Archiv fur Hydrobiologie*, 78, 247-273.

Klug, J.L. (2002), Positive and negative effects of allochthonous dissolved organic matter and inorganic nutrients on phytoplankton growth, *Canadian Journal of Fisheries and Aquatic Sciences*, 59(1), 85-95. http://doi.org/10.1139/f01-194

Kobayashi, T., D.S. Ryder, G. Gordon, I. Shannon, T. Ingleton, M. Carpenter, and S.J. Jacobs (2009), Short-term response of nutrients, carbon and planktonic microbial communities to floodplain wetland inundation, *Aquatic Ecology*, 43(4), 843–858. http://doi.org/10.1007/s10452-008-9219-2

Kone, Y.J.M., G. Abril, K.N. Kouadio, B. Delille, and A.V. Borges (2009), Seasonal variability of carbon dioxide in the rivers and lagoons of Ivory Coast (West Africa), *Estuaries and Coasts*, 32, 246-260. http://doi.org/10.1007/s12237-008-9121-0

Kummu, M., D. Penny, J. Sarkkula, and J. Koponen (2008), Sediment—Curse or blessing for Tonle Sap Lake?, *AMBIO*, 37(3), 158-163. http://doi.org/10.1579/0044-7447(2008)37[158:SCOBFT]2.0.CO;2

Lapierre, J.F. and P.A. del Giorgio (2012), Geographical end environmental divers of regional differences in the lake pCO2 versus DOC relationship across northern landscapes, *Journal of Geophysical Research—Biogeosciences*, 117, G03015. http://doi.org/10.1029/2012JG001945

Lauerwald, R., G.G. Laruelle, J. Hartmann, P. Ciais, and P.A.G. Regnier (2015), Spatial patterns in CO2 evasion from the global river network, *Global Biogeochemical Cycles*, 29, 534-554. http://doi.org/10.1002/2014GB004941

Lehman, P. W., T. Sommer, and L. Rivard (2008), The influence of floodplain habitat on the quantity and quality of riverine phytoplankton carbon produced during the flood season in San Francisco Estuary, *Aquatic Ecology*, 42(3), 363–378. http://doi.org/10.1007/s10452-007-9102-6

Lewis, W.M., S.K. Hamilton, M.A. Rodriguez, J.F. Saunders, and M.A. Lasi (2001), Foodweb analysis of the Orinoco floodplain based on production estimates and stable isotope data, Journal of the North American Benthological Society, 20(2), 241-254. http://doi.org/10.2307/1468319

Longhi, D., M. Bartoli, D. Nizzoli, A. Laini, P. Viaroli (2016), Do oxic-anoxic transitions constrain organic matter mineralization in eutrophic freshwater wetlands, *Hydrobiologia*, 774(1), 81-92. http://doi.org/10.1007/s10750-016-2722-x

Ludwig, , W., J.L. Probst, and S. Kempe (1996), Predicting the oceanic input of organic carbon by continental erosion, Global Biogeochemical Cycles, 10, 23-41. http://doi.org/10.1029/95GB02925

Mackay, A. W., T. Davidson, P. Wolski, R. Mazebedi, W.R.L. Masamba, P. Huntsman-Mapila, and M. Todd (2011), Spatial and seasonal variability in surface water chemistry in the Okavango Delta, Botswana: A multivariate approach, *Wetlands*, 31, 815–829. http://doi.org/10.1007/s13157-011-0196-1

Maeck, A., H. Hofmann, and A. Lorke (2014), Pumping methane out of aquatic sediments: Ebullition forcing mechanisms in an impounded river, *Biogeosciences*, 11, 2925-2938. http://doi.org/10.5194/bg-11-2925-2014

Maloney, K.O., D.P. Morrris, C.O. Moses, and C.L. Osburn (2005), The role of iron and dissolved organic carbon in the absorption of ultraviolet radiation in humic lake water, *Biogeochemistry*, 75(3), 393-407. http://doi/org/10.1007/s10533-005-1675-3

Mann, P. J., R.G.M. Spencer, B.J. Dinga, J.R. Poulsen, P.J. Hernes, G. Fiske, M.E. Salter, Z.A. Wang, K.A. Wang, J. Six, and R.M. Holmes (2014), The biogeochemistry of carbon across a gradient of streams and rivers within the Congo basin, *Journal of Geophysical Research: Biogeosciences*, 119(4), 687-702. http://doi.org/10.1002/2013JG002442

Mantoura, R.F.C., A. Dickson, and J.P. (1978), Complexation of metals with humic materials in natural waters, *Estuarine and Coastal Marine Science*, 6(4), 387-408. http://doi.org/10.1016/0302-3524(78)90130-5

Mayorga, E., A.K. Aufdenkampe, C.A. Masiello, A.V. Krusche, J.I. Hedges, P.D. Quay, J.E. Richey, and T.A. Brown (2005), Young organic matter as a source of carbon dioxide outgassing from Amazonian rivers, *Nature*, 436(7050), 538–41. http://doi.org/10.1038/nature03880

McClain, M. E., E.W. Boyer, C.L. Dent, S.E. Gergel, N.B. Grimm, P.M. Groffman, S.C. Hart, J.W. Harvey, C.A. Johnston, E. Mayorga, W.H. McDowell, and G. Pinay (2003), Biogeochemical Hot Spots and Hot Moments at the Interface of Terrestrial and Aquatic Ecosystems, *Ecosystems*, 6(4), 301–312. http://doi.org/10.1007/s10021-003-0161-9

McNicol, G. and W.L. Silver (2015), Non linear response of carbon dioxide and methane emissions to oxygen availability in a drained histosol, *Biogeochemistry*, 123(1-2), 299-306. http://doi.org/10.1007/s10533-015-0075-6

Meittenen, J., C. Shi, S.C. Liew (2011), Deforestation rates in insular Southeast Asia between 2000 and 2010, *Global Change Biology*, 17(7), 2261-2270. http://doi.org/10.1111/j.1365-2486.2011.02398.x

Melack, J.M. and T.R. Fisher (1983), Diel oxygen variations and their ecological implications in Amazon floodplain lakes, *Archiv fur Hydrobiologie*, 98, 422-442.

Mendoca, R., S. Kosten, S. Sobek, N. Barros, J.J. Cole, L. Tranvik, and F. Roland (2012), Hydroelectric carbon sequestration, *Nature Geoscience*, 5, 838-840. http://doi.org/10.1038/ngeo1653

Mihaljevic, M. and S.F. Filip (2011), Cyanobacterial blooms in a temperate river-floodplain ecosystem: The importance of hydrological extremes, *Aquatic Ecology*, 45(3), 335-349. http://doi.org/10.1007/s10452-011-9357-9

Mladenov, N., D.M. McKnight, P. Wolski, and L. Ramberg (2005), Effects of annual flooding on dissolved organic carbon dynamics within a pristine wetland, the Okavango Delta, Botswana, *Wetlands*, 25(3), 622–638. http://doi.org/10.1672/0277-5212(2005)025[0622:eoafod]2.0.co;2

Montoya, Y. and N. Aguirre (2010), Dynamics of the primary production of phytoplankton in tropical lakes through the flood pulse, Revista Facultad de Ingenieria-Universidad de Antioquia, 55, 76-89.

Montoya, J.V., D.L. Roelke, K.O. Winemiller, J.B. Cotner, J.A. Snider (2006), Hydrological seasonality and benthic algal biomass in a Neotropical floodplain river, *Journal of the North American Benthological Society*, 25(1), 157-170. http://doi.org/10.1899/0887-3593(2006)25[157:HSABAB]2.0.CO;2

Moreira-Turcq, P., M.P. Bonnet, M. Amorim, M. Bernardes, C. Lagane, L. Maurice, M. Perez, and P. Seyler (2013), Seasonal variability in concentration, composition, age, and fluxes of particulate organic carbon exchanged between the floodplain and Amazon River, *Global Biogeochemical Cycles*, 27(1), 119–130. http://doi.org/10.1002/gbc.20022

Mortillaro, J. M., F. Rigal, H. Rybarczyk, M. Bernardes, G. Abril, and T. Meziane, (2012), Particulate organic matter distribution along the lower Amazon River: Addressing aquatic ecology concepts using fatty acids, *PLoS ONE*, 7(9), 1–10. http://doi.org/10.1371/journal.pone.0046141

Murray-Hudson, M., P. Wolski, L. Cassidy, M.T. Brown, K. Thito, K. Kashe, and E. Mosimanyana (2015), Remote sensiving-dervied hydroperiod as a predictor of floodplain vegetation composition, *Wetlands Ecology Management*, 23, 603.

O'Connell, M., D.S. Baldwin, A.I. Robertson, and G. Rees (2000), Release and bioavailability of dissolved organic matter from floodplain litter: Influence of origin and oxygen levels. *Freshwater Biology*, 45(3), 333–342. http://doi.org/10.1046/j.1365-2427.2000.00627.x

Oliveira, M.D., S.K. Hamilton, D.F. Calheiros, and C.M. Jacobi (2010), Oxygen depletion events control the invasive golden mussel (Limneoperna fortunei) in a tropical floodplain, *Wetlands*, 30(4), 705-716. http://doi.org/10.1007/s13157-010-0081-3

Oviedo-Vargas, D., D.P. Genereux, D. Dierick, and S.F. Oberbauer (2015), The effect of regional groundwater on carbon dioxide and methane emissions from a lowland rainforest

stream in Costa Rica, *Journal of Geophysical Research—Biogeosciences*, 120, 2579-2595. http://doi.org/10.1002/2015JG003009

Park, J.H., O.K. Nayna, M.S. Begum, E. Chea, J. Hartmann, R.G. Keil, S. Kumar, X. Lu, L. Ran, J.E. Richey, V.V.S.S. Sarma, S.M. Tareq, D. T. Xuan, and R. Yu (2018), Reviews and sysntheses—Anthropogenic perturbations to carbon fluxes in Asian river systems—Concepts, emerging trends, and research challenges, Biogeosciences, 15, 3049-3069. http://doi.org/10.5194/bg-15-3049-2018

Pettit, N.E., R.J. Naiman, D.M. Warfe, T.D. Jardine, M.M. Douglas, S.E. Bunn, and P.M. Davies (2016), Productivity and connectivity in tropical riverscapes of Northern Australia: Ecological insights for management, *Ecosystems*, 20(3), 492-514.

Placella, S.A., E.L. Brodie, and M.K. Firestone (2012), Rainfall-induced carbon dioxide pulses result from sequential resuscitation of phylogenetically clustered microbial groups, *Proceedings of the National Academy of Sciences of the United States of America*, 109(27), 10931-10936. http://doi.org/10.1073/pnas.1204306109

Pollard, P.C. (2013), In situ rapid measures of total respiration rate capture the super labil DOC bacterial substrates of freshwater, 11, 584-593. http://doi.org/10.4319/lom.2013.11.584

Pollard, P. C. and H.W. Ducklow (2011), Ultrahigh bacterial production in a eutrophic subtropical Australian River: Does viral lysis short-circuit the microbial loop?, *Limnology and Oceanography*, 56(3), 1115–1129. http://doi.org/10.4319/lo.2011.56.3.1115

Raymond, P.A., J. Hartmann, R. Lauerwald, S. Sobek, C. McDonald, M. Hoover, D. Butman, R. Striegl, E. Mayorga, C. Humborg, P. Kortelainen, H. Duerr, M. Meybeck, P. Ciais, and P. Guth (2013), Global carbon dioxide emissions from inland waters, *Nature*, 503, 355-359. http://doi.org/10.1038/nature12760

Reynolds, C.S. and J.P. Descy (1996), The production, biomass, and structure of phytoplantkon in large rivers, *Archiv fur Hydrobiologie*, 12, 487-508. http://doi.org/10.1127/lr/10/1996/161

Richey, J.E., J.M. Melack, A.K. Aufdenkampe, V.M. Ballester, and L.L. Hess (2002), Outgassing from Amazonian rivers and wetlands as a large tropical source of atmospheric CO2, *Nature*, 416, 617-620. http://doi.org/10.1038/416617a

Richey, J.E., A.H. Devol, S.C. Wofsy, R. Victoria, and M.N.G. Riverio (1988), Biogenic gases and the oxidation and reduction of carbon in Amazon River and floodplain waters, *Limnology and Oceanography*, 33(4), 551-561. http://doi.org/10.4319/lo.1988.33.4.0551

Roach, K.A. (2013), Environmental factors affecting incorporation of terrestrial material into large river food webs, *Freshwater Science*, 32(1), 283–298. http://doi.org/10.1899/12-063.1

Sabo, J.L., A. Ruhi, G.W. Holtgrieve, V. Elliott, M.E. Arias, P.B. Ngor, T.A. Raesaenen, and S.

Nam (2017), Designing river flows to improve food security futures in the Lower Mekong Basin, *Science*, 358, 1270. http://doi.org/10.1126/science.aao1053

Sanders, L.M., K. Taffs, D. Stokes, C.J. Sanders, and A. Enrich-Prast (2018), Historic carbon burial spike in an Amazon floodplain lake linked to riparian deforestation near Santarem, Brazil (2018), *Biogeosciences*, 15, 447-455. http://doi.org/10.5194/bg-15-447-2018

Schluenz, B. and R.R. Schneider (2000), Transport of terrestrial organic carbon to the oceans by rivers—Re-estimating flux and burial rates, *International Journal of Earth and Space Sciences*, 88, 599-606. http://doi.org/10.1007/s005310050290

Scofield, V., J.M. Melack, P.M. Barbosa, J.H.F. Amaral, B.R. Forsberg, and V.F. Farjalla (2016), Carbon dioxide outgassing from Amazonian aquatic ecosystems in the Negro River basin, *Biogeochemistry*, 129, 77–91. http://doi.org/10.1007/s10533-016-0220-x

Seekell, D.A., J.F. Lapierre, J. Ask, A.K. Bergstrom, A. Deininger, P. Rodriguez, and J. Karlsson (2015a), The influence of dissolved organic carbon on primary production in northern lakes, *Limnology and Oceanography*, 60, 1276-1285. http://doi.org/10.1002/lno.10096

Seekell, D.A., J.F. Lapierre, and J. Karlsson (2015b), Trade-offs between light and nutrient availability across gradients of dissolved organic carbon concentration in Swedish lakes: Implications for patterns in primary production, *Canadian Journal of Fisheries and Aquatic Sciences*, 72, 1663-1671. http://doi.org/10.1139/cjfas-2015-0187

Selvam, B., J.F. Lapierre, A.R.A. Soares, D. Bastviken, J. Karlsson, and M. Berggren (2019), Photo-reactivity of dissolved organic carbon in the freshwater continuum, *Aquatic Sciences*, 81, 57. http://doi.org/10.1007/s00027-019-0653-0

Sobek, S. T. DelSontro, N. Wongfun, and B. Wehrli (2012), Extreme organic carbon burial fuels intense methane bubbling in a temperate reservoir, *Geophysical Research Letters*, 39, L01401. http://doi.org/10.1029/2011GL050144

Sousa, W.T.Z. (2011), Hydrilla verticillata (Hydrocharitaceae), a recent invader threatening Brazil's freshwater environments: A review of the extent of the problem, *Hydrobiologia*, 6691(1), 1-20. http://doi.org/10.1007/s10750-011-0696-2

State of the Tropics (2019), *State of the Tropics—2019 Report*, James Cook University, Townsville, Queensland.

Sun, T., S. Tang, W. Yang, and X. Shen (2016), Short-term response of aquatic metabolism to hydrologic pulsing in the coastal wetlands of Yellow River Delta, *Wetlands*, 36(S1), 81-94. http://doi.org/10.1007/s13157-015-0710-y

Teixeira-de Mello, F., V.A. de Oliveira, S.M. Loverde-Oliveira, V.L.M. Huszar, J. Barquin, C. Iglesias, T.S.F. Silva, C.H. Duque-Estrada, A. Silio-Calzada, and N. Mazzeo (2016), The structuring role of free-floating plants on the fish community in a tropical shallow lake: An

experimental approach with natural and artificial plants, Hydrobiologia, 778(1), 167-178. http://doi.org/10.1007/s10750-015-2447-2

Thorp, J. H. and M.D. Delong (2002), Dominance of autochthonous autotrophic carbon in food webs of heterotrophic rivers, *Oikos*, 96(3), 543–550. http://doi.org/10.1034/j.1600-0706.2002.960315.x

Thorp, J.H. and M.D. Delong (1994), The riverine productivity model: An heuristic view of carbon sources and organic processing in large river ecosystems, *Oikos*, 70(2), 305-308. http://doi.org/10.2307/3545642

Tockner, K., M.S. Lorang, and J.A. Stanford (2010), River flood plains are model ecosystems to test general hydrogeomorphic and ecological concepts, *River Research and Applications*, 26, 76-86. http://doi.org/10.1002/rra.1328

Tockner, K., D. Pennetzdorfer, N. Reiner, F. Schiemer, and J.V. Ward (1999), Hydrological connectivity and the exchange of organic matter and nutrients in a dynamic river-floodplain system (Danube, Austria), *Freshwater Biology*, 41(3), 521-535. http://doi.org/10.1046/j.1365-2427.1999.00399.x

Toth, L.A. (2015), Invasibility drives restoration of a floodplain plant community, *River Research and Applications*, 31, 1319-1327. http://doi.org/10.1002/rra.2836

Val, J., D. Chinarro, M.R. Pino, and E. Navarro (2016), Global change impacts on river ecosystems: A high-resolution watershed study of Ebro River metabolism, *Science of the Total Environment*, 569, 774-783. http://doi.org/10.1016/j.scitotenv.2016.06.098

Vannote, R.L., G.W. Minshall, K.W. Cummins, J.R. Sedell, and C.E. Cushing (1980), The river continuum concept, *Canadian Journal of Fisheries and Aquatic Sciences*, 37(1), 130-137. http://doi.org/10.1139/f80-017

Vrede, T. and L.J. Tranvik (2006), Iron constraints on planktonic primary production in oligotrophic lakes, *Ecosystems*, 9(7), 1094-1105. http://doi.org/10.1007/s10021-006-0167-1

Vastila, K., M. Kummu, C. Sangmanee, and S. Chinvanno (2010), Modeling climate change impacts on the flood pulse in the Lower Mekong floodplains, 1(1), 67-86. http://doi.org/10.2166/wcc.2010.008

Vasquez, E., E. Ejarque, I. Ylla, A.M. Romaní, and A. Butturini (2015), Impact of drying/rewetting cycles on the bioavailability of dissolved organic matter molecular-weight fractions in a Mediterranean stream, *Freshwater Science*, 34(1), 263–275. http://doi.org/10.1086/679616

Waichmann, A.V. (1996), Autotrophic carbon sources for heterotrophic bacterioplankton in a floodplain lake of central Amazon, *Hydrobiologia*, 341(1), 27-36.

Wainright, S.C., C.A. Couch, and J.L. Meyer (1992), Fluxes of bacteria and organic matter into a blackwater river from river sediments and floodplain soils, *Freshwater Biology*, 28(1), 37-48. http://doi.org/10.1111/j.1365-2427.1992.tb00560.x

Wallace, T.A. and D. Furst (2016), Open water metabolism and dissolved organic carbon in response to environmental watering in a lowland river-floodplain complex, *Marine and Freshwater Research*, 67, 1346-1361. http://doi.org/10.1071/MF15318

Wang, X., Y. He, H. Chen, C. Peng, Q. Zhu, J. Yue, H. Ren, W. Deng, and H. Liu (2017), pCO2 and CO2 fluxes of the metropolitan river network in relation to the urbanization of Chongqing, China, *Journal of Geophysical Research—Biogeosciences*, 122, 470-486. http://doi.org/10.1002/2016JG003494

Wantzen, K. M., Junk, W. J., and Rothhaupt, K.O. (2008), An extension of the flood-pulse concept for lakes, 151–170, *In* K.M. Wantzen (ed.), Ecological Effects of Water-level Fluctuations in Lakes, *Developments in Hydrobiology*, 204.

Ward, D.P., N.E. Pettit, M. Adame, M.M. Douglas, S.A. Setterfield, and S.E. Bunn (2016), Seasonal spatial dynamics of floodplain macrophyte and periphyton abundance in the Alligator Rivers region (Kakadu) of northern Australia, *Ecohydrology*, 9(8), 1675-1686. http://doi.org/10.1002/eco.1757

Ward, C.P., R.L. Sleighter, P.G. Hatcher, and R.M. Corey (2014), Insights into the complete and partial photooxidation of black carbon in surface waters, *Environmental Science and Process Impacts*, 16(4), 721-731. http://doi.org/10.1039/c3em00597f

Weishaar, J.L., G.R. Aiken, B.A. Bergamaschi, M.S. Fram, R. Fujii, and K. Mopper (2003), Evaluation of specific ultraviolet absorbance as an indicator of the chemical composition and reactivity of dissolved organic carbon, *Environmental Science and Technology*, 37(20), 4702-4708. http://doi.org/10.1021/es030360x

Winemiller, K. O., C.G. Montaña, D.L. Roelke, J.B. Cotner, J.V. Montoya, L. Sanchez, M.M. Castillo, and C.A. Layman (2014), Pulsing hydrology determines top-down control of basal resources in a tropical river-floodplain ecosystem, *Ecological Monographs*, 84(4), 621–635. http://doi.org/10.1890/13-1822.1

Winemiller, K.O. and D.B. Jepsen (1998), Effects of seasonality and fish movement tropical river food webs, *Journal of Fish Biology*, 53(sA), 267-296. http://doi.org/10.1111/j.1095-8649.1998.tb01032.x

Winslow, L.A., J.A. Zwart, R.D. Batt, H.A. Dugan, R.I. Woolway, J.R. Corman, and J.S. Read (2016), LakeMetabolizer—An R package for estimating lake metabolism from free-water oxygen using diverse statistical models, *Inland Waters*, 6(4), 622-636. http://doi.org/10.1080/IW-6.4.883

Yoon, T.K., H. Jin, N.H. Oh, and J.H. Park (2017), Technical note—Assessing gas equilibration systems for continuous pCO2 measurements in inland waters, *Biogeosciences*, 13, 3915-3930. http://doi.org/10.5194/bg-13-3915-2016

Yurek, S., D.L. DeAngelis, J.C. Trexler, J.A. Klassen, and L.G. Larsen (2016), Persistence and diversity of directional landscape connectivity improves biomass pulsing in simulations of expanding and contracting wetlands, *Ecological Complexity*, 28, 1-11. http://doi.org/10.1016/j.ecocom.2016.08.004

Yvon-Durocher, G., J.M. Caffrey, A. Cescatti, M. Dossena, P. del Giorgio, J.M. Gasol, J.M. Montoya, J. Pumpanen, P.A. Staehr, M. Trimmer, G. Woodward, and A.P. Allen (2012), Reconciling the temperature dependence of respiration across timescales and ecosystem types, *Nature*, 487(7408), 472-476. http://doi.org/10.1038/nature11205

Zarfl, C., A.E. Lumsdon, J. Berlekamp, L. Tydecks, and K. Tockner (2015), A global boom in hydropower dam construction, *Aquatic Sciences*, 77(1), 161-170. http://doi.org/10.1007/s00027-014-0377-0

Zhang, M., N. Liu, R. Harper, Q. Li, K. Liu, X. Wei, D. Ning, Y. Hou, S. Liu (2017), A global review on hydrological responses to forest change across multiple spatial scales: Importance of scale, climate, forest type and hydrological regime, *Journal of Hydrology*, 546, 44-59. http://doi.org/10.1016/j.jhydrol.2016.12.040

Zuijdgeest, A., S. Baumgartner, and B. Wehrli (2016), Hysteresis effects in organic matter turnover in a tropical floodplain during a flood cycle, *Biogeochemistry*, 131, 49-63. http://10.1007/s10533-016-0263-z

Chapter 2

Methane-derived carbon gas fluxes from a tropical flood-pulse lake

Benjamin L. Miller[1]

Gordon W. Holtgrieve[1]

Mauricio E. Arias[2]

Sophorn Uy[3]

Chheng Phen[4]

1. University of Washington School of Aquatic and Fishery Sciences
2. University of South Florida Department of Civil and Environmental Engineering
3. Inland Fisheries Research and Development Institute of Cambodia
4. Fisheries Administration of Cambodia

1.0 Abstract

The oversaturation and resulting flux of carbon dioxide (CO_2) to the atmosphere within lakes and rivers worldwide has long been attributed to terrestrial-aquatic transfers of inorganic and organic C and subsequent, *in-situ* aerobic respiration. However, anaerobic respiration such as methane production (methanogenesis) and oxidation also results in dissolved CO_2. Tropical rivers like the Mekong have a distinct flood-pulse hydrology, seasonally inundating large floodplains and establishing reducing conditions over thousands of km^2. Incorporating anaerobic respiration from seasonally inundated floodplains may reframe the nature of CO_2 oversaturation within inland waters and challenge our understanding of terrestrial-aquatic transfers, thought to comprise 60 % of terrestrial net ecosystem production. Cambodia's Tonle Sap Lake (TSL) is a little studied flood-pulse ecosystem that inundates >9,000 km^2 of floodplain annually. We hypothesized that CO_2 oversaturation would arise in part from CH_4 production and oxidation in this reduced ecosystem during the high-water flood stage. We also predicted that net heterotrophy and diffusive fluxes of CO_2 and CH_4 would differ by flood stage and lake environment, and show a positive relationship to the amount of time that the TSL floodplain was inundated. We measured the concentrations of respiratory gases (O_2, CO_2, CH_4) and isotopic composition of CO_2 and CH_4 during different flood stages in the TSL. We used these data to model aerobic ecosystem metabolism and diffusive fluxes of CO_2 and CH_4 from TSL to the atmosphere. Stable C isotopes demonstrate that 67-97 % of dissolved CO_2 was derived from oxidation of CH_4. Dissolved CO_2 and CH_4 were unrelated to aerobic respiration and inundation time, which shared a strong, negative relationship. CO_2 and CH_4 diffusion varied with local shifts towards reducing conditions and availability of dissolved O_2 and NO_3^- as electron acceptors. The flood-pulse increased net heterotrophy and diffusion, from 3,700 ±500 mg C-

CO_2 m^{-2} d^{-1} and 0.5 ±0.2 mg C-CH_4 m^{-2} d^{-1} during the rising-water stage to 10,000 ±1,000 mg C-CO_2 m^{-2} d^{-1} and 110 ±40 mg C-CH_4 m^{-2} d^{-1} during the high-water stage. These data highlight that anaerobic metabolism can play a key role in the oversaturation and diffusive flux of CO_2 within inland waters, particularly when these waters expand across the terrestrial landscape.

2.0 Introduction

Globally, most lakes are oversaturated with dissolved carbon dioxide (CO_2) relative to atmospheric concentrations, and few are within ±20 % of atmospheric equilibrium (Cole et al., 1994; Tranvik et al., 2009). Most rivers are also a source of CO_2 to the atmosphere (Park et al., 1969; Raymond et al., 2013). This oversaturation has been attributed to transfers of terrestrial net ecosystem production to aquatic ecosystems (Richey et al., 1988; Kling et al., 1991). Of 4.5 net petagrams of C per year (Pg C y^{-1}) that are fixed by terrestrial ecosystems, 2.7 Pg C y^{-1} are transferred to lakes and rivers (Battin et al., 2009). This transfer can take the form of respiratory CO_2 dissolved within terrestrial ground- and surface waters (Richey et al., 1988; Kling et al., 1991; Jones and Mulholland, 1998), or organic C that is subsequently respired within lakes and rivers (del Giorgio et al., 1999; Cole et al., 2001; Raymond et al., 2016). Of the 2.7 Pg C y^{-1} transferred to lakes and rivers, 2.0 Pg C are returned to the atmosphere each year from the surface of these inland waters (Tarnocai et al., 2009). Accounting for terrestrial-aquatic transfers of C in global mass balances therefore decreases terrestrial net ecosystem production by 60 %.

Tropical rivers contribute disproportionately to these global mass balances (Raymond et al., 2013). The Amazon River alone is responsible for >20 % of mean annual riverine discharge (Ward et al., 2015). Yet, few studies focus on the mechanisms of terrestrial-aquatic transfers and respiration of C by tropical rivers relative to temperate watersheds (Raymond et al., 2013), with

most of these conducted in one watershed, the Amazon (Richey et al., 1988; Devol et al., 1988; Mayorga et al., 2005; see Borges et al., 2015 for a notable exception in the Congo).

Terrestrial-aquatic transfers and respiration of C in tropical rivers are likely influenced by their unique hydrology. Temperature and solar irradiance are relatively constant in tropical ecosystems, leaving changes in precipitation as the primary physical variable affecting these watersheds on an annual basis (Winemiller et al., 2014). Along the Intertropical Convergence Zone, precipitation is often monsoonal and predictable, causing similarly predictable expansion and contraction of rivers over their surrounding terrestrial landscapes. "Intermittently flooded land" makes up 10 % of continental surface area, with floodplains associated with tropical rivers and lakes constituting an even smaller share (Downing, 2009; Abril and Borges, 2019). This means that a small amount of continental surface area is potentially highly reactive for terrestrial-aquatic transfers and respiration of C.

Junk et al. (1989) first characterized the predictable annual flooding of tropical rivers across their floodplains and the blurring of classical aquatic and terrestrial boundaries as the Flood-pulse Concept (FPC). Junk et al. (1989) hypothesized that, as river waters inundate floodplain soils, methanogenesis and other forms of anaerobic respiration will become up-regulated. During floodplain inundation, steadily increasing CH_4 diffusion as redox conditions conducive to its production develop has been observed (Bianchi et al., 1996; Hamilton et al., 1997). Vertical and horizontal redox gradients have also been observed in the Amazon (Richey et al., 1988), Pantanal (Devol et al., 1995; Hamilton et al., 1997), Mekong (Holtgrieve et al., 2013), and other tropical watersheds, and with them the anaerobic respiration of floodplain organic C. Richey et al. (1988) estimated that 50 % of Amazonian organic C respiration is anaerobic. Others have estimated that methanogenesis and other forms of anaerobic respiration

comprise 30-80 % of bacterial production in temperate lakes (Rudd and Hamilton, 1978; Fallon et al., 1980; Kuivila et al., 1988; Bedard and Knowles, 1991). Methanogenesis rates are highly correlated to temperature, and may be higher and more persistent in the tropics (Yvon-Durocher et al., 2012; Yvon-Durocher et al., 2014). However, none have quantified the relative contribution of methanogenesis to dissolved C gases and atmospheric fluxes throughout the flood-pulse in large tropical rivers.

The Mekong River is a dramatic example of a flood-pulse ecosystem. Each June through September, monsoonal rains in this watershed increase water levels by up to 15 m, and discharge from 16,000 m^3 s^{-1} to 39,000 m^3 s^{-1} (Arias et al., 2013). Increases in discharge in the lower Mekong cause flows in one tributary, the Tonle Sap River, to reverse from southeast to northwest, flooding Tonle Sap Lake (TSL). During the TSL flood-pulse, lake depths increase by up to 7 m and surface area increases five-fold, from approximately 3,000 km^2 to 15,000 km^2 (Holtgrieve et al., 2013). It is largely unknown how dissolved C gases, atmospheric fluxes, and ecosystem metabolism vary throughout the flood-pulse, and between flood-pulse lakes and their floodplains. Holtgrieve et al. (2013) show that respiration is consistently greater than primary production (i.e., net heterotrophy) throughout the flood-pulse in TSL, and that rates of primary production change little over the flood-pulse. However, they present no metabolism estimates from different environments created by the TSL flood-pulse for comparison, nor do they include information on dissolved C gases and atmospheric fluxes during different flood stages.

Until recently, the Mekong was one of the world's last, largely free-flowing tropical flood-pulse rivers (Stone et al., 2011; Hetch et al., 2019). Arias et al. (2013) project that a combination of climate change and hydropower development on the Mekong will decrease

flood-pulse extent in TSL by 60 ±30 %. This makes understanding how the lake's natural flooding transfers C timely and important.

To determine how this dramatic seasonal hydrologic regime drives aerobic and anaerobic respiration, we measured the concentrations and isotopic composition of respiratory gases (O_2, CO_2, CH_4) during different stages of the TSL flood-pulse, and across different lake environments. We hypothesized that CH_4 production and oxidation during the high-water stage of the flood-pulse would contribute to the lake's oversaturation in CO_2, and the subsequent diffusion of this gas to the atmosphere. We further predicted that net heterotrophy, dissolved C gases, and their diffusive fluxes to the atmosphere would increase with water levels and floodplain inundation. We find that a high percentage of dissolved CO_2 sampled was derived from CH_4. We also show that the expanse of the flood-pulse over floodplain environments during the high-water stage results in sharp increases in ecosystem respiration and diffusive fluxes of CO_2 and CH_4 to the atmosphere. These results highlight that widespread oversaturation of CO_2 within inland waters and resulting atmospheric fluxes may arise in part from anaerobic metabolism.

3.0 Methods

3.1 Sampling Locations

Field sampling occurred during the rising-water, high-water, and falling-water stages of two annual flood-pulses, from September 2014 to September 2016. Lake level data—by which broad flood stages are defined—have been collected from a gauging station at Kampong Luong since 1990 (Figure 1). The rising-water stage of the flood-pulse is characterized by increasing discharge in the Mekong as a result of the monsoon, and course-reversal of the Tonle Sap River from downstream to upstream into TSL from May through September of each year. Lake level

and area reach their maximum in October and November, the high-water stage. Floodwaters contract or "fall" from December through April.

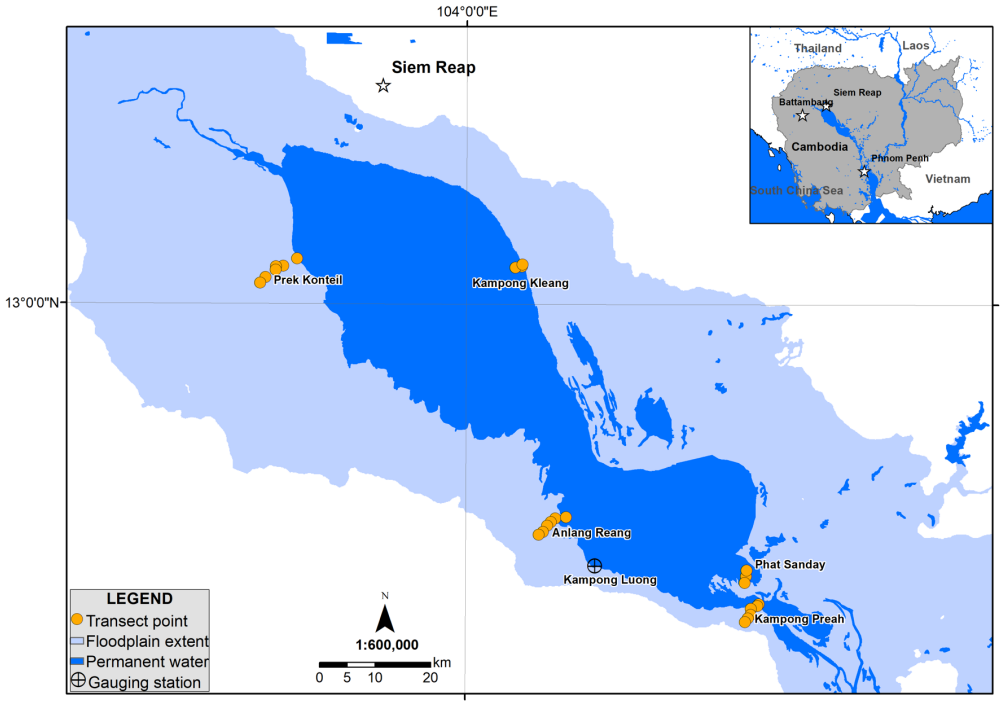

Figure 1. Sampling locations and location of the gauging station at Kampong Luong in TSL, Cambodia, with relative extent of lake and floodplain environments.

Lake sampling focused on three, core locations broadly corresponding to the southwest (Kampong Preah), central (Anlang Reang) and northwest (Prek Konteil) regions of the lake basin (Figure 1). Each of these sampling locations consisted of a transect of six points extending from the open water environment (Transect Point 1), through the edge environment (Transect Point 2) and into the floodplain (Transect Points 4-6). The edge environment is characterized by a transition from the open water environment to rooted terrestrial floodplain vegetation. Two additional locations were sampled for greater spatial coverage corresponding to the southeast (Phat Sanday) and northeast (Kampong Kleang) region of the lake; these locations consisted of three transect points at open water, transitional edge, and floodplain environments. Where water

depth exceeded 0.5 m, discrete samples were drawn from both 0.1 m below the water surface and at 0.5 m above the lake bottom.

3.2 Dissolved Carbon Gases

At each sampling event, partial pressures of CO_2 and CH_4 were quantified as the average of three 74 mL gas-tight serum bottles of water collected at each site and depth. To avoid pseudo-replication in statistical analyses, averaged values measured at each site, depth, and flood stage were considered a single value for that site, depth, and flood stage. Single values across the five sampling locations were considered "true" replicates (n=5). The same applies to all sampling described hereafter.

Samples (n=83, total) were preserved in the field with 74 uL of 50 % m/v zinc chloride solution and placed on ice for transport to the Royal University of Phnom Penh Department of Chemistry where they were stored at 4° C until analysis. For analysis, samples were displaced with helium to roughly equal parts headspace and water, left to equilibrate for 12 h, and analyzed for headspace CO_2 and CH_4 using a gas chromatograph with a flame ionization detector (FID) and nitrogen carrier (SRI 8610*c* GC). Prior to sample analysis, standard curves were generated using 305.0 and 2,030.0 ppm CO_2 in balance with nitrogen and 10.1, 50.5, and 497.0 ppm CH_4 in balance with nitrogen.

3.3 Isotopic Composition of Dissolved Carbon Gases

Following analysis for dissolved C gases, a subset of samples (n=47) from the transects at Prek Konteil, Anlang Reang, and Kampong Preah during high- and falling-water stages of the flood-pulse were inverted, placed on ice, and transported to the University of Washington for isotopic analysis. A 1 mL headspace sample was analyzed for $^{13}C/^{12}C$ of CO_2 and CH_4 simultaneously using a cavity ring-down spectrometer (Picarro G2201*i*) with a small sample

introduction module (Picarro A0314 SSIM, School of Environmental and Forest Sciences). Isotopic compositions of C-CO_2 and C-CH_4 are reported in delta notation following the equation:

$$\delta^{13}C = \left(\frac{R_{sample}}{R_{standard}} - 1\right) \times 10^3 \quad (1)$$

Where $\delta^{13}C$ is the isotopic signature of dissolved C-CO_2 or C-CH_4 in units of per mil (‰), R_{sample} is the ratio of heavy to light isotope in the samples ($^{13}C/^{12}C$ of CO_2 or CH_4), and $R_{standard}$ is the $^{13}C/^{12}C$ value of Vienna Pee Dee Belemnite standard (VPDB equal to 98.9:1.1).

The respiratory C gases resulting from methanogenesis are extremely depleted in ^{13}C relative to other sources of these gases in aquatic ecosystems, such as the aerobic respiration of phytoplankton, periphyton, macrophytes, and terrestrial C_3 and C_4 plants (Hedges, 1986; Whiticar and Faber, 1986; Hecky and Hesslein, 1995; Vuorio et al., 2006). This extreme depletion results from discrimination against ^{13}C in favor of ^{12}C during acetate fermentation and carbonate reduction, the two primary methanogenic pathways (Whiticar, 1999). Magnitudes of this fractionation vary by methanogenic pathway, which is easily distinguishable using the difference fraction factor, ε_C, between δ^{13}C-CO_2 and δ^{13}C-CH_4 (simply, δ^{13}C-CO_2 minus δ^{13}C-CH_4; Whiticar, 1999). The isotopic composition of C-CH_4 and C-CO_2 produced during methanogenesis by acetate fermentation have a ε_C values ranging from 39 to 58 ‰. For methanogenesis by carbonate reduction, which is less common in freshwaters and associated with substrate depletion, ε_C ranges from 49 to 95 ‰ (Whiticar, 1999). For oxidation of CH_4 to CO_2, ε_C ranges from <5 to 30 ‰ (Whiticar, 1999).

To verify methanogenic pathway, we also calculated the apparent fractionation factor, α_{app}, during methanogenesis following Conrad (2005):

$$\alpha_{app} = \frac{(R_{CO_2})}{(R_{CH_4})} \quad (2)$$

where values of α_{app} <1.06 indicate methanogenesis by acetate fermentation and values >1.06 indicate carbonate reduction.

3.4 Carbon Gas Fluxes

Net diffusive fluxes of CO_2 and CH_4 (mg C m^{-2} d^{-1}) from TSL to the atmosphere were modeled using surface water partial pressures and the thin boundary-layer equation:

$$F_E = k \times K_H(pGas_w - pGas_a) \quad (3)$$

where k is the gas transfer velocity (cm h^{-1}), $pGas_w$ is the partial pressure of a gas in water (µatm), $pGas_a$ is the partial pressure of a gas in water at equilibrium with ambient air (µatm), and K_H is a water temperature-dependent Henry's constant (mmol kg^{-1} atm^{-1}; Wilhelm et al., 1977) (n=83). The gas transfer velocity, k (cm h^{-1}), was determined using the following relationships:

$$k = k_{600}\left(\frac{Sc}{600}\right)^{-0.66} \quad (4)$$

$$Sc = a - bT + cT^2 - dT^3 \quad (5)$$

where Sc is the Schmidt number, T is the water temperature (ºC), a, b, c, and d are dimensionless constants for CO_2 and CH_4 (Wanninkhof, 1992; Crusius and Wanninkhof, 2003), and k_{600} (cm h^{-1}) is the gas transfer velocity at a Schmidt number of 600. Although Crusius and Wanninkhof (2003) assume a k_{600} of 1.0 cm h^{-1} at wind speeds <3.7 m s^{-1}, k_{600} was calculated using wind speed following Cole and Caracao (1998):

$$k_{600} = 2.07 + 0.215\,(U_{10})^{1.7} \quad (6)$$

where U_{10} is the wind speed at 10 m above the water surface. Wind speed was measured from a height of 10 m every 30 minutes at Phnom Penh International Airport, the site of the only continuous, archived wind speed measurements in Cambodia. Daily means and standard deviations of windspeed were run through 10,000 Monte Carlo simulations in R, and the error from these simulations was applied to flux estimates following Taylor (1997).

Importantly, our study omits CH_4 bubbling or ebullition, shown to be a large fraction of total CH_4 emissions from inland waters in recent years (Joyce and Jewel, 2003; Del Sontro et al., 2011). Omission was based on logistical constraints and tested hypotheses. The mean water depth of our sampling locations was 0.6 m, precluding the 2-m inverted funnels typically used to measure ebullition in lakes (though Crawford et al., 2014 presents a novel construction for ebullition measurements in shallow streams). In addition, oxidation of CH_4 within bubbles is minimal during their rapid ascent from sediments to the surface means that oxidation (Ostrovsky et al., 2008), meaning that they unlikely to contribute to dissolved CO_2 in the water column.

3.5 Dissolved Oxygen

Dissolved O_2 (mg L^{-1}) and water temperature (°C) at each site and depth were quantified using a multi-parameter sonde calibrated just prior to sampling with water-saturated air (YSI 6920) (*n*=279). Additionally, we collected water samples (*n*=83) to measure the ratio of dissolved O_2 to argon (Ar) at a subset of sites and depths during the rising-, high-, and falling-water stages of the flood-pulse. Dissolved O_2 and Ar occur in the atmosphere at a ratio of approximately 22.5 to 1, with *in-situ* production and respiration in water increasing and decreasing this ratio, allowing the ratio to be used as an indicator for metabolic state. Samples were collected using 12 mL exetainers (Labco) pre-sparged with helium and submerged completely to avoid interference by atmospheric O_2, killed with 12 uL of of 50 % m/v zinc chloride solution, inverted, placed on ice, and transported to the University of Washington for analysis using a continuous flow isotope ratio mass spectrometer following Holtgrieve et al. (2010) (ThermoFisher Scientific Delta V IRMS, School of Oceanography).

We also deployed continuously logging dissolved O_2 (mg L^{-1}) and water temperature (°C) sensors for a minimum of 20 h in open, edge, and floodplain environments of Prek Konteil,

Anlang Reang, and Kampong Preah during the rising-, high-, and falling-water stages of the flood-pulse (n=24). We modeled the ecosystem metabolic parameters aerobic gross primary production (*GPP*), aerobic ecosystem respiration (*ER*), and aerobic net ecosystem production (*NEP*) using these diel data in the "LakeMetabolizer" R package (Winslow et al., 2016; R Core Team, 2019). Model inputs include hourly dissolved oxygen (mg L^{-1}), hourly water temperature (°C), and hourly photon flux for photosynthetically active radiation (PAR; uE s^{-1} m^{-2}). The model performs maximum likelihood parameter estimation for *GPP* per unit PAR and *ER* per unit log-transformed water temperature, as well as the variance of observational and process error. It incorporates a log-linear light saturation function, an Arrhenius temperature dependence for respiration, and k_{600} for reaeration of dissolved O_2 using windspeed following Cole and Caraco (1998). PAR was not measured directly, but calculated from full-spectrum irradiance based on latitude, longitude, aspect, slope, transmissivity data and the "astrocalc4r" function in the "fishmethods" R package (Gates, 1966; Jellison and Melack, 1993; Nelson, 2019; R Core Team, 2019).

3.6 Hypothesis Tests

All hypothesis tests were conducted using the statistical and data visualization software R (R Core Team, 2019). We assessed normality in the data using quantile-quantile plots and Shapiro-Wilk Tests, and heteroscedasticity in the data using Bartlett Tests for Homogeneity of Variance. Partial pressures and diffusive fluxes of CO_2 and CH_4 followed non-normal distributions with unequal variances. We compared mean partial pressures and diffusive fluxes across sites and flood stages using non-parametric Wilcoxon Rank-sum Tests. We used a Bonferroni correction to initial critical α-values of 0.05 in order to compensate for loss in

statistical power over subsequent comparisons (Zar, 2010). The corrected α for comparisons between flood stages and sampling environments was 0.025.

To assess whether differences between means were independent of sample size and ecologically as well as statistically significant, we calculated effect sizes following Cohen (1988):

$$d = \frac{\mu_i - \mu_j}{\sqrt{\frac{\sigma_i^2 + \sigma_j^2}{2}}} \quad (8)$$

Where d is a descriptive measure corresponding to a small (0.0-0.4), medium (0.5-0.7), or large (0.8-2.0) effect size, $\mu_{i,j}$ is the mean, and $\sigma_{i,j}$ is the standard deviation. Large effect sizes are considered ecologically significant. Absolute Cohen's *d*-values for effect size are reported with each α-value.

We investigated controls on net CO_2 and CH_4 diffusion during the high-water stage of the flood-pulse using mixed effects models. Mixed effects models allowed our heteroscedastic data to vary independently across the random effects of site. The slope of each fixed effect relative to each random effect was also allowed to vary independently following Bates et al. (2015):

$$y_i = \beta_{0,i} + \beta_i x_i \ldots + (1 \mid g_i) + (0 + x_i \mid g_i) \ldots + \varepsilon_y \quad (9)$$

Where y_i is diffusive flux of CO_2 or CH_4, $\beta_{0,i}$ is the intercept of y_i, β_i is the coefficient for each effect, x_i, and g_i is a random effect, site, and ε_y is the error associated with y_i. Small sample size-corrected Akaike Information Criterion (AIC_C) was used for model selection following Burnham and Anderson (2004). The likelihood of each model in describing CO_2 and CH_4 diffusion relative to the other models was expressed in terms of ΔAIC_c and ΔAIC_c weight, w_i, following Burnham and Anderson (2004):

$$\Delta AIC_c = AIC_{c,i} - AIC_{c,min} \quad (10)$$

$$w_i = \frac{e^{-0.5\Delta AIC_{c,i}}}{\sum e^{-0.5\Delta AIC_{c,i}}} \quad (11)$$

Where $AIC_{c,min}$ is the lowest AIC_c value in a group of candidate models. Information on all model covariates, including election acceptors, nutrients, chlorophyll, and inundation time, is included in Appendix 2A.

4.0 Results

4.1 Dissolved Gas Partial Pressures by Flood Stage

Aqueous PCO_2 at all sites was above atmospheric equilibrium throughout the flood-pulse, but increased sharply from 4,700 ±500 uatm during the rising-water stage to 12,000 ±1,000 uatm during the high-water stage (p<0.001, d=1.5) (Table 2; Figure 2a). PCO_2 over the course of the flood-pulse showed a second increase during falling-water in March, when some of the highest partial pressures of this gas were measured, though this change was not significant from the previous stage. Aqueous PCH_4 also increased sharply from 50 ±20 uatm during the rising-water stage to 9,000 ±4,000 uatm during the high-water stage (p<0.001, d=0.9) (Figure 2b). Despite relatively high PCH_4, near-atmospheric equilibrium (~1.9 ±1 uatm) was measured at 25 % of sites sampled during the rising and falling water stages of the flood-pulse.

Table 2. Mean aqueous partial pressures (uatm) ±SE, diffusive fluxes (mg C m^{-2} d^{-1}) ±SE, and k_{600} (cm h^{-1}) ±SE for CO_2 and CH_4 at the surface of TSL in open-water, edge, and floodplain environments during the rising-, high-, and falling-water stages of the flood-pulse. Wilcoxon *p*-values for statistical differences and absolute Cohen's *d*-values for effect sizes are shown for pairwise comparisons across environments and flood stages. Means that are significantly different according to the Bonferroni-corrected α of 0.025 with low, medium, and high effect size are starred.

	k_{600} (cm h^{-1})	PCO_2 (uatm)	CO_2 Diffusion (mg C m^{-2} d^{-1})	PCH_4 (uatm)	CH_4 Diffusion (mg C m^{-2} d^{-1})	*n*
Rising	2.51 ±0.02	4700 ±500	3700 ±500	50 ±20	0.5 ±0.2	20
Open	2.50 ±0.04	3800 ±600	2900 ±500	20 ±9	0.19 ±0.08	7
Edge	2.55 ±0.03	5000 ±1000	4000 ±1000	30 ±10	0.2 ±0.1	6
Floodplain	2.48 ±0.02	6000 ±1000	4500 ±900	110 ±50	1.2 ±0.5	7
Open, Edge						
Edge, Floodplain						
Open, Floodplain				*p*= 0.025, *d*=1.0***	*p*=0.025, *d*=1.0***	
High	2.71 ±0.04	12000 ±1000	10000 ±1000	9000 ±4000	110 ±40	18
Open	2.72 ±0.05	14000 ±1000	12000 ±1000	5000 ±2000	50 ±20	3
Edge	2.71 ±0.06	13000 ±2000	11000 ±2000	19000 ±9000	200 ±100	3
Floodplain	2.71 ±0.03	12000 ±1000	10000 ±900	9000 ±2000	100 ±20	12
Open, Edge						
Edge, Floodplain						
Open, Floodplain						
Falling	2.47 ±0.02	9000 ±2000	7000 ±2000	400 ±300	4 ±3	22
Open	2.47 ±0.01	8000 ±1000	6000 ±1000	30 ±10	0.3 ±0.1	10
Edge	2.47 ±0.02	10000 ±2000	8000 ±2000	900 ±400	9 ±4	9
Floodplain	2.440 ±0.001	5100 ±400	3600 ±300	19 ±4	0.17 ±0.04	3
Open, Edge						
Edge, Floodplain						
Open, Floodplain						
Rising, High	*p*<0.001, *d*=1.5***	*p*<0.001, *d*=1.6***	*p*<0.001, *d*=1.6***	*p*<0.001, *d*=0.9***	*p*<0.001, *d*=0.9***	
High, Falling	*p*<0.001, *d*=1.8***	p=0.029, *d*=0.4	*p*=0.015, *d*=0.5**	*p*<0.001, *d*=0.8***	*p*<0.001, *d*=0.8***	
Rising, Falling						

Statistically different with low effect size (*d*=0.0-0.4)*, medium effect size (*d*=0.5-0.7)**, and high effect size (*d*≥0.8)***

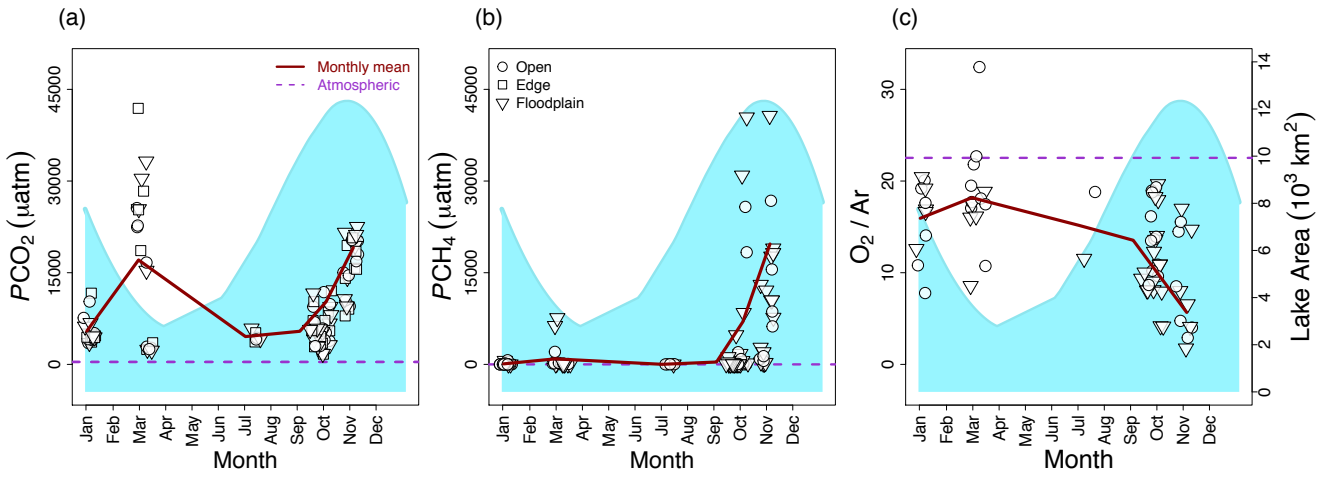

Figure 2. **(a)** Aqueous PCO_2 (uatm), **(b)** aqueous PCH_4 (uatm), and **(c)** O_2 / Ar (± SE) in open, edge, and floodplain environments of TSL throughout the flood-pulse. Historic lake area (from 2007, in 10^3 km^2) throughout the flood-pulse estimated from water levels recorded from the Kampong Luong gauging station is shown on a secondary *y*-axis. A red trendline follows monthly means for these values, and a purple dashed line marks atmospheric equilibrium.

Sharp increases in PCO_2 and PCH_4 during the high-water stage coincided with a substantial decline in dissolved oxygen (O_2; Figure 2c). O_2/Ar of <22.5 indicated net heterotrophy throughout the flood-pulse, but decreased significantly from the rising- to high-water stage (p<0.001, d=0.9) (Figure 2c). By contrast, the sharp increase in PCO_2 during the falling-water stage coincided with a similar increase in O_2/Ar to near atmospheric equilibrium.

4.2 Sources of Dissolved Gases by Flood Stage

Dissolved CO_2 was decoupled from dissolved O_2 during all flood stages. An equimolar consumption of dissolved O_2 and production of dissolved CO_2 is expected in aquatic ecosystems during *in-situ* aerobic respiration under steady state conditions (m=-1.0). By contrast, there were approximately 0.6 mmol O_2 L^{-1} consumed for each mmol CO_2 produced in TSL during the rising-water stage of the flood-pulse, and very little of this O_2 deficit could account for the excess CO_2 measured during the high- and falling-water stages (Figure 3).

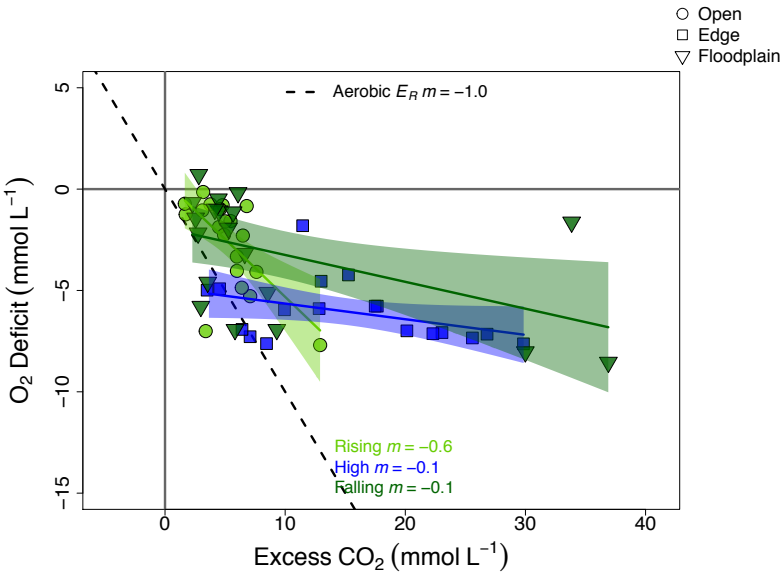

Figure 3. Dissolved O_2 deficit and excess dissolved CO_2 relative to atmospheric equilibrium in open, edge, and floodplain environments of TSL during the rising-, high-, and falling water stages of the flood-pulse. Grey lines show atmospheric equilibrium at 0 mmol L^{-1} excess CO_2 or O_2 deficit. A slope (*m*) of -1.0 for represents the equimolar consumption of dissolved O_2 and production of dissolved CO_2 expected during *in-situ* aerobic respiration (black dashed line). Subsequent *m*-values for the rising-, high-, and falling-water stages of the flood-pulse likewise represent mmol O_2 L^{-1} consumed in the numerator for each mmol CO_2 L^{-1} produced in the denominator.

Nearly all aqueous PCO_2 measured at Prek Konteil, Anlang Reang, and Kampong Preah during the high- and falling-water stages of the flood-pulse was highly depleted in ^{13}C relative to other sources of this gas in aquatic ecosystems. Here, we define high relative depletion of $\delta^{13}C$-CO_2 as <-35 ‰. During the high-water stage, $\delta^{13}C$-CO_2 ranged from -78 ‰ to -11 ‰, with few values above -35 ‰ (n=5 of 30) (Figure 4a). During the high-water stage, there was also a strong relationship between $\delta^{13}C$-CO_2 and aqueous PCH_4 (R^2=0.41, p<0.001). During the falling-water stage, $\delta^{13}C$-CO_2 ranged from -49 ‰ to -31 ‰, with 42 % of values above -35 ‰ (n=7 of 12) (Figure 4b).

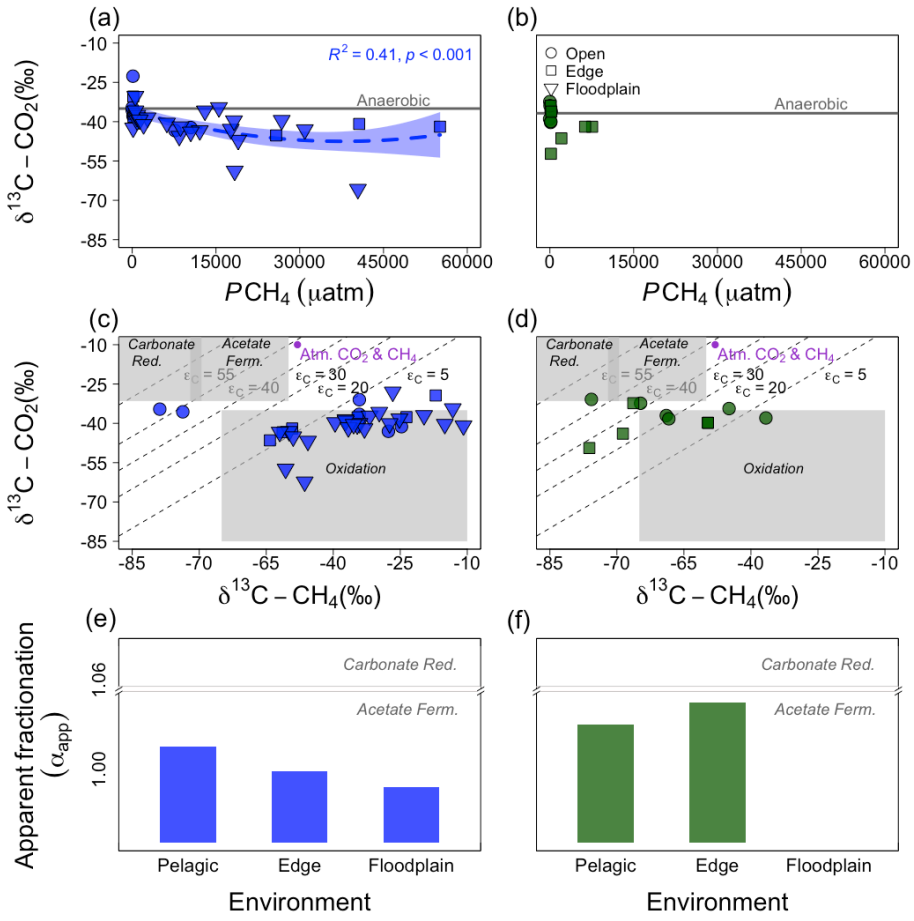

Figure 4. Relationships between δ^{13}C-CO_2 and PCH_4 measured in open, edge, and floodplain environments at Prek Konteil, Anlang Reang, and Kampong Preah during the **(a)** high- and **(b)** falling-water stages of the flood-pulse. A grey line marks depletion of δ^{13}C-CO_2 at -35 ‰, values below which indicate an anaerobic or methanogenic origin. δ^{13}C-CO_2 and δ^{13}C-CH_4, as well as the differences between the two (δ^{13}C-CO_2 – δ^{13}C-CH_4, or ε_C), are shown for **(c)** high- and **(d)** falling-water stages of the flood-pulse. Zones of CH_4 oxidation, methanogenesis by acetate fermentation, and methanogenesis by carbonate reduction are shaded in grey. The apparent fraction (α_{app}) between δ^{13}C-CO_2 and δ^{13}C-CH_4 during methanogenesis in open, edge, and floodplain environments during the **(e)** high- and **(f)** falling-water stages of the flood-pulse are also shown.

Nearly all aqueous PCH_4 measured at Prek Konteil, Anlang Reang, and Kampong Preah during the high- and falling-water stages of the flood-pulse was enriched in ^{13}C relative to values expected from the two primary methanogenic pathways. The δ^{13}C-CH_4 produced via the acetate fermentation pathway of methanogenesis ranges from -65 to -50 ‰, while carbonate reduction

produces δ^{13}C-CH_4 ranging from -110 to -60 ‰ (Whiticar and Faber, 1986). During the high-water stage, δ^{13}C-CH_4 ranged from -78 ‰ to as high as -11 ‰, with few values below -50 ‰ (n=6 of 35), indicating oxidation of CH_4. All values below -50 ‰ were sampled along the Anlang Reang transect. During the falling-water stage, δ^{13}C-CH_4 was considerably more depleted and ranged from -94 ‰ to -38 ‰, with most values below -50 ‰ (n=8 of 12). This corresponded with less depletion in the δ^{13}C-CO_2 during this stage.

Differences between δ^{13}C-CO_2 and δ^{13}C-CH_4, or ε_C values, of <31 ‰ also indicated oxidation of CH_4 (Barker and Fritz, 1981; Whiticar, 1999). During the high-water stage, 97 % of ε_C values were <31 ‰ (Figure 4c). This proportion fell to 67 % of ε_C values <31 ‰ during the falling-water stage of the flood-pulse (Figure 4d). Of the ε_C values above 31 ‰ during the high- and falling-water stages, only one exceeded 58 ‰, indicating acetate fermentation as the predominant methanogenic pathway.

An α_{app} of <1.06 during the high-water stage of the flood-pulse further indicated methanogenesis via acetate fermentation. This α_{app} increased from floodplain to edge to open environments, perhaps as a result of increasing substrate limitation where sites were inundated longer (i.e., open; Figure 4e). During the falling-water stage, increasing α_{app} suggests that acetate became limiting to the production of CH_4 across sampling environments, leading to methanogenic inputs to aqueous $P$$CH_4$ via carbonate reduction (Figure 4f).

4.3 Diffusive CO_2 and CH_4 Fluxes by Flood Stage

Partial pressures of CO_2 above atmospheric equilibrium in surface waters led to net diffusive fluxes from TSL to the atmosphere, ranging from 1,095 to 36,748 mg C-CO_2 m^{-2} d^{-1} (Table 2). The flood-pulse nearly tripled mean CO_2 diffusion, from 3,700 ±500 mg C m^{-2} d^{-1} during the rising-water stage to 10,000 ±1,000 mg C m^{-2} d^{-1} during the high-water stage

(p<0.001, d=1.6) (Figures 5a and 5b). CO_2 diffusion then declined during falling-water (10,000 ±1,000 mg C m^{-2} d^{-1} to 7,000 ±2,000 mg C m^{-2} d^{-1}; p=0.015, d=0.5) to rates not significantly different from those measured during the rising-water stage of the flood-pulse (Figure 5c).

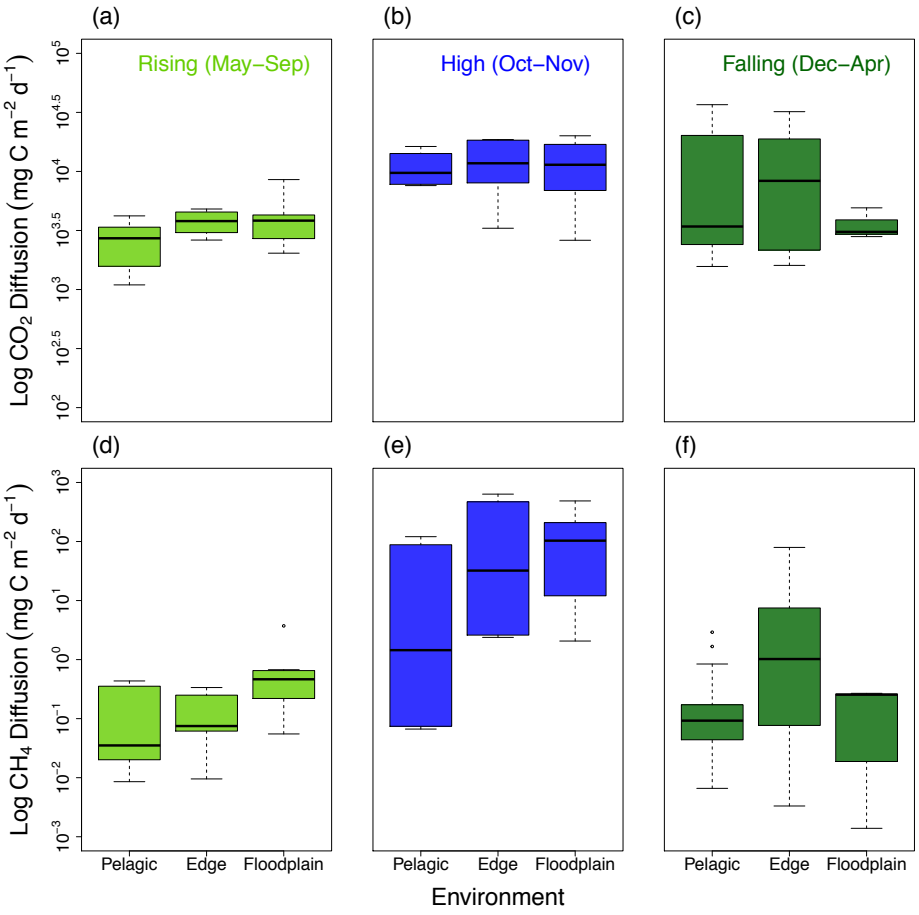

Figure 5. CO_2 diffusion from TSL to the atmosphere. Values are given for open, edge, and floodplain environments during the **(a)** rising- (May-September), **(b)** high- (October-November), and **(c)** falling-water (December-April) stages of the flood-pulse. CH_4 diffusion from Tonle Sap Lake to the atmosphere is also shown for each environment during the **(d)** rising-, **(e)** high-, and **(f)** falling-water stages. CH_4 diffusion during the high-water stage is skewed by high values measured at Prek Konteil and Anlang Reang.

Mean CH_4 diffusion from the lake to the atmosphere was low during the rising-water stage (0.5 ±0.2 mg C m^{-2} d^{-1}), but increased by approximately 21,900 % during the high-water stage to 110 ±40 mg C m^{-2} d^{-1}. As with CO_2, diffusive CH_4 fluxes were significantly greater

during the high-water stage (Figure 5e) than during the rising- ($p<0.001$, $d=0.9$) (Figure 5d) and falling-water ($p<0.001$, $d=0.8$) (Figure 5f) stages. Because partial pressures and diffusive fluxes of CO_2 and CH_4 were not significantly different during the rising- and falling-water stages, they did not appear to follow hysteresis patterns with flood stage; magnitudes were comparable during flood stages with different rising or falling trajectories but identical water levels.

CO_2 and CH_4 diffusion resulted both from large partial pressure gradients between the lake and atmosphere and gas transfer velocities mediated by local meteorological conditions (k_{600}; Table 2). Mean k_{600}, which is dependent on wind speed, increased significantly from rising- to high-water (2.51±0.02 cm h^{-1} to 2.71 ±0.04 cm h^{-1}; $p<0.001$, $d=1.5$). Mean k_{600} decreased significantly from high- to falling-water (2.71 ±0.04 cm h^{-1} to 2.47 ±0.02 cm h^{-1}; $p<0.001$, $d=1.8$).

4.4 Diffusive CO_2 and CH_4 Fluxes by Environment

Both aqueous PCH_4 and resulting CH_4 diffusion were higher on the floodplain than in open environments during the falling-water stage of the flood-pulse ($p=0.025$, $d=1.0$). There were no other significant differences in net diffusive CO_2 and CH_4 fluxes by environment, meaning that there was greater variation in these fluxes by flood stage. Inundation time integrates spatial and temporal elements of the flood-pulse; each of the different environments sampled—open, edge, and floodplain—was inundated by flood waters for different amounts of time. Open environments were located in the main body of TSL, and thus were inundated for periods of time ranging from 281 to 365 days. Edge environments were inundated from 281 to 301 days per year. Floodplain environments experienced the largest range of inundation times as the flood-pulse advanced during the rising-water stage and receded during the falling-water

stage, from 54 to 275 days per year. However, there were no significant relationships between CO_2 and CH_4 diffusion and inundation time (Figures 6a and 6b).

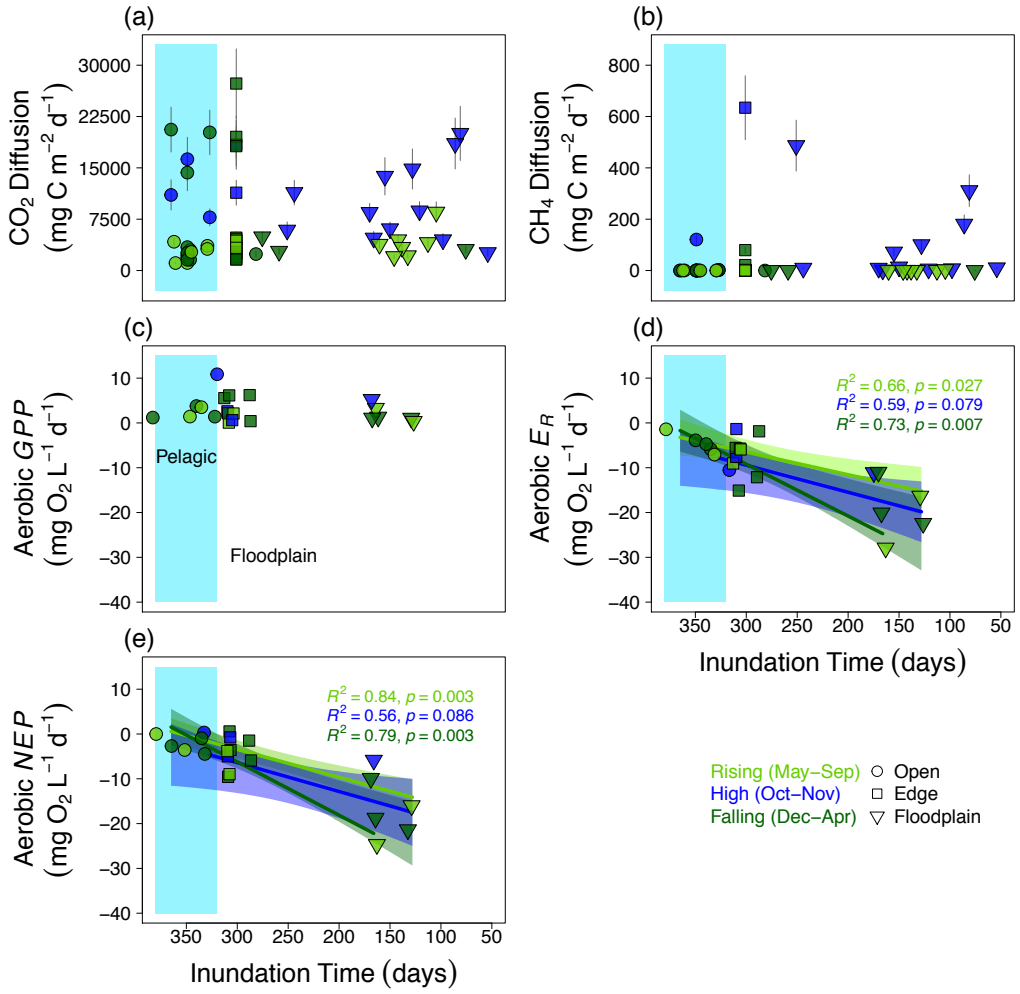

Figure 6. Relationships between **(a)** diffusive CO_2 fluxes, **b)** diffusive CH_4 fluxes, **(c)** aerobic *GPP*, **(d)** aerobic *ER*, **(e)** aerobic *NEP*, and inundation time in open, edge, and floodplain environments of TSL during the rising-, high-, and falling-water stages of the flood-pulse. CO_2 and CH_4 diffusion include errors propagated from variance in aqueous PCO_2, PCH_4, and Monte Carlo simulations of k_{600}.

GPP was also constant throughout the flood-pulse at sites experiencing variable inundation times (Figure 6c). However, there were significant linear model fits between inundation time, aerobic *ER*, and aerobic *NEP* (Figures 6d and 4e). Aerobic *ER* was greatest in floodplain sites inundated for <170 days per year, ranging from -5 to -25 mg O_2 L^{-1} d^{-1} and

driving negative *NEP* (i.e., net heterotrophy). The slopes (*m*) for inundation time and aerobic *NEP* increased as the flood-pulse progressed throughout the rising- (m=0.06, R^2=0.84, p=0.003), high- (m=0.06, R^2=0.56, p=0.086), and falling-water (m=0.12, R^2=0.79, p=0.003) stages. Thus, *ER* and net heterotrophy increased in floodplain environments throughout the flood-pulse.

4.5 Controls on CO_2 and CH_4 Diffusion

Mixed effects modeling at Prek Konteil, Anlang Reang, and Kampong Preah during the high-water stage of the flood-pulse suggested that net diffusive fluxes of CO_2 and CH_4 were most likely controlled by changing redox conditions between bottom and surface waters. AICc model selection revealed that CO_2 diffusion was most strongly related to total manganese concentrations within bottom waters (Mn_{Tot}; AICc weight=0.89, R^2=0.81, p<0.001) (Table S1). Diffusive CO_2 fluxes from the surface of the lake to the atmosphere increased with Mn_{Tot} concentrations within bottom waters (Figure 7a). CH_4 diffusion declined dramatically when dissolved O_2 within surface waters was above 1 mg L^{-1} (AICc weight=0.99, R^2=0.38, p<0.001) (Figure 7b). Diffusive fluxes of both CO_2 and CH_4 were also related to changing bottom water NO_3^- concentrations (AICc weight=0.05, R^2=0.42, p<0.001 for CO_2 and AICc weight=0.005, R^2=0.22, p=0.002 for CH_4). CO_2 and CH_4 diffusion decreased as bottom water NO_3^- concentrations increased. Collectively, these results show that the greatest diffusive fluxes of CO_2 and CH_4 occurred under strongly reducing conditions and lower concentrations of the thermodynamically favorable electron acceptors O_2 and NO_3^-.

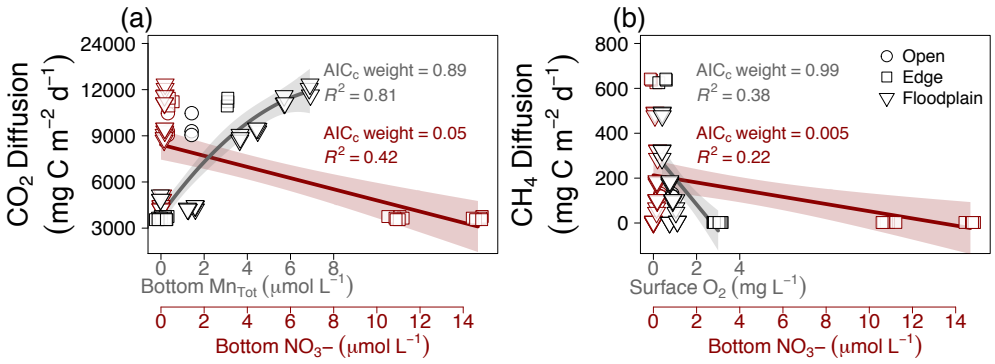

Figure 7. Relationships between **(a)** CO_2 and **(b)** CH_4 diffusion (mg C L^{-1} d^{-1}) and the two most important covariates as indicated by AICc model selection in open, edge, and floodplain environments at Prek Konteil, Anlang Reang, and Kampong Preah during the high-water stage of the flood-pulse. CO_2 and CH_4 diffusion include errors propagated from variance in aqueous PCO_2, PCH_4, and Monte Carlo simulations of k_{600}.

5.0 Discussion

5.1 Respiratory gases (CO_2, CH_4, O_2) show flood-driven net heterotrophy in TSL

Ecologists have attributed supersaturation of inland waters with CO_2 to transfers of this gas from terrestrial groundwaters (Richey et al., 1988; Kling et al., 1991; Jones and Mulholland, 1998), terrestrial surface runoff (Raymond et al., 2016), or respiration of terrestrial organic C *in-situ* (Cole et al., 1994; del Giorgio and Peters, 1994). When "plumbing" the global C cycle, Cole et al. (2007) assumed a unidirectional transfer of C from land to water, and assigned only three fates to this C: Burial within sediments, diffusive flux of CO_2 to the atmosphere, and export to the oceans. Recently, Abril and Borges (2019) proposed the bidirectional expansion and contraction of floodwaters over the terrestrial landscape as a major revision to the "active pipe" model presented by Cole et al. (2007).

Our data, collected from the extensively flooded environments in and around TSL, supports this conceptual revision by showing the importance of the flood-pulse to remineralization of terrestrial organic C through both aerobic and anaerobic pathways. Measurements throughout two annual Lower Mekong and TSL flood-pulses showed that

aqueous PCO_2 increased dramatically with water levels during the high-water stage (Figure 2a). This increase is consistent with results by Richey et al. (2002) from the Amazon River, who document a similar increase in aqueous PCO_2 with water level and floodplain area inundated (2,950 to >44,000 uatm, compared with 1,058 to 44,516 uatm measured by our study; Table 2). Aqueous PCO_2 spanning several orders of magnitude has also been measured in African flood-pulse rivers, ranging from 300 to 16,492 uatm in the Congo (Borges et al., 2015) and from atmospheric equilibrium (400 uatm) to over 12,500 uatm in Senegal's Lukulu River (Zuijdgeest et al., 2016). Though aqueous PCO_2 data from the Amazon closely tracks the hydrograph of this river (Devol et al., 1995), mean aqueous PCO_2 does not decrease immediately during the falling-water stage of the Lukulu River or TSL flood-pulses. Instead, aqueous PCO_2 in the Lukulu remains elevated, and in TSL shows a second sharp increase during the falling-water stage in March, when some of the highest partial pressures of this gas were measured both years of sampling (Figure 2a). The sharp increase in aqueous PCO_2 during the falling-water stage corresponds to a similar increase in O_2/Ar to near atmospheric equilibrium (Figure 2c**)**. An increase in O_2/Ar indicates greater primary production and/or gas exchange. Based on their review of the flood-pulse literature, Miller et al. (*in review*; see Chapter 1) find that receding flood waters consolidate floodplain organic matter and re-oxygenate stratified and hypoxic floodplain water masses, leading to greater respiration. This respiration leads to the release of inorganic nutrients via remineralization, blooms of cyanobacteria and other phytoplankton, and—subsequently—respiration of this new and relatively labile biomass, (Miller et al., *in review*; see Chapter 1).

We hypothesized that diffusive CO_2 and CH_4 fluxes, *GPP*, *ER*, and finally *NEP* would trend with the amount of time sites were submerged, i.e., inundation time. Weak net

heterotrophy in open-water environments together with strong net heterotrophy in floodplain environments established and maintained increasingly negative aerobic *NEP* across a gradient of flooding throughout the flood pulse (Figures 6d and 6e). *GPP* did not change (Figure 6c), which is consistent with previous findings by Holtgrieve et al. (2013). We are aware of no other studies that report aerobic metabolic parameters across a gradient of inundation time in a tropical flood pulse system. Our hypothesis that diffusive C gas fluxes would trend with inundation time along with these aerobic metabolic parameters was not supported by our data (Figures 6a and 6b); anaerobic respiration and changing redox conditions were likely greater controls on diffusion of respiratory C gases at the surface.

5.2 Dissolved CO_2 and its subsequent flux to the atmosphere are derived in large part from oxidation of CH_4

Sharp increases in aqueous PCO_2 during the high-water stage of the flood-pulse in TSL corresponded to similar increases in aqueous PCH_4 (Table 2; Figure 2b). Junk et al. (1989) early predicted that flood-pulse river waters expanding over their surrounding floodplains would create large expanses of saturated and reduced soils, and redox conditions favorable to anaerobic respiration. Such predictions are consistent with findings by early studies in the Amazon by Richey et al. (1988) and Devol et al. (1988), who use balance of dissolved CO_2, CH_4, and O_2 to estimate that anaerobic respiration comprises 50% of total respiration in their study system. Dissolved CO_2 throughout the TSL flood-pulse was out of balance with dissolved O_2 deficits. During the rising-water stage, 0.6 mmol O_2 was consumed for each mmol CO_2 produced (m=0.6 in Figure 3), meaning that 40 % of dissolved CO_2 during rising-water originated from sources other than *in-situ* aerobic respiration. The proportion of dissolved CO_2 originating from sources other than *in-situ* aerobic respiration increased to 90% throughout the high- and falling-water

stages of the flood-pulse (*m*=-0.1 and *m*=-0.1, respectively, in Figure 3). These other sources include the groundwater inputs documented by Richey et al. (1988), Kling et al. (1991), and Jones and Mulholland (1998), the terrestrial surface runoff documented by Raymond et al. (2016) among others, or anaerobic respiration.

Our isotopic data shows that some of the CO_2 supersaturation long observed within inland waters may actually result from *in-situ* production and oxidation of CH_4. Measurements of $\delta^{13}C\text{-}CO_2$ indicated that much of the dissolved CO_2 sampled originated from anaerobic metabolism of organic C to CH_4, and its subsequent oxidation to CO_2. Much of the aqueous PCO_2 measured in open, edge, and floodplain environments at Prek Konteil, Anlang Reang, and Kampong Preah during the high- and falling-water stages of the flood-pulse (86 % and 63 %, respectively) was depleted in $^{13}C/^{12}C$ to -35 ‰ or less, reaching -77 ‰ (mean -41.9 ±0.8 ‰) (Figures 4a and 4b). We attribute this depletion in $^{13}C/^{12}C\text{-}CO_2$ to a methanogenic origin. In a review of isotopic values for different primary producers in tropical and temperate lakes, including unpublished data for phytoplankton, periphyton, macrophytes, and terrestrial plants collected throughout the 2010 flood pulse in TSL by Holtgrieve, none exceed -35 ‰ (Table 3). There is little to no fractionation during respiration; $\delta^{13}C$ values are conserved from C fixation at the base of the food web through higher trophic levels (Emerson and Hedges, 2008). Although some have reported $\delta^{13}C$ values for phytoplankton that exceed -40 ‰ (McCallister and del Giorgio, 2008; De Kluijver et al., 2014), respiratory $\delta^{13}C\text{-}CO_2$ reported for the De Kluiver et al. (2014) dataset is comparatively enriched (-9 to -21 ‰), suggesting that these depleted phytoplankton do not contribute appreciably to dissolved CO_2 relative to terrestrial vegetation in these net heterotrophic lakes. According to these values, aerobic respiration of phytoplankton,

periphyton, macrophytes, and terrestrial C_3 and C_4 plants cannot alone explain the level of $\delta^{13}C$-CO_2 depletion measured in TSL.

Table 3. Ranges of $\delta^{13}C$ (‰) values for phytoplankton, periphyton, macrophytes, terrestrial C_3 plants, and terrestrial C_4 plants measured in tropical and temperate lakes and the Amazon River. Assuming little or no fractionation during respiration, these values would be reflected in any resulting respiratory $\delta^{13}C$-CO_2.

	Location	$\delta^{13}C$ (‰)	Study	*n*
Phytoplankton	Lake Malawi, Africa (Transboundary)	-25 to -21	Hecky and Hesslein, 1995	3
	Tonle Sap Lake, Cambodia	-30 to -19	Holtgrieve, *unpubl.*	6
	Pyhajarvi Lake, Finland	-30 to -6	Vuorio et al., 2006	32
	Koylionjarvi Lake, Finland	-32 to -24	Vuorio et al., 2006	47
	Kirkkojarvi Lake, Finland	-32 to -18	Vuorio et al., 2006	39
	Kuralanjarvi Lake, Finland	-34 to -22	Vuorio et al., 2006	25
Periphyton	Lake Malawi, Africa (Transboundary)	-15 to -8	Hecky and Hesslein, 1995	5
	Tonle Sap Lake, Cambodia	-33 to -21	Holtgrieve, *unpubl.*	17
	ELA 240, Ontario	-20 to -17	Hecky and Hesslein, 1995	4
Macrophytes	Lake Malawi, Africa (Transboundary)	-20 to -10	Hecky and Hesslein, 1995	2
	Lake Kyoga, Uganda	-28 to -12	Hecky and Hesslein, 1995	5
	Amazon River, Brazil	-28 to -12	Hedges et al., 1986	4
	ELA 240, Ontario	-12 to -11	Hecky and Hesslein, 1995	2
Terrestrial C_3 plants	Amazon River, Brazil	-30 to -25	Hedges et al., 1986	16
	Tonle Sap Lake, Cambodia	-31 to -26	Holtgrieve, *unpubl.*	7
	ELA 240, Ontario	-29 to -28	Hecky and Hesslein, 1995	2
	ELA 373, Ontario	-29	Hecky and Hesslein, 1995	1
Terrestrial C_4 plants	Amazon River, Brazil	-12	Hedges et al., 1986	1

The α_{app} between $\delta^{13}C\text{-}CO_2$ and $\delta^{13}C\text{-}CH_4$ showed that the predominant methanogenic pathway in TSL is likely acetate fermentation (Figures 4d and 4e), which has been shown to produce $\delta^{13}C\text{-}CH_4$ values in tropical lake sediments from the Amazon and Pantanal ranging from -84 ±2 to -62.3 ±0.9 ‰ (Conrad et al., 2010; Conrad et al., 2011). The same study inhibited acetate fermentation in favor of carbonate reduction, which produced $C\text{-}CH_4$ even more depleted in ^{13}C / ^{12}C (Conrad, 2010). This is compared with a mean $\delta^{13}C\text{-}CH_4$ of -43 ±2 ‰ measured at our sampling sites, with $\delta^{13}C\text{-}CH_4$ values reaching -11 ‰ (Figures 4c and 4d). These comparatively enriched $\delta^{13}C\text{-}CH_4$ values indicate the preferential oxidation of lighter, $^{12}C\text{-}CH_4$ by methanotrophic bacteria and archaea (Whiticar and Faber, 1986).

Difference fractionation factors between $\delta^{13}C\text{-}CO_2$ and $\delta^{13}C\text{-}CH_4$ further support oxidation; for methanotrophy in natural systems, the magnitudes of isotope effects between $\delta^{13}C\text{-}CO_2$ and $\delta^{13}C\text{-}CH_4$ ranges from ε_C=5-20 ‰ (Whiticar, 1999), with laboratory experiments yielding values of ε_C as high as 31 ‰ (Barker and Fritz, 1981). Most of our ε_C values were less than 31 ‰ during the high-water (97 %) and falling-water (67 %) stages.

The contribution of anaerobic processes is largely ignored in studies of C cycling in freshwaters, but this contribution is likely to be large given the areal extent and discharge of flood-pulse rivers, globally. The subtropics and tropics are home to many high order flood pulse rivers, such as the Amazon, Orinoco, Parana, Congo, Okavango, Zambezi, Oubangui, Ganges, Indus, Yangtze, Irrawaddy, and Mekong, which are collectively responsible for much of global, mean annual discharge (Ward et al., 2015). Cole et al. (2007) acknowledge that inclusion of floodplains in "plumbing" the global C cycle would increase their land-water flux estimate by some 48 %, from 1.9 to 2.8 Pg C y^{-1} (Richey et al., 2002). They further acknowledge that CH_4 diffusion comprises a small part of the annual water-atmosphere C flux (Melack et al., 2004),

though Bastviken et al. (2011) have since estimated that CH_4 diffusion from freshwaters corresponds to 0.65 Pg C y^{-1}. This number is only increasing with attention to CH_4 bubbling or ebullition (Joyce and Jewel, 2003; Del Sontro et al., 2011), which our study omits. Fluxes of CH_4 as a greenhouse gas from the surfaces of lakes (e.g., Sanches et al., 2019), rivers (e.g., Streigl et al., 2012), and reservoirs (e.g., St. Louis et al., 2000) to the atmosphere have been often studied in recent years. Few have studied the contribution of oxidized methanogenic C to DIC (Rudd and Hamilton, 1978; Gu et al., 2004), or how coupled methanogenesis and methanotrophy contribute C to aquatic food webs (Bastviken et al., 2003; Kankaala et al., 2006).

There is a broader lack of accounting for anaerobic processes in studies of ecosystem metabolism. Current estimates of *ER* in the literature rely almost exclusively on daily measurements of net oxygen depletion, the electron acceptor for the aerobic respiration of organic C. These estimates fail to include methanogenesis and anaerobic methanotrophy as respiratory pathways. Given the massive, hypoxic aquatic ecosystem represented by the Amazon River floodplain, alone (>100,000 km^2; Richey et al., 1988), anaerobic processes generally and methanogenesis and methanotrophy specifically are likely to be important to the overall balance of primary production and respiration in flood-pulse ecosystems and perhaps beyond. This raises central questions about accounting for C in aquatic ecosystems, and alters conventional understanding of *NEP*. Revised C accounting is needed for tropical flood-pulse rivers and lakes with sizeable contributions to the DIC and heterotrophic food web by CH_4.

5.3 Changes in local redox environments appear to control CO_2 and CH_4 diffusion

Mixed effects modeling of data collected during the high-water stage of the flood pulse provided another line of evidence that much of the dissolved CO_2 measured was derived from methanogenesis and methanotrophy, rather than aerobic respiration. Diffusive CO_2 fluxes from

the surface of TSL to the atmosphere increased with Mn_{Tot} concentrations in bottom waters (Figure 7a). This may have resulted from Mn-dependent anaerobic oxidation of CH_4 in the hypoxic (<4 mg O_2 L^{-1}) water column of TSL. Aerobic oxidation of CH_4 is a well-known fate for CH_4 in lake water columns (Bastviken et al., 2002), but anaerobic oxidation has only recently been reported at the sediment-water interface of freshwater lakes (Deutzmann et al., 2011; Martinez-Cruz et al., 2018; Su et al., 2019). Many of the anaerobic oxidation pathways reported by these authors are mediated by sulfate and iron, rather than Mn, as electron acceptors. Mn-dependent anaerobic oxidation of CH_4 has been shown in reduced wetland (Liu et al., 2019) and marine sediments (Beal et al., 2009). However, a large fraction of dissolved Mn_{Tot}, Mn^{2+}, is also simply more soluble in hypoxic waters. Thus, anaerobic oxidation of CH_4 may not necessarily be driven by changes in Mn_{Tot}, but by changes to its solubility and the local redox environment. CO_2 and CH_4 diffusion also decreased as bottom water NO_3^- and surface water O_2 concentrations increased (Figures 7a and 7b). The introduction of NO_3^- to bottom waters and dissolved O_2 to surface waters marks a further shift in the local redox environment. In a hypoxic ecosystem where flood waters inundate soils to create anaerobic conditions, NO_3^- would be quickly removed not only as the primary substrate for denitrification, but also as a thermodynamically-favorable electron acceptor (along with O_2). Any introductions of NO_3^- and O_2 would alter local redox conditions and make methanogenesis, CH_4 diffusion, and CH_4-derived CO_2 diffusion less likely to occur.

6.0 Conclusion

The Lower Mekong and TSL flood-pulse blurs classical ecosystem boundaries between the terrestrial and the aquatic. This and other tropical flood pulses around the world inundate floodplains many times the spatial extent of the rivers, themselves, affecting ecosystem function

in profound ways. Contrary to the predictions of Junk and others (1989) from work in the Amazon, we show that the flood-pulse drives net heterotrophy in Tonle Sap Lake. Resulting C gas fluxes to the atmosphere are derived in large part from anaerobic oxidation of floodplain C. Anaerobic metabolism has been largely ignored in studies of freshwater C cycling and ecosystem metabolism, with implications for C accounting in other flood pulse and hypoxic ecosystems, worldwide.

7.0 Acknowledgements

We gratefully acknowledge the assistance of the Cambodian Inland Fisheries Research and Development Institute staff and the inhabitants of the floating villages on Tonle Sap Lake. Their engagement, logistical support, and kindness made this study possible and surpassingly enjoyable. We would like to thank Vittoria Elliott of the Smithsonian Institute and Chey Thavy, Vannmei Ly, and David Ford of Royal University of Phnom Penh for further in-country support. Matthew Bonnema guided our application of satellite backscatter data. We would also like to thank Daniel Schindler, Jeffrey Richey, David Butman, and two anonymous reviewers for helpful comments during the preparation of this manuscript. This research was supported by the National Science Foundation (EAR 1740042) and Margaret A. Cargill Foundation. B.L.M. was additionally supported by a National Science Foundation Graduate Research Fellowship (DGE 1256260), a National Security Education Boren Fellowship, and a University of Washington School of Aquatic and Fishery Sciences Graduate Fellowship. All data and data products presented in figures and analyses are available by following the link: https://github.com/blm8/Tonle-Sap-Lake-Carbon-Fluxes.git.

8.0 Literature Cited

Abril, G. and A.V. Borges (2019), Ideas and perspectives—Carbon leaks from flooded land—Do we need to replumb the inland water active pipe?, *Biogeosciences*, 16, 769-784.

http://doi.org/10.5194/bg-16-769-2019

Arias, M.E., T.A. Cochrane, M. Kummu, H. Lauri, G.W. Holtgrieve, J. Koponen, and T. Piman (2014), Impacts of hydropower and climate change on drivers of ecological productivity of Southeast Asia's most important wetland, *Ecological Modelling*, 272, 252-263. http://doi.org/10.1016/j.ecolmodel.2013.10.015

Arias, M.E., T.A. Cochrane, D. Norton, T.J. Killeen, and P. Khon (2013), The flood pulse as the underlying driver of vegetation in the largest wetland and fishery of the Mekong Basin, *AMBIO*, 42(7), 864-876. http://doi.org/10.1007/s13280-013-0424-4

Arias, M.E., T.A. Cochrane, T. Piman, M. Kummu, B.S. Caruso, and T.J. Killeen (2012), Quantifying changes in flooding and habitats in the Tonle Sap Lake (Cambodia) caused by water infrastructure development and climate change in the Mekong Basin, *Journal of Environmental Management*, 112, 53-66. http://doi.org/10.1016/j.jenvman.2012.07.003

Barker, J.F. and P. Fritz (1981), Carbon isotope fractionation during microbial methane oxidation, *Nature*, 293, 289-291.

Bastviken, D., L. Tranvik, J.a. Downing, P.M. Crill, and A. Enrich-Prast (2011), Freshwater methane emissions offset the continental carbon sink, Science, 331(6013), 50. http://doi/10.1126/science.1196808

Bastviken, D., J. Ejlertsson, I. Sundh, and L. Tranvik (2003), Methane as a source of carbon and energy for lake pelagic foodwebs, *Ecology*, 84(4), 969-981. http://doi.org/10.1890/0012-9658(2003)084[0969:MAASOC]2.0.CO;2

Bastviken, D., J. Ejlertsson, and L. Tranvik (2002), Measurement of methane oxidation in lakes—A comparison of methods, *Environmental Science and Technology*, 36, 3354-3361. http://doi.org/10.1021/es010311p

Bates, D., M. Maechler, B. Bolker, and S. Walker (2015), Fitting linear mixed effects models using lme4, *Journal of Statistical Software*, 67(1). http://doi.org/10.18637/jss.v067.i07

Battin, T. J., L.A. Kaplan, S. Findlay, C.S. Hopkinson, E. Marti, A.I. Packman, J.D. Newbold, and F. Sabater (2009), Biophysical controls on organic carbon fluxes in fluvial networks, *Nature Geoscience*, 2(8), 595–595. http://doi.org/10.1038/ngeo602

Bayley, P.B. (1995), Understanding large river-floodplain ecosystems, *BioScience*, 45(3), 153-158. http://doi.org/10.2307/1312554

Beal, E.J., C.H. House, and V.J. Orphan (2009), Manganese- and iron-dependent marine methane oxidation, *Science*, 325(5937), 184-187. http://doi.org/10.1126/science.1169984

Bedard, C. and R. Knowles (1991), Hypolimnetic O2 consumption, denitrification, and methanogenesis in a thermally stratified lake, *Canadian Journal of Fisheries and Aquatic Sciences*, 54, 1639-1645. http://10.1139/cjfas-54-7-1639

Bianchi, T.S., M.E. Freer, R.G. Wetzl (1996), Temporal and spatial variability, and the role of dissolved organic carbon (DOC) in methane fluxes from the Sabine River floodplain (southeast Texas, USA), *Archiv Fur Hydrobiologie*, 136(2), 261-287.

Borges, A.V., G. Abril, F. Darchambeau, C.R. Teodoru, J. Deborde, L.O. Vidal, T. Lamber, and S. Bouillion (2015), Divergent biophysical controls of aquatic CO2 and CH4 in the world's two largest rivers, *Scientific Reports*, 5, 15614. http://doi.org/10.1038/srep15614

Burnham, K.P. and D.R. Anderson (2004), Multimodel inference—Understanding AIC and BIC in model selection, *Sociological Methods and Research*, 33(2), 261-304. http://doi.org/10.1177/0049124104268644

Cohen, J. (1988), Statistical power analysis for the behavioral sciences (2nd ed.), Lawrence Earlbaum Associates, Hillsdale, New Jersey, U.S.A.

Cole, J.J., Y.T. Prairie, N.F. Caraco, W.H. McDowell, L.V. Tranvik, R.G. Streigl, C.M. Duarte, P. Kortelainen, J.A. Downing, J.J. Middleburg, and J. Melack (2007), Plumbing the global carbon cycle—Integrating inland wters into the terrestrial carbon budget, *Ecosystems*, 10, 171-184. http://doi.org/10.1007/s10021-006-9013-8

Cole, J.J. and N.F. Caracao (2001), Carbon in catchments: Connecting terrestrial carbon losses with aquatic metabolism, *Marine and Freshwater Research*, 52, 101-110.

Cole, J.J. and N.F. Cole (1998), Atmospheric exchange of carbon dioxide in a low wind oligotrophic lake measured by the addition of SF6, *Limnology and Oceanography*, 43(4), 647-656. http://doi.org/10.4319/lo.1998.43.4.0647

Cole, J.J., N.F. Caraco, G.W. Kling, and T.K. Kratz (1994), Carbon dioxide supersaturation in the surface waters of lakes, *Science*, 265(5178), 1568-1570. http://doi.org/10.1126/science.265.5178.1568

Conrad, R., M. Noll, P. Clause, M. Klose, W.R. Bastos, and A. Enrich-Prast (2011), Stable carbon isotope discrimination and microbiology of methane formation in tropical anoxic lake sediments, *Biogeosciences*, 8, 795-814. http://doi.org/10.5194/bg-8-795-2011/

Conrad, R., M. Klose, P. Claus, and A. Enrich-Prast (2010), Methanogenic pathway, 13C isotope fractionation, and archaeal community composition in the sediment of two clear-water lakes of Amazonia, *Limnology and Oceanography*, 55(2), 689-702. http://doi.org/10.4319/lo.2010.55.2.0689

Conrad, R. (2005), Quantification of methanogenic pathways using stable carbon isotopic signatures—A review and a proposal, *Organic Geochemistry*, 36, 739-752.

http://doi.org/10.1016/j.orggeochem.2004.09.006

Crawford, J.T., E.H. Stanley, S.A. Spawn, J.C. Finlay, L.C. Loken, and R.G. Streigl (2014), Ebullitive methane emissions from oxygenated wetland streams, Global Change Biology, 20, 3408-3422. http://doi.org/10.1111/gcb.12614

Crusius, J. and R. Wanninkhof (2003), Gas transfer velocities measured at low wind speed over a lake, *Limnology and Oceanography*, 48(3), 1010-1017. http://doi.org/10.4319/lo.2003.48.3.1010

De Kluijver, A., P.L. Schoon, J.A. Downing, S. Schouten, and J.J. Middleburg (2014), Stable carbon isotope biogeochemistry of lakes along a trophic gradient, *Biogeosciences*, 11, 6615-6646. http://doi.org/10.5194/bgd-11-6615-2014

Del Giorgio, P.A., J.J. Cole, N.F. Caraco, and R.H. Peters (1999), Linking planktonic biomass and metbolism to net gas fluxes in northern temperate lakes, *Ecology*, 80(4), 1422-1431. http://doi.org/10.1890/0012-9658(1999)080[1422:LPBAMT]2.0.CO;2

Del Giorgio, P.A. and R.H. Peters (1994), Patterns in planktonic P:R ratios in lakes—Influence of lake trophy and dissolved organic carbon, *Limnology and Oceanography*, 39(4), 772-787. http://doi.org/10.4319/lo.1994.39.4.0772

Del Sontro, T., M.J. Kunz, T. Kempter, A. Wuest, B. Wehrli, and D.B. Senn (2011), Spatial heterogeneity of methane ebullition in a large tropical reservoir, *Environmental Science and Technology*, 45, 9866-9873. http://doi.org/10.1021/es2005545

Deutzmann, J.S., P. Stief, J. Brandes, and B. Schink (2014), Anaerboic methane oxidation coupled to denitrification is the dominant methane sink in a deep lake, *Proceedings of the National Academy of Sciences*, 111(51), 18273-18278. http://doi.org.10.1073/pnas.1411617111

Devol, A.H., B.R. Forsberg, J.E. Richey, and T.P. Pimentel (1995), Seasonal variation in chemcial distributions in the Amazon (Solimenos) River—A multiyear time series, *Global Biogeochemical Cycles*, 9(3), 307-328. http://doi.org/10.1029/95GB01145

Devol, A.H., J.E. Richey, W.A. Clark, and S.L. King (1988), Methane emissions to the troposphere from the Amazon floodplain, *Journal of Geophysical Research—Atmospheres*, 93(D2), 1583-1592. http://doi.org/10.1029/JD093iD02p01583

Downing, J.A. (2009), Global limnology—Upscaling aquatic services and processes to planet Earth, Internationale Vereinigung fuer Theoretische und Angewandte Limnologie—Verhandlungen, 30(8), 1149-1166.

Emerson, S. and J. Hedges (2008), Chemical Oceanography and the Marine Carbon Cycle, Cambridge University Press, Cambridge, New York, USA.

Fallon, R.D., S. Harris, R.S. Hanson, and T.D. Brock (1980), The role of methane in internal carbon cycling in Lake Mendota during summer stratification, *Limnology and Oceanography*, 25, 357-360. http://doi.org/10.4319/lo.1980.25.2.0357

Gates, D.M. (1966), Spectral distribution of solar radiation at the earth's surface, *Science*, 151(3710), 523-529. http://doi.org/10.1126/science.151.3710.523

Gorelick, N., M. Hancher, M. Dixon, S. Ilyushchenko, D. Thau, and R. Moore (2017), Google Earth Engine: Planetary-scale geospatial analysis for everyone, *Remote sensing of Environment*, 202, 18-27. http://doi.org/10.1016/j.rse.2017.06.031

Gu, B., C.L. Schelske, and D.A. Hodell (2004), Extreme 13C enrichments in a shallow hypereutrophic lake—Implications for carbon cycling, *Limnology and Oceanography*, 49(4), 1152-1159. http://doi.org/10.4319/lo.2004.49.4.1152

Hamilton, S. K., S.J. Sippel, D.F. Calheiros, and J.M. Melack (1997), An anoxic event and other biogeochemical effects of the Pantanal wetland on the Paraguay River, *Limnology and Oceanography*, 42(2), 257–272. http://doi.org/10.4319/lo.1997.42.2.0257

Hecky, R.E. and R.H. Hesslein (2001), Contributions of benthic algae to lake food webs as revealed by stable isotope analysis, *Freshwater Science*, 14(4), 631-653.

Hedges, J.I., W.A. Clark, P.D. Quay, J.E. Richey, A.H. Devol, and M. Santos (1986), Compositions and fluxes of particulate organic material in the Amazon River, *Limnology and Oceanography*, 31(4), 717-738. http://doi.org/10.4319/lo.1986.31.4.0717

Hetch, J., G. Lacombe, M.E. Arias, T.D. Dang, and T. Piman (2019), Hydropower dams of the Mekong River basin—A review of their hydrological impacts, *Journal of Hydrology*, 568, 285–300. https://doi.org/10.1016/j.jhydrol.2018.10.045

Holtgrieve, G.W., M.E. Arias, K.N. Irvine, D. Lamberts, E.J. Ward, M. Kummu, J. Koponen, J. Sarkkula, and J.E. Richey, (2013), Patterns of ecosystem metabolism in the Tonle Sap Lake, Cambodia with links to capture fisheries, *PLoS ONE*, 8(8), e71395. http://doi.org/10.1371/journal.pone.0071395

Holtgrieve, G.W., D.E. Schindler, T.A. Branch, and Z. Teresa-A'mar (2010), Simultaneous quantification of aquatic ecosystem metabolism and reaeration using a Bayesian statistical model of oxygen dynamics, Limnology and Oceanography, 55(3), 1047-1063. http://doi.org/10.4319/lo.2010.55.3.1047

IPCC (2007), Climate change 2007—Synthesis report, Contribution of Working Groups I, II, and III to the Fourth Assessment Report of the Intergovernmental Panel on Climate Change, Core Writing Team, R.K. Pachauri, and L.A. Meyer (eds.), IPCC, Geneva, Switzerland

Jellison, R. and J.M. Melack (1993), Algal photosynthetic activity and its response to meromixis in hypersaline Mono Lake, California, *Limnology and Oceanography*, 38(4), 818-837. http://doi.org/10.4319/lo.1993.38.4.0818

Jones, J.B. and P.J. Mulholland (1998), Carbon dioxide variation in a hardwood forest stream—An integrative measure of whole catchment soil respiration, *Ecosystems*, 1, 183-196. http://doi.org/10.1007/s100219900014

Joyce, J. and P.W. Jewell (2003), Physical controls on methane ebullition from reservoirs and lakes, *Environmental and Engineering Geoscience*, 9(2), 167-178.

Junk, W.J., P.B. Bayley, and R.E. Sparks (1989), The flood pulse concept in river-floodplain systems, 110-127, *In* D.P. Dodge (ed.), Proceedings of the International Large River Symposium, *Canadian Special Publication of Fisheries and Aquatic Sciences*, 106.

Kling, G.W., G.W. Kipphut, and M.C. Miller (1991), Arctic lakes and rivers as gas conduits to the atmosphere—Implications for tundra carbon budgets, *Science*, 251, 298-301. http://doi.org/10.1126/science.251.4991.298

Kuivila, K.M., J.W. Murray, A.H. Devol, M.E. Lidstrom, and C.E. Reimers (1988), Methane cycling in the sediments of Lake Washington, *Limnology and Oceanography*, 33, 571-581. http://doi.org/10.4319/lo.1988.33.4.0571

Lauri, H., H. de Moel, P.J. Ward, T.A. Rasanen, M. Keskinen, and M. Kummu (2012), Future changes in Mekong River hydrology—Impact of climate change and reservoir operation on discharge, *Hydrology and Earth System Sciences Discussion*, 9, 6569-6614. http://doi.org/10.5194/hessd-9-6569-2012

Liu, W., H. Xiao, H. Ma, Y. Li, T.M. Adyel, and J. Zhai (2019), Reduction of methan emissions from manganese-rich constructed wetlands—Role of manganese-dependent anaerobic methane oxidation, *Chemical Engineering Journal*. http://doi.org/10.1016/j.cej.2019.123402

Martinez-Cruz, K., M.C. Lewis, I.C. Herriott, A. Sepulveda-Jauregui, K.W. Anthony, F. Thalasso, M.B. Leigh (2017), Anaerboic oxidation of methane by aerboic methanotrophs in sub-Arctic lake sediments, *Science of the Total Environment*, 607-608, 23-31. http://doi.org/10.1016/j.scitotenv.2017.06.187

Mayorga, E., A.K. Aufdenkampe, C.A. Masiello, A.V. Krusche, J.I. Hedges, P.D. Quay, J.E. Richey, and T.A. Brown (2005), Young organic matter as a source of carbon dioxide outgassing from Amazonian Rivers, *Nature*, 436, 538-541. http://doi.org/10.1038/nature03880

McCallister, S.L. and P.A. Del Giorgio (2008), Direct measurement of the d13C signature of carbon respirared by bacteria in lakes—Linkages to potential carbon sources, ecosystem bseline metabolism, and CO2 fluxes, *Limnology and Oceanography*, 53(4), 1204-1216.

http://doi.org/10.4319/lo.2008.53.4.1204

Melack, J., L.L. Hess, M. Gastil, B.R. Forsberg, S.K. Hamilton, I.B.T. Lima, E. Marcia, and L. de Moraes-Novo (2004), Regionalization of methane emissions in the Amazon Basin with microwave remote sensing, *Global Change Biology*, 10, 530-544. http://doi.org/10.1111/j.1365-2486.2004.00763

MRC (2009), Mekong River Commission Spatial Database, Mekong River Commission, Vientiane, Lao PDR. http://www.mrcmekong.org/spatial/data_catalog.htm

Nelson, G.A. (2019), fishmethods—Fishery Science Methods and Models, R package version 1.11-1, http://CRAN.R-project.org/package=fishmethods.

Ostrovsky, I., D.F. McGinnis, L. Lapidus, and W. Eckert (2008), Quanitfying gas ebulllition with echosounder—The role of methane transport by bubbles in a medium-sized lake, Limnology and Oceanography—Methods, 6, 18. http://doi.org/10.4319/lom.2008.6.105

Park, P.K., L.I. Gordon, S.W. Hager, and M.C. Cissell (1969), Carbon dioxide partial pressure in the Columbia River, *Science*, 166(3907), 867-868. http://doi.org/10.1126/science.166.3907.867

R Core Team (2019), R—A language and environment for statistical computing, R Foundation for Statistical Computing, Vienna, Austria, http://www.R-project.org/.

Raymond, P.A., J.E. Saiers, and W.V. Sobczak (2016), Hydrological and biogeochemical controls on watershed dissolved organic matter transport—Pulse-shunt concept, Ecology, 97(1), 5-16. http://doi.org/10.1890/14-1684.1

Raymond, P.A., J. Hartmann, R. Lauerwald, S. Sobek, C. McDonald, M. Hoover, D. Butman, R. Striegl, E. Mayorga, C. Humborg, P. Kortelainen, H. Duerr, M. Meybeck, P. Ciais, and P. Guth (2013), Global carbon dioxide emissions from inland waters, *Nature*, 503, 355-359. http://doi.org/10.1038/nature12760

Richey, J.E., J.M. Melack, A.K. Aufdenkampe, V.M. Ballester, and L.L. Hess (2002), Outgassing from Amazonian rivers and wetlands as a large tropical source of atmospheric CO2, *Nature*, 416, 617-620. http://doi.org/10.1038/416617a

Richey, J.E., A.H. Devol, S.C. Wofsy, R. Victoria, and M.N.G. Riverio (1988), Biogenic gases and the oxidation and reduction of carbon in Amazon River and floodplain waters, *Limnology and Oceanography*, 33(4), 551-561. http://doi.org/10.4319/lo.1988.33.4.0551

Rudd, J.W.M., and R.D. Hamilton (1978), Methane cycling in a eutrophic hield lake and its effects on who lake metabolism, *Limnology and Oceanography*, 23, 337-348. http://doi.org/10.4319/lo.1978.23.2.0337

Sabo, J.L., A. Ruhi, G.W. Holtgrieve, V. Elliott, M.E. Arias, P.B. Nor, T.A. Raesaenen, and S.

Nam (2017), Designing river flows to improve food security futures in the Lower Mekong Basin, *Science*, 358(6368), 270-281. http://doi.org/10.1126/science.aao1053

Sanches, L.F., B. Guenet, C.C. Marinho, N. Barros, and F. de Assis Esteves (2019), Global regulation of methane emission from natural lakes, Scientific Reports, 9(255), 1-10. http://doi.org/10.1038/s41598-018-3619-5

Stone, R. (2011), Mayheem on the Mekong, *Science*, 333(6044), 814-818. http://doi.org/10.1126/science.333.6044.814

St. Louis, V.L., C. Kelly, E. Duchemin, J.W.M. Rudd, and D.M. Rosenberg (2000), Reservoir surfaces as sources of greenhouse gases to the atmosphere—A global estimate, *Bioscience*, 50(9), 766-775. http://doi.org/10.1641/0006-3568(2000)050[0766:RSASOG]2.0.CO;2

Streigl, R.G., M.M. Dornblaser, C.P. McDonald, J.R. Rover, and E.G. Stets (2012), Carbon dioxide and methane emissions from the Yukon River system, *Global Biogeochemical Cycles*, 26, GB0E05. http://doi.org/10.1029/2012GB004306

Su, G., J. Zopfi, H. Yao, L. Steinle, H. Niemann, and M.F. Lehmann (2019), Manganese/iron-supported sulfate-dependent anaerboic oxidation of methane by archea in lake sediments, *Limnology and Oceanography*, *In press*. http://doi.org/10.1002/lno.11354

Taylor, J.R. (1997), An introduction to error analysis—The study of uncertainties in physical measurements, 2nd ed., University Science Books, Sausilito, California, USA.

Tarnocai, C., C.G. Canadell, E.A.G. Schuur, P. Kuhry, G. Mazhitova, and S. Zimov (2009), Soil organic carbon pools in the northern circumpolar permafrost region, *Global Biogeochemical Cyles*, 23(2), GB2023. http://doi.org/10.1029/2008GB003327

Torres, R., P. Snoeij, D. Geudtner, D. Bibby, M. Davidson, E. Attema, P. Potin, B. Rommen, N. Floury, M. Brown, I.N. Traver, P. Deghaye, B. Duesmann, B. Rosich N. Miranda, C. Bruno, M. L'Abbate, R. Croci, and F. Rostan (2012), GMES Sentinel-1 mission, *Remote Sensing of Environment*, 120, 9-24. http://doi.org/10.1016/j.rse.2011.05.028

Tranvik, L.J., J.A. Downing, J.B. Cotner, S.A. Loiselle, R.G. Streigl, T.J. Bellatore, P. Dillon, K. Findlay, K. Fortino, L.B. Knoll, P.L. Kortelainen, T. Kutser, S. Larsen, I. Laurion, D.M. Leech, S. L. McCallister, D.M. McKnight, J.M. Melack, E. Overholt, J.A. Porter, Y. Prairie, W.H. Renwick, F. Roland, B.S. Sherman, D.W. Schindler, S. Sobek, A. Tremblay, M.J. Vanni, A.M. Verschoor, E. von Wachenfeldt, and G.A. Weyhenmeyer (2009), Lakes and reservoirs as regulators of carbon cycling and climate, *Limnology and Oceanography*, 54(6), 2298-2314. http://doi.org/10.4319/lo.2009.54.6_part_2.2298

Vuorio, K., M. Meili, and J. Sarvala (2006), Taxon-specific variation in the stable isotopic signatures ($\delta^{13}C$ and $\delta^{15}N$) of lake phytoplankton, *Freshwater Biology*, 51, 807-822. http://doi.org/10.1111/j.1365-2427.2006.01529.x

Wanninkhof, R. (1992), Relationship between wind speed and gas exchange over the ocean, *Journal of Geophyscial Research—Oceans*, 97(C5), 7373-7382. http://doi.org/10.1029/92JC00188

Ward, N.D., A.V. Krusche, H.O. Sawakuchi, D.C. Brito, A.C. Cunha, J.M.S. Moura, R. da Silva, P.L. Yager, R.G. Keil, and J.E. Richey (2015), The compositional evolution of dissolved and aprticulate organic matter along the lower Amazon River—Obidos to the ocean, *Marine Chemistry*, 177, 244-256. http://doi.org/10.1016/j.marchem.2015.06.013

Whiticar, M.J. (1999), Carbon and hydrogen isotope systematics of bacterial formation and oxidation of methane, *Chemical Geology*, 161, 291-314. http://doi.org/10.1016/S0009-2541(99)00092-3

Whiticar, M.J. and E. Faber (1986), Methane oxidation in sediment and water column environments—Isotopic evidence, *Organic Geochemistry*, 10(4-6), 759-768. http://doi.org/10.1016/S0146-6380(86)80013-4

Wilhelm, E., Rubin Battino, and R.J. Wilcock (1977), Low-pressure solubility of gases in liquid water, *Chemical Reviews*, 77(2), 219-262. http://doi.org/10.1021/cr60306a003

Winemiller, K. O., C.G. Montaña, D.L. Roelke, J.B. Cotner, J.V. Montoya, L. Sanchez, M.M. Castillo, and C.A. Layman (2014), Pulsing hydrology determines top-down control of basal resources in a tropical river-floodplain ecosystem, *Ecological Monographs*, 84(4), 621–635. http://doi.org/10.1890/13-1822.1

Winslow, L.A., J.A. Zwart, R.D. Batt, H.A. Dugan, R.I. Woolway, J.R. Corman, and J.S. Read (2016), LakeMetabolizer—An R package for estimating lake metabolism from free-water oxygen using diverse statistical models, *Inland Waters*, 6(4), 622-636. http://doi.org/10.1080/IW-6.4.883

Yvon-Durocher, G., A.P. Allen, D. Bastviken, R. Conrad, C. Gudasz, A. St. Pierre, N. Thanh-Duc, and P. Del Giorgio (2014), Methane fluxes show consistent temperature dependence across microbial to ecosystem scales, *Nature*, 507(7493), 488-491. http://doi.org/10.1038/nature13164

Yvon-Durocher, G., J.M. Caffrey, A. Cescatti, M. Dossena, P. del Giorgio, J.M. Gasol, J.M. Montoya, J. Pumpanen, P.A. Staehr, M. Trimmer, G. Woodward, and A.P. Allen (2012), Reconciling the temperature dependence of respiration across timescales and ecosystem types, *Nature*, 487(7408), 472-476. http://doi.org/10.1038/nature11205

Zar, J.H. (2010), Biostatistical Analysis, Pearson, Upper Saddle River, New Jersey, USA.

Zuijdgeest, A., S. Baumgartner, and B. Wehrli (2016), Hysteresis effects in organic matter turnover in a tropical floodplain during a flood cycle, *Biogeochemistry*, 131, 49-63. http://10.1007/s10533-016-0263-z

Chapter 3

High methanogenic fixation of carbon in a flood-pulse lake food web

Benjamin L. Miller[1]

Mauricio E. Arias[2]

Sodavy Gnim[3,4]

Chheng Phen[4]

G.W. Holtgrieve[1]

1. University of Washington, School of Aquatic and Fishery Sciences
2. University of South Florida, Department of Civil and Environmental Engineering
3. Cambodian Forestry Administration
4. Cambodian Fisheries Administration

1.0 Abstract

Lake food webs can receive carbon (C) from multiple aerobic and anaerobic energetic pathways, including methane (CH_4) production and oxidation. Metabolism measured at the base of lake food webs to date has focused on photosynthesis and whole-ecosystem aerobic respiration (*ER*). However, the anaerobic production and subsequent oxidation of CH_4 (methanogenesis and methanotrophy, respectively) may be particularly important in tropical lakes and rivers that annually expand over their surrounding floodplains, creating thousands of km^2 of reduced habitat. We hypothesized that rates of methanogenesis, methanotrophy, and their contribution to ecosystem metabolism in a "flood-pulse" lake would increase with flood duration, and differ across lake environments. We also predicted that upper trophic levels would incorporate this methanogenic C into their biomass. To evaluate these hypotheses, we quantified areal rates of methanogenesis and methanotrophy using bottle incubations and a vertical advection model, and compared them to diel oxygen estimates of gross primary production (*GPP*), net primary production (*NPP*), and *ER*. We also sampled invertebrates, several fish species, and other members of the local food web for $^{13}C/^{12}C$ as a tracer of methanogenic C at higher trophic levels. Methanogenesis comprised up to 36 ±7 % of C fixed through *GPP* and methanotrophy comprised up to 11 ±3 % of *NPP*. Rates of both methanogenesis and methanotrophy were small compared to *ER*. Methanogenesis and *GPP* were each significantly greater at the edge of Tonle Sap Lake than in open-water or floodplain environments, perhaps due to greater water column stability here. Methanogenesis and methanotrophy were greatest during full flooding, but neither were correlated with flood duration as expected. By contrast, *ER* was strongly related to inundation time. Certain invertebrates and fish species were highly depleted in $^{13}C/^{12}C$ ($\delta^{13}C$<-35 ‰), indicating transfer of methanogenic C to higher trophic levels. Collectively, these results demonstrate that there is significant cycling of C through

anaerobic pathways during the flood pulse, contributing to the overall energetic base of this lake food web.

2.0 Introduction

Traces of methanogenic carbon (C) detected within the biomass of chironomids (Jones et al., 1999; Bunn and Boon, 2003), zooplankton (Bastviken et al., 2003; Kankaala et al., 2006), and fish (Sanseverino et al., 2013) offer tantalizing evidence for partial support of lake food webs by CH_4 production (i.e., methanogenesis). Yet, studies of the energetic base of lake food webs have traditionally focused on photosynthesis and whole-ecosystem aerobic respiration (*ER*). The fraction of food web support by methanogenesis relative to aerobic metabolism is therefore almost entirely unresolved in lakes and other freshwaters (Shelley et al., 2014).

Methanogenesis can introduce C to lake food webs in the absence of O_2 via two primary pathways, CO_2 reduction (eq. 1) and acetate fermentation (eq. 2; Whiticar and Faber, 1986):

$$CO_2 + 8H^+ + 8e^- \rightarrow CH_4 + 2H_2O \quad (1)$$

$$CH_3COOH \rightarrow CH_4 + CO_2 \quad (2)$$

Acetate fermentation is predominant in lake sediments, and has also been shown in the water column in recent years (Bogard et al., 2014). It is estimated that roughly 70 % of the methanogenesis in freshwater sediments is carried out via acetate fermentation (Winfrey et al., 1977; Whiticar, 1999). The Wood-Ljungdhal pathway is common form of acetogenesis involving the reduction of two CO_2 molecules to form an essential precursor for acetate fermentation (Ljungdahl, 1986; Berg, 2011). Furthermore, recent work on floodplains of the Brazilian Pantanal showed that between 50 % and 90 % of methanogenesis was carried out via CO_2 reduction (Conrad et al., 2011). Both the Wood-Ljungdahl pathway and prevalence of CO_2 reduction in the Pantanal highlight that methanogenesis can involve the reduction of CO_2 in freshwaters, a defining feature of autotrophy.

Methanogenesis is alternately presented in the oceanographic and limnological literatures as 1) a form of autotrophy involving the reduction of CO_2 not unlike photosynthesis (Dilling and Cypionka, 1990; Kellermann et al., 2012; Greening et al., 2016) or 2) the terminal process for respiration of organic matter when dissolved O_2 and all other electron acceptors are depleted (Zeikus and Winfrey, 1976; Bastviken et al., 2003). Those who have measured methanogenesis in lakes typically consider it a fraction of respiration, ranging from 20 % to 100 % of *ER* (Rudd and Hamilton, 1978; Heesen and Nygaard, 1992; Mattson and Likens, 1993; Boon and Mitchell, 1995; Hamilton et al., 1995; Utsumi et al., 1998; Bastviken et al., 2003). This disciplinary divide may stem from the predominance of CO_2 reduction in marine ecosystems and acetate fermentation in freshwater ecosystems. In either case, methanogenesis "fixes" inorganic C (CO_2 reduction) or introduces C that is otherwise unavailable (acetate fermentation) to the base of the food web. Thus, it is comparable to photosynthetic Gross Primary Production (*GPP*; Figure 1).

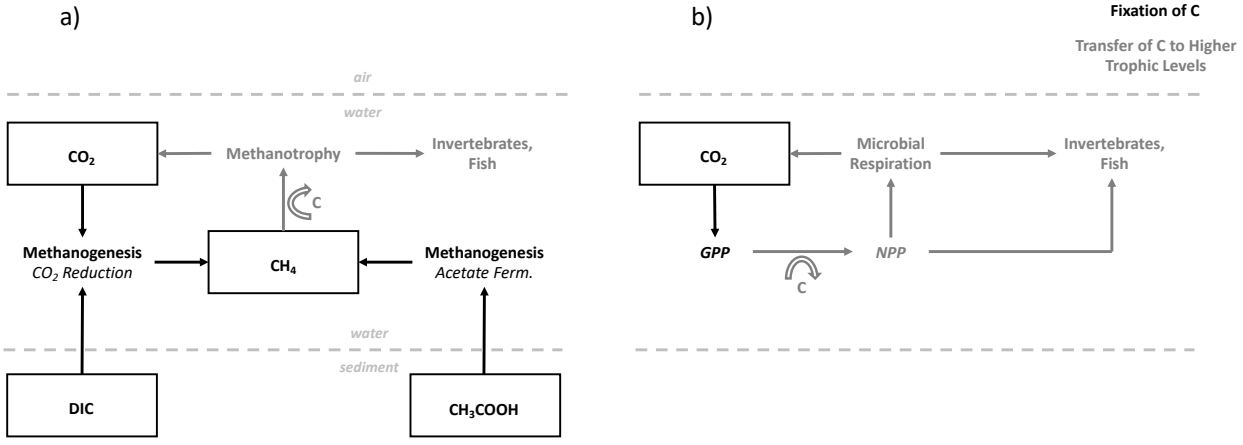

Figure 1. a) Methanogenesis via CO_2 reduction and acetate fermentation, and oxidation by methanotrophs. b) *GPP* by primary producers and *ER* by other members of the microbial community are also shown. Methanogenesis and *GPP* are processes that lead to the fixation of C (black). Methanotrophy and *ER* are processes that transfer C to higher trophic levels, such as fish (gray).

Methanogenic C can subsequently be oxidized by methanotrophic bacteria in a variety of lake environments:

$$CH_4 + (2 - x)O_2 \rightarrow (1 - x)CO_2 + xCH_2O + (2 - x)H_2O \quad (3)$$

Where *x* is the C conversion efficiency of methanotrophy, or the fraction of CH_4 oxidized actually assimilated into methanotrophic biomass, CH_2O (Urmann et al., 2009; Trimmer et al., 2015) (Figure 1a, Table 1). This fraction has recently been shown to be approximately 50 % (Trimmer et al., 2015), which is within the range reported by others previously (Whalen et al., 1990; Roslev et al., 1997; Bastviken et al., 2003). As shown in eq. 3, methanotrophic bacteria typically utilize dissolved O_2 as an electron acceptor where freshwaters transition from anaerobic to aerobic conditions. In lakes, such transitions occur at the sediment-water interface (Kuivila et al., 1991), between bottom and surface waters in lakes that undergo thermal stratification (Bedard and Knowles, 1991), and so-called microzones of anoxia in the water column (Carlton and Wetzel, 1988). Anaerobic methanotrophy utilizing a diverse array of electron acceptors, including nitrate, iron, and sulfate has also been shown at the sediment-water interface in temperate lakes (Deutzmann et al., 2011; Martinex-Cruz et al., 2018; Su et al., 2019). Collectively, these studies show that lakes can harbor a wide range of potential methanotrophic habitats.

Table 1. Summary of pathways for C fixation at the base of freshwater food webs, and—subsequently—transfer to higher trophic levels. Both were measured and compared in this study.

Fixation of C at the Base of Food Webs (mg C m^{-2} d^{-1})	**Transfer of C to Higher Trophic Levels** (mg C m^{-2} d^{-1})
Gross Primary Production (*GPP*)	Net Primary Production (*NPP*)
Methanogenesis	Methanotrophy

Methanogenesis and methanotrophy may be particularly important to the overall energetic base of food webs in tropical flood-pulse lakes and rivers. Tropical flood-pulse lakes and rivers fed by monsoonal precipitation expand over their surrounding floodplains on a highly predictable, annual basis

(Junk et al., 1989; Wantzen et al., 2008). Respiration of abundant floodplain organic matter progressively depletes dissolved O_2 and other electron acceptors in the overlying water column (Junk et al., 1989). This leads to vertical redox gradients between bottom and surface waters and horizontal redox gradients from the central "pulsing" water body through its floodplain, widespread methanogenesis and methanotrophy may be widespread (Junk et al., 1989; Holtgrieve et al., 2013). Cambodia's Tonle Sap Lake (TSL), on a tributary of the Lower Mekong, is a flood-pulse ecosystem that also harbors one of the most productive freshwater fisheries in the world (Arias et al., 2014; Sabo et al., 2017). Preliminary measurements of *GPP* suggest that photosynthesis cannot alone account for the fish biomass caught annually in TSL, implicating other energetic pathways on a floodplain spanning >9,000 km^2 as being critically important to local food web productivity (Holtgrieve et al., 2013).

The biomass of methanotrophic bacteria available for transfer to higher trophic levels can be compared to the fraction of *GPP* ultimately available to heterotrophic organisms after metabolic requirements of primary producers have been met, namely, Net Primary Production (*NPP*):

$$NPP = GPP - R_A \quad (4)$$

Where R_A is autotrophic respiration. R_A is commonly assumed—and recently empirically shown—to be approximately 40 % of *GPP* (Hall and Beaulieu, 2013; Holtgrieve et al., 2013). *NPP* is transferred to higher trophic levels directly or following microbial respiration (Figure 1b, Table 1).

Stable isotopes of C ($^{13}C/^{12}C$) provide a useful tracer for methanogenic C at higher trophic levels in lake food webs (Bastviken et al., 2003; Kankaala et al., 2006). Methanogenic C is highly depleted in ^{13}C relative to ^{12}C compared to other C sources to lake food webs (Whiticar and Faber, 1986). This depletion in $^{13}C/^{12}C$ is conserved from methanotrophs to higher trophic levels (Peterson and Fry, 1987; Jones et al., 1999). In lake sediments, invertebrate chironomid larvae highly depleted in ^{13}C relative to ^{12}C were among the first indications of methanogenic C in lake food webs (Jones et al., 1999; Bunn and

Boon, 2003). Later, it was suggested that the $^{13}C/^{12}C$ depletion of zooplankton indicated feeding on methanotrophic bacteria (Bastviken et al., 2003; Kankaala et al., 2006). Evidence for methanotrophy within the biomass of higher-trophic level consumers, such as invertebrates and fish, remains understudied (Sanseverino et al., 2013).

We compared 1) the fixation of C by methanogenesis and *GPP* and 2) the transfer of C to higher trophic levels by methanotrophy and *NPP* in TSL. We carried out these metabolic measurements during two flood stages, in different lake environments, and across a gradient of inundation time. We hypothesized that rates of methanogenesis, methanotrophy, their importance to ecosystem metabolism would be greatest during the high-water stage of the flood-pulse, and increase from the central "pulsing" body of TSL through its floodplain. We predicted that methanogenic C would be detectable at higher trophic levels of the TSL food web using $^{13}C/^{12}C$. We show high methanogenic fixation of C relative to *GPP* throughout the flood-pulse, as well as trophic transfers methanogenic C by methanotrophy great enough be detected within TSL invertebrates and fishes. A strong correlation between inundation time and *ER* further demonstrates contributions of C through both aerobic and anaerobic pathways to the overall energetic base of this lake food web during the flood-pulse.

3.0 Methods

3.1 Sampling Locations

Field sampling occurred during the high-water and falling-water stages of the TSL flood-pulse in October 2015 and March 2016, respectively. Lake level data—by which broad flood stages are defined—have been collected from a gauging station at Kampong Luong since 1990 (Figure 2). The flood-pulse begins with an increase in discharge within the Mekong River following the monsoon and course-reversal of its tributary, the Tonle Sap River, from downstream to upstream into TSL from May

through September of each year. Lake level and area reach their maximum in October and November, the full flooding or "high-water" stage. Floodwaters contract or "fall" from December through April.

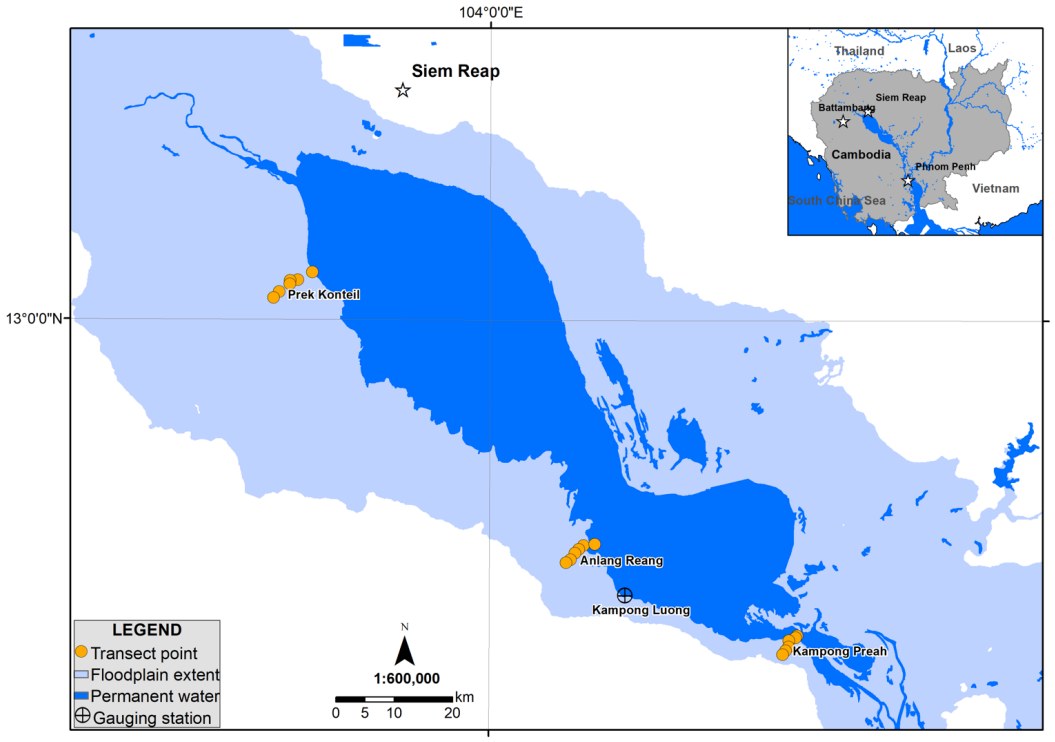

Figure 2. Sampling locations At Prek Konteil, Anlang Reang, and Kampong Preah and location of the gauging station at Kampong Luong in TSL, Cambodia.

Field sampling focused on three, core sampling locations broadly corresponding to the southwest (Kampong Preah), central (Anlang Reang) and northwest (Prek Konteil) lake basin (Figure 1). Each of these sampling locations consisted of a transect of six points extending from the open-water environment (Transect Point 1), through the edge environment (Transect Point 2) and into the floodplain (Transect Points 4-6). The edge environment is characterized by a transition from the open-water environment to rooted terrestrial floodplain vegetation.

3.2 Dissolved CH_4 and CO_2

Partial pressures of CH_4 were quantified as the average of three 74 mL gas-tight serum bottles of water collected at each transect point and depth during the high-water (*n*=54) and falling-water (*n*=18) stages of the flood-pulse. Samples were collected in vertical profile at six transect points during the high-water stage and two transect points during the falling-water stage, when the extent of the flood-pulse extended only as far as Transect Point 2. Vertical profiles consisted of samples drawn from 0.1 m depth (lake surface) and 0.5 m above sediments (lake bottom), and up to 3 depths in between at a minimum of 0.25 m increments. Samples were preserved in the field with 74 uL of 50 % m/v zinc chloride solution and placed on ice for transport to the Royal University of Phnom Penh Department of Chemistry, where they were stored at 4 °C until analysis. For analysis, samples were displaced with helium to roughly equal parts headspace and water, left to equilibrate for 12 h, and analyzed for headspace CH_4 using a gas chromatograph with a flame ionization detector (FID) and nitrogen carrier (SRI 8610*c* GC). Prior to sample analysis, standard curves were generated using 10.1, 50.5, and 497.0 ppm CH_4 in balance with nitrogen.

3.4 Isotopic Composition of CH_4 and CO_2

Following analysis for *P*CH_4, samples (*n*=72) from the transects at Prek Konteil, Anlang Reang, and Kampong Preah were sealed with Apiezon grease, inverted, placed on ice, and transported back to the University of Washington for analysis of isotopic composition of C-CH_4 and C-CO_2 using a cavity ring-down mass spectrometer (Picarro G2201*i* combined CO_2-CH_4 Isotopic Analyzer) with a small sample introduction module (Picarro A0314 SSIM). Isotopic compositions of C-CH_4 and C-CO_2 are reported in delta notation (‰) following the equation:

$$\delta^{13}C = \left(\frac{R_{sample}}{R_{standard}} - 1\right) \times 10^3 \quad (5)$$

Where $\delta^{13}C$ is the isotopic signature of dissolved C-CO_2 or C-CH_4 in units of per mil (‰), R_{sample} is the ratio of heavy to light isotope in the samples ($^{13}C/^{12}C$ of CO_2 or CH_4), and $R_{standard}$ is the $^{13}C/^{12}C$ value of Vienna Pee Dee Belemnite standard (VPDB equal to 98.9:1.1).

To determine methanogenic pathway, we calculated the apparent fractionation factor, α_{app}, during methanogenesis following Conrad (2005):

$$\alpha_{app} = \frac{(R_{CO_2})}{(R_{CH_4})} \quad (6)$$

where values of α_{app} <1.06 indicate methanogenesis by acetate fermentation and values >1.06 indicate carbonate reduction.

3.3 Methanogenesis

Methanogenesis in lake sediments was measured by sealing three, 1 cm^3 sediment cores taken with a stainless-steel corer in three 74 mL gas-tight serum bottles at each transect point during the high-water (*n*=54) and falling-water (*n*=18) stages of the flood-pulse. The remaining volume of these bottles was filled with bottom water collected 0.5 m above the sediments. Three, additional bottles were filled with bottom water, only. All bottles were incubated at ambient temperatures and sampled from a 50 % helium headspace displaced with degassed water each day, for seven days. *P*CH_4 was analyzed as described previously and corrected for progressively decreasing headspace-to-water ratios. Net oxidation of CH_4 measured in bottles containing bottom water, only, was added to net production of CH_4 measured in the bottles containing a combination of sediment cores and bottom water and considered gross production. Each sediment core was dried at 100 °C for three hours and weighed. Gross production rates were then corrected for sediment core weight and scaled to mg C-CH_4 m^{-3} d^{-1}. Previously published studies of CH_4 production in lake sediment cores show that rates measured at the sediment-water interface are relatively consistent to a sediment depth of 0.1 m (Thebrath et al., 1993; Whiticar, 1999). Thus, this volumetric rate was multiplied by 0.1 m to obtain an areal rate in terms of

mg C-CH_4 m^{-2} d^{-1}. Each transect sampled during the high- and falling-water stages included negative control incubations amended with a 74 uL of 50 % m/v zinc chloride solution.

As stated previously, methanogenesis can also occur in the water column. We estimated gross water column methanogenesis using the vertical depletion of δ^{13}C-CH_4 (see Section 3.4). Although rates of water column methanogenesis were comparatively minor, we added the two rates to obtain total methanogenesis (mg C-CH_4 m^{-2} d^{-1}).

3.4 Methanotrophy

Methanotrophy in the water column was measured using an open-system vertical advection model following Happel et al. (1994), and since Bastviken et al. (2002) and Barbosa et al. (2018):

$$f_{Open} = \frac{(\delta_s - \delta_b)}{((\alpha - 1)\ 1000)} \quad (7)$$

where f_{Open} is the fraction of δ^{13}C-CH_4 in bottom waters that is subsequently depleted via water column methanogenesis or enriched via methanotrophy, δ_s is the δ^{13}C-CH_4 measured at the surface, δ_b is the δ^{13}C-CH_4 measured at the bottom, α is the fractionation factor of 1.02 for oxidation estimated by Bastviken et al. (2002). We modified f_{Open} as expressed by Equation 5 to reflect discrete changes over a vertical depth profile of δ^{13}C-CH_4:

$$f_{Open} = \frac{(\delta_{Zi} - \delta_{Zi-1})}{((\alpha - 1)\ 1000)} \quad (8)$$

Where Z_i is the shallower depth measured in profile and Z_{i-1} is the deeper depth. The diffusive flux of CH_4 from TSL to the atmosphere is effectively the fraction of CH_4 from sediments that evades oxidation by methanotrophs within the water column. Using the open-system, vertical advection model expressed by Equation 7, it can be related to the fraction of CH_4 produced or oxidized within the water column, such that:

$$Gross\ Methanotrophy_{\ Water\ column} = F_{wa} \left(\sum f_{Open,Enrichment\ from\ Zi-1\ to\ Zi} \right) CCE \quad (9)$$

$$Gross\ Methanogenesis_{\,Water\ column} = F_{wa}\left(\sum f_{Open,Depletion\ from\ Zi-1\ to\ Zi}\right) \quad (10)$$

where F_{wa} is the diffusive flux of CH_4 from TSL described elsewhere (Miller et al., *in review*) and *CCE* is the C conversion efficiency for methanotrophy (0.5; Trimmer et al., 2015).

3.5 Aerobic Metabolic Parameters

The aerobic metabolic parameters *GPP*, *NPP*, *ER*, and net ecosystem production (*NEP*), or the difference between GPP and *ER*, were estimated using diel dissolved O_2 data and the "LakeMetabolizer" R package (Winslow et al., 2016; R Core Team, 2019). We deployed continuously logging dissolved O_2 (mg L^{-1}) and water temperature (°C) sensors for a minimum of 20 h in open-water, edge, and floodplain environments during the high-water and falling-water stages of the flood pulse (n=20). The metabolism model incorporates a log-linear light saturation function, an Arrhenius temperature dependence for respiration, and a k_{600} for reaeration of dissolved O_2 following Cole and Caraco (1998), all within a maximum likelihood framework. Other model inputs include hourly photon flux for photosynthetically active radiation (uE s^{-1} m^{-2}). Photosynthetically active radiation was not measured directly, but calculated from full-spectrum irradiance (Gates, 1966; Jellison and Melack, 1993). We modeled hourly irradiance using latitude, longitude, aspect, slope, transmissivity data and the "astrocalc4r" function in the "fishmethods" R package (Nelson, 2019; R Core Team, 2019). The model returns a metabolism estimate in terms of mg O_2 m^{-3} d^{-1}. R_A was assumed to be 40 % of *GPP*, yielding *NPP* (Hall and Beaulieu, 2013). For *GPP* and *NPP*, we assumed an assimilation of 1.2 mol CO_2 for each mol O_2 produced during photosynthesis following Holtgrieve et al. (2013). For *ER*, we assumed an equimolar consumption of O_2 and production of CO_2. CO_2 was then converted to C-CO_2 in order to express aerobic metabolic parameters in terms of mg C m^{-3} d^{-1}. We then multiplied this volumetric rate by mixing depth to obtain an areal rate in terms of mg C m^{-2} d^{-1}. By this accounting, a positive *GPP* value represents fixation or gain of C and a negative *ER* value represents a loss of C.

Mixing depths during the high-water stage of the flood-pulse were evaluated with dissolved O_2 (mg L^{-1}) profiles measured at each transect point using a multi-parameter sonde calibrated just prior to sampling with water-saturated air (YSI 6920). Dissolved O_2 data were plotted over depth (m) using the statistical and data visualization software R (R Core Team, 2019), smoothed using a loess spanning function of 0.2, and interrogated for inflection points. The depth of these inflection points at each transect was considered the mixing depth. Stratification of dissolved O_2 occurred during the high-water stage despite negligible temperature differences of <1-2 °C between bottom and surface waters, which always exceeded 25 ºC in this tropical lake. Stratification did not occur during the falling-water stage, when total water depth was used rather than mixing depth to obtain an areal rate in terms of mg C m^{-2} d^{-1}.

3.6 Food Web Samples

Zooplankton were collected using three vertical tows from 0.5 m above the sediments to the surface (80 um mesh) in open-water, edge, and floodplain environments during the high-water and falling-water stages of the flood pulse. In the same environments, gill nets and locally-made bamboo shrimp traps were deployed for a minimum of 10 hours. Captured representatives from each fish and snake species (n=4, each) were subsampled and dissected for 2 cm^2 of dorsal muscle tissue. All shrimp and mollusks were collected from bamboo traps. To avoid pseudo-replication, averaged values measured at each site and flood stage were considered a single value for that site and flood stage. Single values across sites were considered “true” replicates.

All zooplankton, invertebrate, and fish tissues were placed on ice, transported back to the Cambodian Inland Fisheries Research and Development Institute, and were freeze-dried for 48 hours (VirTis BenchTop, SLC). Exoskeletons and shells were removed from the shrimps and mollusks, respectively. These tissues were then transported back to the University of Washington, where they were

homogenized in a ball mill, packed into tin capsules (~0.340mg), and run using an elemental analyzer (CE Instruments 2500 NA Elemental Analyzer, Conflo IV) interfaced with an Isotope Ratio Mass Spectrometer (DeltaV IRMS) for a continuous flow-based measure for carbon ($^{13}C/^{12}C$) and nitrogen ($^{15}N/^{14}N$) stable isotope ratios. Laboratory working standards were glutamic acid 1 ($\delta^{13}C$=-28.3 ‰ vs VPDB, $\delta^{15}N$=-4.6 ‰ vs air), glutamic acid 2 ($\delta^{13}C$=-13.7 ‰, $\delta^{15}N$=-5.7 ‰), and sockeye salmon ($\delta^{13}C$=-21.3 ‰, $\delta^{15}N$=11.3 ‰). Resulting data are reported in delta notation following Equation 1, which describes the per mil (‰) deviation in the ratio of the heavy-to-light isotope relative to international standards, in this case Vienna Pee Dee Belemnite (VPDB) for C and air for nitrogen (N_2).

3.7 Hypothesis Tests

All hypothesis tests were conducted using the statistical and data visualization software R (R Core Team, 2019). We assessed normality in the data using quantile-quantile plots and Shapiro-Wilk Tests, and heteroscedasticity in the data using Bartlett Tests for Homogeneity of Variance. Rates of methanogenesis, methanotrophy, GPP, and E_R followed non-normal distributions with unequal variances. We compared the means of these metabolic rates across sites and flood stages using non-parametric Wilcoxon Rank-sum Tests. We used a Bonferroni correction to initial critical α-values of 0.05 in order to compensate for loss in statistical power over subsequent comparisons (Zar, 2010). The corrected α for comparisons between flood stages and lake environments was 0.025.

To assess whether differences between means were independent of sample size and ecologically as well as statistically significant, we calculated effect sizes following Cohen (1988):

$$d = \frac{\mu_i - \mu_j}{\sqrt{\frac{\sigma_i^2 + \sigma_j^2}{2}}} \quad (11)$$

Where d is a descriptive measure corresponding to a small (0.0-0.4), medium (0.5-0.7), or large (0.8-2.0) effect size, $\mu_{i,j}$ is the mean, and $\sigma_{i,j}$ is the standard deviation. Absolute Cohen's *d*-values for effect size are reported with each α-value.

We investigated potential biogeochemical controls on methanogenesis and methanotrophy during the high-water stage of the flood-pulse using mixed effects models. Mixed effects models allowed our heteroscedastic data to vary independently across the random effects of site. The slope of each fixed effect relative to each random effect was also allowed to vary independently following Bates et al. (2015):

$$y_i = \beta_{0,i} + \beta_i x_i \ldots + (1 \mid g_i) + (0 + x_i \mid g_i) \ldots + \varepsilon_y \quad (12)$$

Where y_i is the metabolic rate, $\beta_{0,i}$ is the intercept of y_i, β_i is the coefficient for each effect, x_i, and g_i is a random effect, site, and ε_y is the error associated with y_i. Small sample size-corrected Akaike Information Criterion (AIC_C) was used for model selection following Burnham and Anderson (2004). The likelihood of each model in describing metabolic rates relative to the other models was expressed in terms of ΔAIC_c and ΔAIC_c weight, w_i, following Burnham and Anderson (2004):

$$\Delta AIC_c = AIC_{c,i} - AIC_{c,min} \quad (13)$$

$$w_i = \frac{e^{-0.5\Delta AIC_{c,i}}}{\sum e^{-0.5\Delta AIC_{c,i}}} \quad (14)$$

Where $AIC_{c,min}$ is the lowest AIC_c value in a group of candidate models. Information on all model covariates, including election acceptors, nutrients, chlorophyll, and inundation time, is included in Appendix 3A.

4.0 Results

4.1 Distribution of δ^{13}C-CH_4 within the Water Column

The open-system vertical advection model indicated both methanotrophy and methanogenesis in the water column of TSL. According to the distribution of δ^{13}C-CH_4 in the water column, between 0 %

to >100 % of dissolved CH_4 was oxidized by methanotrophic bacteria from 0.5 m above the sediments to 0.1 m below the surface. Net methanogenesis in this column of water ranged from 0 % to 56 % (Table 2).

Like others in recent years, we measured gross methanogenesis within the water column under wide-ranging dissolved O_2 levels (Grossart et al., 2011; Bogard et al., 2014; Li et al., 2019). Dissolved O_2 at Kampong Preah during the high-water stage, for example, ranged from 73.8 ±0.9 % saturation in the open-water environment to 14 ±2 % in the floodplain environment. Depth profiles of δ^{13}C-CH_4 here indicated alternating zones of methanotrophy and methanogenesis (Figure 2; see Figures S1 and S2 for Anlang Reang and Prek Konteil). On the floodplain at Kampong Preah, the preferential consumption of ^{12}C by methanotrophs and vertical enrichment in ^{13}C-CH_4 toward the surface appeared to roughly correspond with increases in dissolved O_2. Water column methanogenesis was 22 ±5 % of CH_4 production in the sediments. The greatest gross water column methanogenesis rates, 18 ±2 and 15 ±2 mg C-CH_4 m^{-2} d^{-1}, were measured at Prek Konteil during the high-water stage.

Table 2. Mean δ^{13}C-CH_4 ±SE (‰) in bottom and surface waters, net percent change in δ^{13}C-CH_4 between bottom and surface waters, mean C-CH_4 diffusion (mg m^{-2} d^{-1}) from sediments to water, mean C-CH_4 diffusion (mg m^{-2} d^{-1}) from water to the atmosphere, water depth (m), and mean gross C-CH_4 methanogenesis and methanotrophy ±SE (mg m^{-2} d^{-1}) within the water column calculated using percent change in δ^{13}C-CH_4 by each depth sampled at Prek Konteil, Anlang Reang, and Kampong Preah.

	Bottom δ^{13}C-CH_4 (‰)	**Surface δ^{13}C-CH_4** (‰)	**Net Change in δ^{13}C-CH_4** (%)	**Water-atm. Diffusion** (mg C-CH_4 m^{-2} d^{-1})	**Water Depth** (m)	**Gross Water Column Methanogenesis** (mg C-CH_4 m^{-2} d^{-1})	**Gross Water Column Methanotrophy** (mg C-CH_4 m^{-2} d^{-1})
Prek Konteil							
High-water							
T1	-26 ±1	-27.02 ±0.02	+7 %	120 ±10	4.00	18 ±2	-4.5 ±0.5
T2	-50.7 ±0.3	-49.65 ±0.04	-5 %	630 ±70	4.25	7.6 ±0.9	-21 ±3
T3	-45.68 ±0.07	-15.0 ±0.3	-100 %[a]	72 ±8	3.00	3.6 ±0.4	-60 ±10
T4	-37.10 ±0.06	-33.16 ±0.07	-20 %	100 ±10	2.00	0	-10 ±2
T5	-36.75 ±0.04	-37.35 ±0.06	+3 %	310 ±40	1.75	15 ±2	-2.6 ±0.3
T6	-35.33 ±0.09	-29.7 ±0.4	-28 %	180 ±20	1.25	4.9 ±0.6	-27 ±3
Falling-water							
T1	-64 ±1	-76 ±6	+56 %	0.041 ±0.004	0.75	0.051 ±0.003	-0.013 ±0.002
T2	-94 ±2	-66 ±1	[a]-100 %	79 ±7	0.50	0	-1.1 ±0.1
Anlang Reang							
High-water							
T1	-78 ±6	-80 ±10	+9 %	0.07 ±0.02	5.50	0.079 ±0.5	-0.035 ±0.001
T2	-53.6 ±0.3	-17 ±1	-100 %[a]	2.4 ±0.3	4.00	3.9 ±0.01	-4.1 ±0.5
T3	-49.7 ±0.2	-46.45 ±0.04	-16 %	490 ±60	1.75	0	-40 ±5
T4	-50.56 ±0.04	-10 ±10	-100 %[a]	2.1 ±0.2	3.50	0	-0.62 ±0.05
T5	-48.8 ±0.2	-20 ±20	-100 %[a]	6.7 ±0.8	1.50	1.1 ±0.1	-2.8 ±0.4
T6	-44 ±3	-39.5 ±0.4	-21 %	10 ±1	1.00	2.2 ±0.3	-2.2 ±0.3
Falling-water							
T1	-59.6 ±0.8	-58 ±2	-9 %	0.041 ±0.004	1.50	0.012 ±0.001	-0.075 ±0.001
T2	-49.5 ±0.2	-49.7 ±0.5	0 %	79 ±7	0.50	0.63 ±0.0.6	0
Kampong Preah							
High-water							
T1	-70 ±20	-33 ±2	-100 %[a]	1.4 ±0.1	6.75	2.9 ±0.2	-1.3 ±0.1
T2	-34.4 ±0.4	-23.46 ±0.09	-55 %	2.6 ±0.2	3.00	0.41 ±0.04	-0.9 ±0.1
T3	-19.6 ±0.2	-25 ±2	+28 %	9.0 ±0.8	2.75	2.7 ±0.2	-0.12 ±0.01
T4	-52.08 ±0.04	-32.0 ±0.6	-100 %[a]	8.9 ±0.8	2.75	1.4 ±0.2	-5.2 ±0.5
T5	-40 ±4	-13.1 ±0.7	-100 %[a]	5.8 ±0.5	2.25	1.4 ±0.1	-4.5 ±0.4
T6	-34.8 ±0.7	-33.9 ±0.3	-4 %	14 ±1	0.50	1.1 ±0.1	-0.25 ±0.03
Falling-water							
T1	-38 ±2	-46 ±7	+42 %	2.9 ±0.3	1.75	2.1 ±0.2	-0.45 ±0.04
T2	-76 ±2	-69 ±3	-37 %	21 ±2	0.75	0	-3.9 ±0.4

[a]Change exceeded 100% within the water column

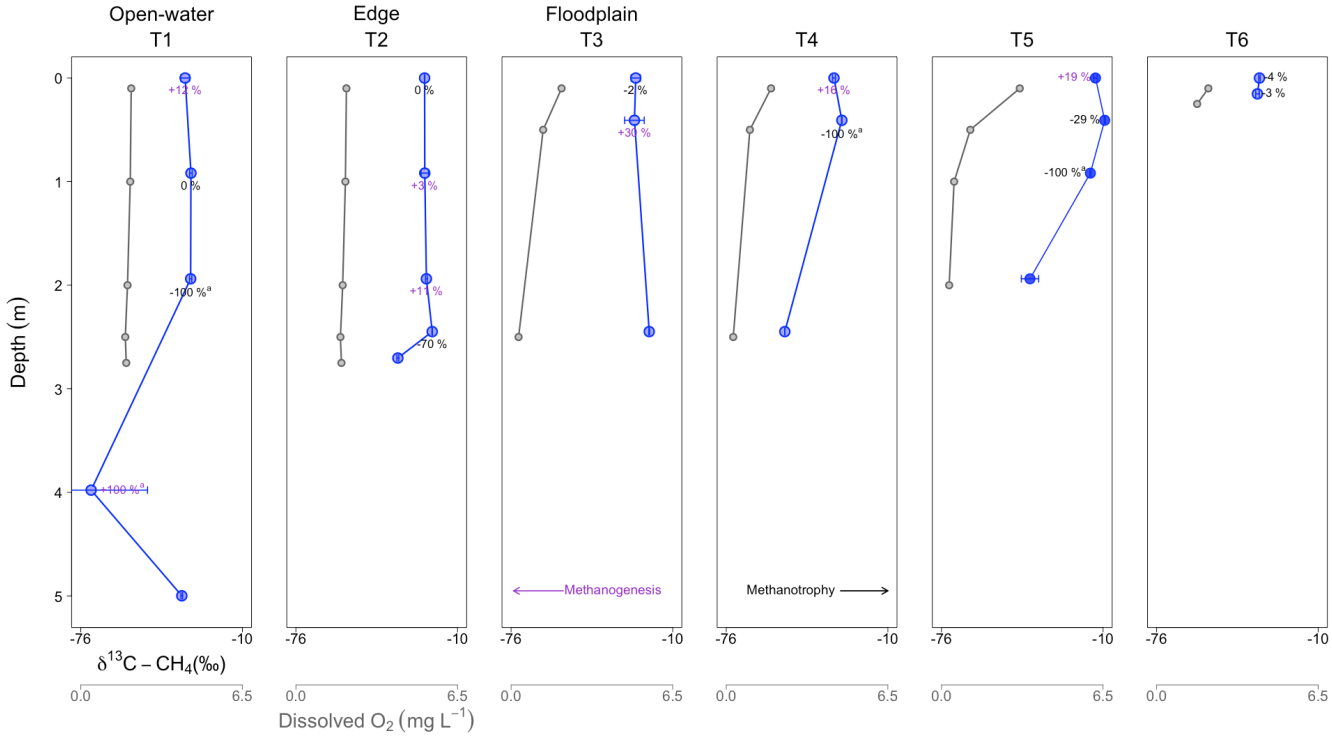

Figure 3. Methanotrophy and methanogenesis in the water column expressed as a percent change between the δ^{13}C-CH_4 ±SE (‰) measured at each depth based on an open-system vertical advection model in open-water, edge, and floodplain environments during the high-water stage of the TSL flood-pulse along the Kampong Preah transect (T1-T6). Depletion of ^{13}C-CH_4 indicates water column methanogenesis, whereas enrichment of ^{13}C-CH_4 indicates preferential consumption of ^{12}C-CH_4 by methanotrophic bacteria. Methanotrophy frequently coincided with increases in dissolved O_2 (mg L^{-1}) at depth.

4.2 Fixation of C by Environment and Flood Stage

Areal C fixation rates varied by environment, though not flood stage, in TSL. During the high-water stage of the flood-pulse, an average of 100 ±20 mg C-CH_4 m^{-2} d^{-1} was fixed through methanogenesis compared to 400 ±70 mg C-CO_2 m^{-2} d^{-1} through photosynthesis (Table 3). Rates of methanogenesis were significantly greater at the edge of TSL than in open-water (p=0.010, d=1.6) or floodplain (p<0.001, d=1.3) environments during this flood stage. Methanogenesis was 9 ±3 % of *GPP* in open-water environments, 36 ±7 % of *GPP* in edge environments, and 20 ±4 % of *GPP* in floodplain

environments during the high-water stage, making it an important component of ecosystem metabolism (Figure 3a). Mixed effects modeling showed that methanogenesis shared a strong positive relationship with floodplain water depth, which was greatest at the edge of TSL during this flood stage (AICc weight=0.99, R^2=0.30, p<0.001; Table S1). *GPP* was also significantly greater at the edge than in open-water (p=0.010, d=1.6) or floodplain (p<0.001, d=1.3) environments, making the edge of TSL a hotspot for C fixation during the high-water stage.

Table 3. Mean methanogenesis (mg C-CH_4 m^{-2} d^{-1}) ±SE, *GPP* (mg C-CO_2 m^{-2} d^{-1}) ±SE, and the fraction that methanogenesis comprises of *GPP* (%) ±SE in TSL. Values are given for open-water, edge, and floodplain environments during the high- (October) and falling-water (March) stages of the flood pulse. Wilcoxon p-values for statistical differences and absolute Cohen's d-values for effect sizes are shown for pairwise comparisons across lake environments and flood stages. Means that are significantly different according to the Bonferroni-corrected α of 0.025 with low, medium, and high effect size across lake environments and flood stages are starred. Effect sizes exceed 0.8, indicating both statistical and ecological significance.

	Methanogenesis (mg C-CH_4 m^{-2} d^{-1})	***GPP*** (mg C-CO_2 m^{-2} d^{-1})	**Fraction Methanogenesis of *GPP***	***n***
High-water[a]	100 ±20	400 ±50	25 ±6 %	51
Open-water	33 ±9	360 ±60	9 ±3 %	8
Edge	270 ±40	750 ±100	36 ±7 %	9
Floodplain	70 ±10	350 ±60	20 ±4 %	34
Open-water, Edge	p=0.010, d=1.6***	p=0.010, d=1.6***	-	
Edge, Floodplain	p<0.001, d=1.3***	p<0.001, d=1.3***	-	
Open-water, Floodplain	-	-	-	
Falling-water[a]	130 ±70	500 ±200	30 ±20 %	17
Open-water	200 ±100	900 ±200	20 ±10 %	8
Edge	30 ±20	140 ±50	20 ±20 %	9
Open-water, Edge	p=0.010, d=1.4***	p=0.010, d=1.4***	-	
High-water, Falling-water	-	-	-	

Statistically different with low effect size (d=0.0-0.4)*, medium effect size (d=0.5-0.7)**, and high effect size ($d \geq 0.8$)***
Overall mean across sites[a]

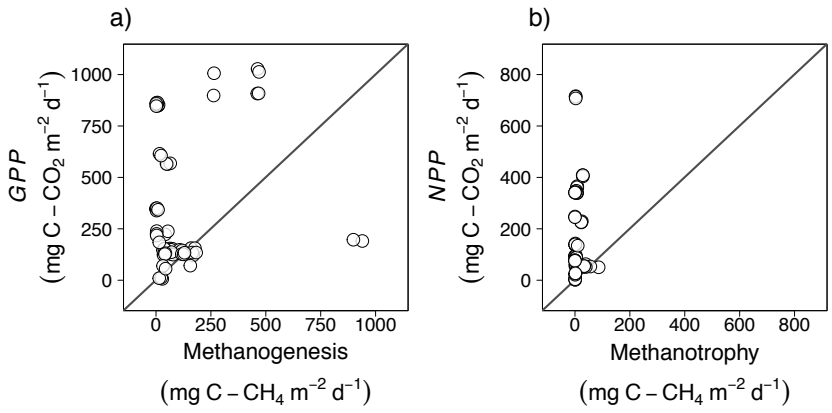

Figure 3. a) Ratios of C fixed through methanogenesis (mg C-CH_4 m^{-2} d^{-1}) and *GPP* and b) ratios of C transferred to higher trophic levels through methanotrophy (mg C-CH_4 m^{-2} d^{-1}) and *NPP* (mg C-CO_2 m^{-2} d^{-1}) in TSL.

Neither methanogenesis nor *GPP* changed significantly from the high-water stage to the falling-water stage. In contrast to the high-water stage, falling-water methanogenesis was significantly greater in the open-water environment (200 ±20 mg C-CH_2 m^{-2} d^{-1}) than at the edge of TSL (30 ±20 mg C-CH_2 m^{-2} d^{-1}; p=0.010, d=1.4). This was also true of *GPP*. Thus, lake environment was a more important driver of C fixation through methanogenesis and *GPP* at the base of the TSL food web than flood stage.

The production pathway for CH_4 seemed to vary slightly by flood stage. An α_{app} of <1.06 during the high-water stage indicated that most methanogenic C was produced via acetate fermentation (Figure 4a). This α_{app} increased from floodplain to edge to open environments, perhaps as a result of increasing substrate limitation where sites were inundated longer (i.e., open-water, see below; Whiticar and Faber, 1986). During the falling-water stage, increasing α_{app} suggests that acetate became limiting to the production of CH_4 across lake environments, leading to increasing inputs of methanogenic C produced via CO_2 reduction (Figure 4b).

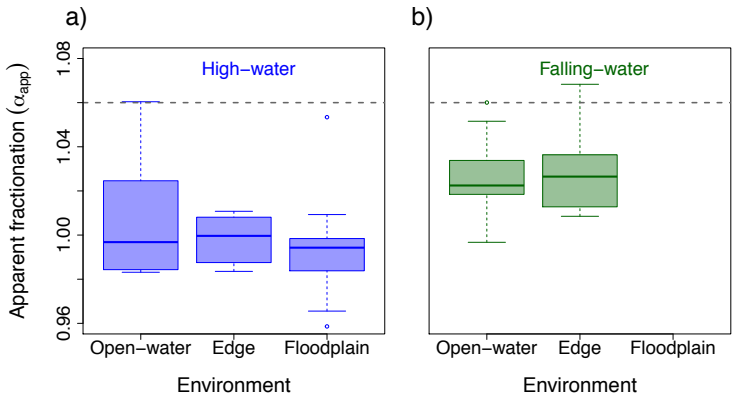

Figure 4. The apparent fractionation (α_{app}) between δ^{13}C-CO_2 and δ^{13}C-CH_4 during methanogenesis in open-water, edge, and floodplain environments during the a) high- and b) falling-water stages of the flood-pulse. An α_{app}<1.06 (grey line) indicates methanogenesis via acetate fermentation, and α_{app}>1.06 indicates methanogenesis via CO_2 reduction.

4.3 Transfer of C to Higher Trophic Levels by Environment and Flood Stage

Unlike methanogenesis, methanotrophy was remarkably consistent across lake environments during the high-water stage of the flood-pulse (Table 4). Because of its relationship to *GPP* (see eq. 4), *NPP* was significantly greater at the edge of TSL than in open-water (p=0.009, d=1.6) or floodplain (p<0.001, d=1.3) environments during this flood stage. Methanotrophy transferred C to higher trophic levels at rates that were an order of magnitude lower than C transferred by *NPP* during the high-water stage. Methanotrophy comprised 10 ±4 % of *NPP* in open-water environments, 13 ±4 % of *NPP* in edge environments, and 16 ±4 % of *NPP* in floodplain environments during this flood stage (Figure 3b). Throughout the high-water stage, methanotrophy comprised a smaller but still measurable share of *NPP* (4 ±1 % to 11 ±3 %) compared with methanogenesis relative to *GPP* (25 ±6 % to 36 ±7 %).

Methanotrophy decreased significantly from 10 ±2 mg C-CH_2 m^{-2} d^{-1} during the high-water stage to 1.5 ±0.6 mg C-CH_2 m^{-2} d^{-1} during the falling-water stage (p<0.001, d=1.1). Methanotrophy as a percentage of *NPP* decreased from 6 ±1 % during the high-water stage to 0.8 ±0.4 % during the falling-

water stage. Declining methanotrophy as a share of C transfers to higher trophic levels was due in part to *NPP*—like *GPP*—remaining relatively consistent over this period.

Table 4. Mean methanotrophy (mg C-CH_4 m^{-2} d^{-1}) ±SE, *NPP* (mg C-CO_2 m^{-2} d^{-1}) ±SE, and the fraction that methanotrophy comprises of *NPP* (%) ±SE in TSL. Values are given for open-water, edge, and floodplain environments during the high- (October) and falling-water (February) stages of the flood pulse. Wilcoxon *p*-values for statistical differences and absolute Cohen's *d*-values for effect sizes are shown for pairwise comparisons across environments and flood stages. Means that are significantly different according to the Bonferroni-corrected α of 0.025 with low, medium, and high effect size across environments and flood stages are starred. Effect sizes exceed 0.8, indicating both statistical and ecological significance.

	Methanotrophy (mg C-CH_4 m^{-2} d^{-1})	***NPP*** (mg C-CO_2 m^{-2} d^{-1})	**Fraction Methanotrophy of *NPP***	***n***
High-water[a]	10 ±2	170 ±20	6 ±1 %	51
Open-water	10 ±4	140 ±30	7 ±3 %	8
Edge	13 ±4	300 ±40	4 ±1 %	9
Floodplain	16 ±3	140 ±20	11 ±3 %	34
Open-water, Edge	-	*p*=0.009, *d*=1.6***	-	
Edge, Floodplain	-	*p*<0.001, *d*=1.3***	-	
Open-water, Floodplain	-	-	-	
Falling[a]	1.5 ±0.6	200 ±60	0.8 ±0.4 %	17
Open-water	0.9 ±0.5	400 ±100	0.2 ±0.1 %	8
Edge	2 ±1	60 ±20	3 ±2 %	9
Open-water, Edge	-	*p*=0.010, *d*=1.4***	-	
High, Falling	*p*<0.001, *d*=1.1***	-	-	

Statistically different with low effect size (*d*=0.0-0.4)*, medium effect size (*d*=0.5-0.7)**, and high effect size (*d*≥0.8)***
Mean across sites[a]

Methanotrophy showed a strong positive relationship to its substrate, *P*CH_4 (R^2=0.49, *p*<0.001; Figure 5a). Methanotrophy also shared a strong negative relationship with dissolved O_2 during the high-water stage (AICc weight=0.99, R^2=0.33, *p*<0.001; Table S1) and overall (R^2=0.33, *p*<0.001; Figure 5b). Because dissolved O_2 is the electron acceptor for aerobic CH_4 oxidation in freshwaters, this relationship was the inverse of what would be expected for this reaction. The greatest rates of methanotrophy occurred in hypoxic waters (<2 mg O_2 L^{-1}) under strongly reducing conditions (Figure 5c), indicating the potential importance of anaerobic methanotrophy in TSL.

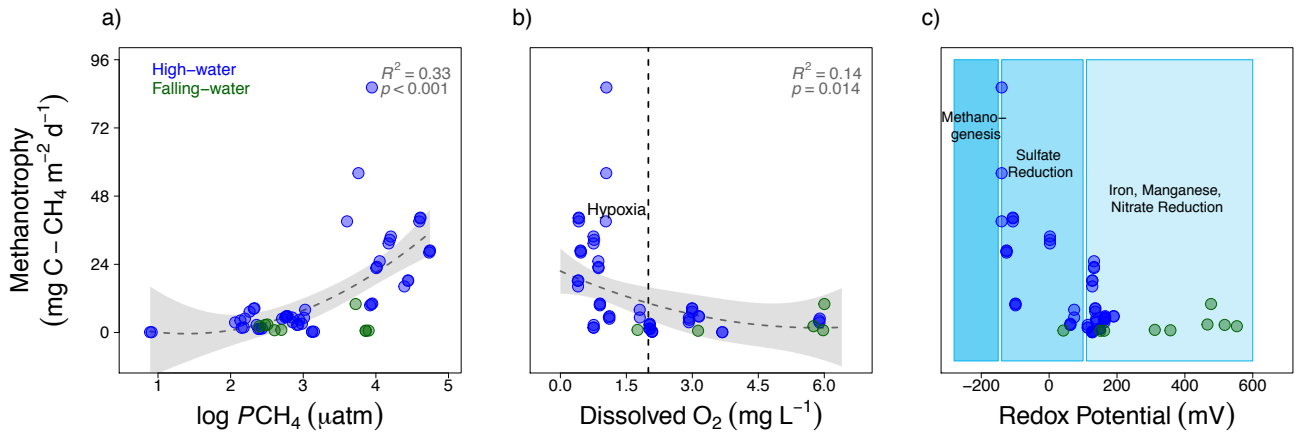

Figure 5. a) Rates of methanotrophy increase with greater availability of dissolved CH_4, b) though not dissolved O_2, which is the electron acceptor for aerobic CH_4 oxidation. Gray shading represents 95 % confidence interval of the regression line. c) The greatest rates of methanotrophy occurred under strongly reducing conditions.

4.4 Metabolic Parameters Across a Gradient of Inundation Time

Inundation time integrates spatial and temporal elements of the flood-pulse; each of the different environments sampled—open-water, edge, and floodplain—was inundated by flood waters for different amounts of time. Open environments were located in the main body of TSL, and thus were inundated for periods of time ranging from 281 to 365 days. Edge environments were inundated from 281 to 301 days per year. Floodplain environments experienced the largest range of inundation times as the flood-pulse advanced during the rising-water stage and receded during the falling-water stage, from 54 to 275 days per year.

There were no significant relationships between methanogenesis, methanotrophy, and inundation time. *GPP* and *NPP* were similarly consistent across a gradient of flooding (Figure 6a). However, there was a strong linear relationship between aerboic *ER* and inundation time (m=5.5, R^2=0.54, p<0.001) (Figure 6b), with the highest rates of *ER* occurring at sites inundated the least amount of time on the floodplain, or newly flooded sites. Driven by *ER*, *NEP* shared a similarly strong linear relationship with inundation time (m=5.5, R^2=0.60, p<0.001) (Figure 6c).

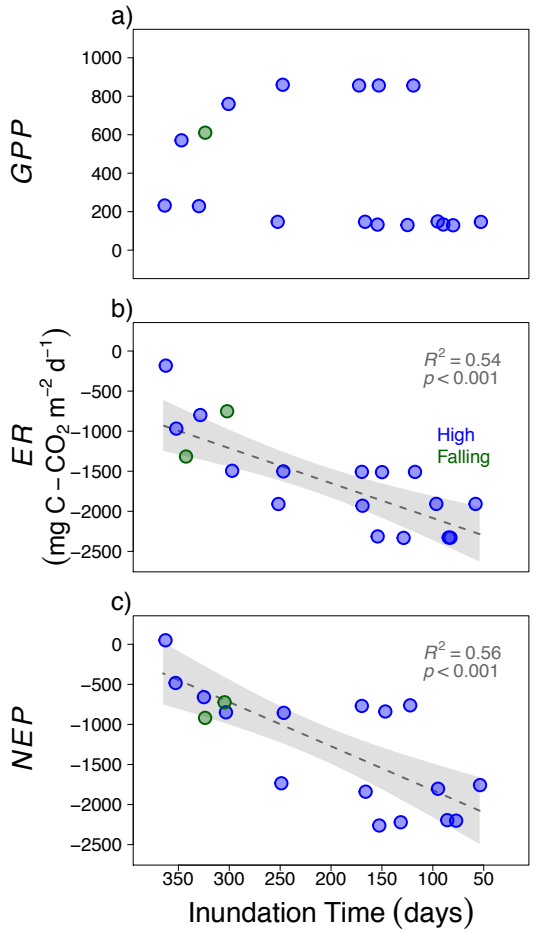

Figure 6. *GPP*, *ER*, and *NEP*, in mg C-CO_2 m^{-2} d^{-1}, in TSL during the high- and falling-water stages of the flood pulse over a gradient of flooding or inundation times (days). Gray shading represents 95 % confidence interval of the regression line.

4.5 Methanogenic C in the Food Web

Shrimp, benthic invertebrates, and many fish species showed depletion in $^{13}C/^{12}C$ relative to primary producers, indicating some contribution by methanogenic C to their biomass (Table 5, Figures 7a and 7b). The fish species *Parambassis wolfii*, *Rasbora sp.*, *Cirrhinus lobatus*, *Paralaubucher typus*, *Xenochrophis piscator*, and *Puntius brevis* were all depleted in $^{13}C/^{12}C$ to $\delta^{13}C$>-30 ‰. Freshwater shrimp ($\delta^{13}C$=-38 ±1 ‰) and *Trichogaster sp.* ($\delta^{13}C$=-35.4 ±0.2 ‰) were the members of the TSL food web that were most depleted in $^{13}C/^{12}C$. By comparison, the

$\delta^{13}C$ of phytoplankton we measured in TSL was -24.1 ±0.7 ‰, and the $\delta^{13}C$ of terrestrial C_3 plants that others have measured was -28.0 ±0.7 ‰ (Holtgrieve, *unpubl.*). In the case of the benthic catfish *Mystus mysticetus* ($\delta^{13}C$=-31.7 ±0.5 ‰), individual depletion of ^{13}C / ^{12}C shared a relationship with methanotrophy (R^2=0.50), reaching -34.1 ‰ where methanotrophy was greatest, though the significance of this relationship was limited by a low number of influential data points in the regression (p=0.289; Figure 7c).

Table 5. Members of the TSL food web measured for stable C (‰) ±SE and N (‰) ±SE isotope ratios, ordered by mean $\delta^{15}N$ signatures.

	Species	*n*	δ^{15}N (‰)	δ^{13}C (‰)
Phytoplankton		3	3 ±1	-24.1 ±0.7
Zooplankton		6	4.6 ±0.8	-28 ±1
Benthic Invertebrate		8	6.8 ±0.6	-30.7 ±0.8
Shrimp		3	7 ±1	-38 ±1
Larval Dragonfly		3	7.9 ±0.6	-28 ±0.2
Attached Invertebrate		4	8 ±1	-28.8 ±0.5
Fish	Overall	45	9.9 ±0.2	-30.6 ±0.4
	Parambassis wolfii	3	7.9 ±0.1	-31.7 ±0.1
	Rasbora sp.	5	9.1 ±0.6	-32.7 ±0.8
	Cirrhinus lobatus	4	8.9 ±0.7	-30.5 ±0.9
	Mystus mysticetus	4	10.1 ±0.5	-31.7 ±0.5
	Paralaubuca typus	5	10.2 ±0.5	-30.2 ±0.7
	Xenochrophis piscator	3	10.3 ±0.1	-30.8 ±0.1
	Labeo chrysophekadion	3	10.3 ±0.4	-29.0 ±0.6
	Puntioplites proctozysron	4	10.8 ±0.2	-27 ±1
	Anabas testudineus	3	10.9 ±0.2	-29.8 ±0.1
	Puntius brevis	3	11 ±2	-30.1 ±0.3
	Notopterus notopterus	3	11.7 ±0.1	-29.6 ±0.1
	Trichogaster sp.	5	5.7 ±0.3	-35.4 ±0.2
Snake	*Enhydris enhydris*	6	10.5 ±0.5	-29.9 ±0.8

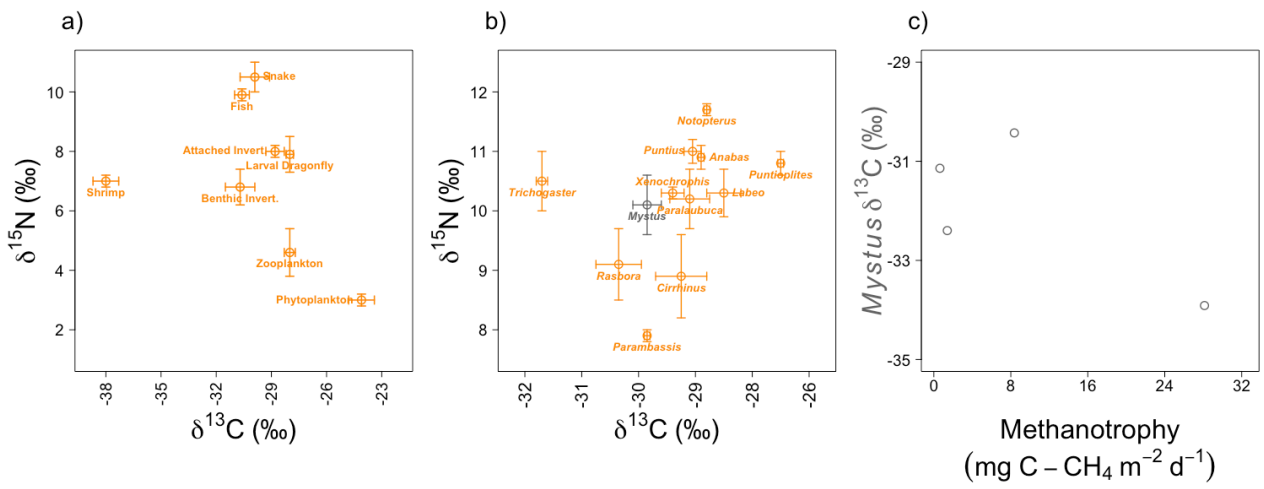

Figure 7. Stable C (‰) and N (‰) isotope ratios measured in a) members of the TSL food web and b) the fish community. c) *Mystus mysticetus* tended to show the greatest depletion in $\delta^{13}C$ where methanotrophy rates were greatest (R^2=0.50), though a low number of influential data points limited the significance of this relationship (p=0.289).

5.0 Discussion

5.1 C fixation through methanogenesis comprised a sizeable fraction of *GPP*

Methanogenesis was shown to be a sizeable fraction of *GPP* in TSL (Figure 3a), ranging from 9 ±3 % to 36 ±7 %, with a mean of 25 ±6 %, during the high-water stage (Table 3). Rates of methanogenesis and *GPP* remained statistically consistent from the high-water stage to the falling-water stage of the flood-pulse. Methanogenesis in TSL (1-469 mg C-CH_4 m^{-2} d^{-1}) was measured at rates comparable to other studies (10-130 mg C-CH_4 m^{-2} d^{-1} in Lake Washington by Rudd and Hamilton, 1978; 60-1,140 mg C-CH_4 m^{-2} d^{-1} in Lake Constance by Thebrath et al., 1993).

While rates of methanogenesis did not change across flood stages, they were significantly greater at the edge of TSL than in other sampling environments. Zeikus and Winfrey (1976), Rudd and Hamilton (1978), and Kuivila et al. (1988) long ago showed the importance of water depths to maintaining high rates of methanogenesis in lakes. Water depths great enough to isolate reduced habitat in the sediments from reaeration at the surface, yet shallow enough to

maintain a range of optimal temperatures for archaeal growth and production (15 °C to 30 °C) tend to be a critical determinant of methanogenesis (Zeikus and Winfrey, 1976; Rudd and Hamilton, 1978; Kuivila et al., 1988). During the high-water stage in TSL, the edge environment combined water depths of at least 3 m, hypoxic conditions (< 2 mg O_2 L^{-1}), and water temperatures of at least 25 °C to "fix" more C through methanogenesis than did the open-water or floodplain environments. As flood waters receded during the falling-water stage, water depths decreased at the edge and in TSL as a whole decreased, perhaps explaining the significantly greater rates of methanogenesis in the open-water environment than at the edge of the lake during this flood stage.

The standard errors of both methanogenesis and *GPP* increased during the falling-water stage, perhaps as a result of a less stable water column as flood waters receded. Turbulence at the surface has been shown to interfere with methanogenesis (Zeikus and Winfrey, 1976) and increase the error associated with free-water measurements of dissolved O_2 and *GPP* (Winslow et al., 2016). Water column stability may partially explain significant differences in methanogenesis and *GPP* across different lake environments measured by our study.

Rates of *GPP* at the edge (630 ±90 mg C-CO_2 m^{-2} d^{-1}) were nearly twice those measured in open-water (300 ±50 mg C-CO_2 m^{-2} d^{-1}) and floodplain (320 ±50 mg C-CO_2 m^{-2} d^{-1}) environments. The flood-pulse is a disturbance regime, and the edge in TSL can be described in terms of intermediate disturbance (Connell et al., 1978; Junk et al., 1989). This is the environment of TSL that is aquatic enough to support growth of phytoplankton (Moreira-Turcq et al., 2013) and macrophytes (Toth, 2015), but terrestrial enough to support growth of rooted vegetation, all of which can be colonized by periphyton (Nunes da Cunha and Junk, 2001; Bleich et al., 2015; Ferreira-Junior et al., 2016). Edge environments in flood-pulse ecosystems are

therefore broadly characterized by both 1) intermediate disturbance and 2) transitions between the aquatic and terrestrial environment, two characteristics that can increase diversity of primary producers and *GPP*.

5.2 C Transfer to higher trophic levels through methanotrophy comprised up to 11 ±3 % of *NPP*

Methanotrophy comprised a small share of C transfers to higher trophic levels relative to *NPP* (4 ±1 % to 11 ±3 %; Table 4, Figure 3b). Unlike other metabolic parameters, methanotrophy decreased significantly from the high-water stage to the falling-water stage. During this flood stage, the water column was shallower (0.5 m to 1.8 m) and presumably less methanotroph habitat was present (compared with 0.5 m to 6.5 m) (Kuivila et al., 1988; Bastviken et al., 2002).

Methanotrophy in TSL was measured at rates that were comparable to other ecosystems, including a similarly "pulsing" lake in the Amazon (Barbosa et al., 2018). Using methods identical to those in this study, Barbosa et al. (2018) measured 1-132 mg C-CH_4 m^{-3} d^{-1} in the Amazon. Rates measured in other tropical lakes and reservoirs ranged from 0 to 165 mg C-CH_4 m^{-3} d^{-1} (Jannasch, 1975; Almeida et al., 2016). For comparison, volumetric rates of methanotrophy in TSL, before multiplying by mixing depth (m), ranged from 17 to 27 mg C-CH_4 m^{-3} d^{-1} during the high-water stage of the flood-pulse and from 1 to 4 mg C-CH_4 m^{-3} d^{-1} during the falling-water stage.

No other study has directly compared methanotrophy to other mechanisms for C transfer to higher trophic levels in a tropical lake food web, like *NPP* (Table 1, Figures 1a and 1b). Recently, Shelley et al. (2014) compared methantrophy (4-15 mg C-CH_4 m^{-2} d^{-1}) to *NPP* in a network of English streams. In these temperate streams, rates of methanotrophy relative to *NPP*

ranged from 1 % to 46 %, strikingly similar to those measured in our tropical flood-pulse lake (0-86 mg C-CH_4 m^{-2} d^{-1}, 4 ±1 % to 11 ±3 %).

Some of the methanotrophy in TSL may have been anaerobic. Methanotrophy shared a negative relationship with dissolved O_2 (R^2=0.14, p=0.010) and tended to occur under hypoxic, strongly reducing conditions within redox potential ranges that indicated reduction of sulfate and metals such as iron (Figures 5b and 5c). Iron has been shown to be a thermodynamically favorable electron acceptor for anaerobic CH_4 oxidation in hypoxic temperate lake environments (Martinez-Cruz et al., 2018; Su et al., 2019), but anaerobic CH_4 oxidation has yet to be shown in tropical lakes.

Methanotrophy rates were typically an order of magnitude lower than methanogenesis rates. Consumption of dissolved CH_4 via methanotrophy increased with greater availability of dissolved CH_4 in the water column (R^2=0.33, p<0.001; Figure 5a). However, dissimilar production and consumption rates led to high PCH_4 in the water column (8-55,753 uatm) and diffusion to the atmosphere (Miller et al., *in review*). Globally, methanogenesis would seem to be greater than methanotrophy, based on widespread atmospheric CH_4 diffusion from freshwaters (St. Louis et al., 2000; Streigl et al., 2012; Crawford et al., 2014; Sanches et al., 2019).

5.3 *ER* was strongly related to inundation time

We hypothesized that methanogenesis and methanotrophy would occur along a gradient of inundation time. This was true of aerobic *ER* only, which increased with shorter inundation times on the floodplain. Water residence time tends to be a "master variable" in terms of biological utilization of flooded organic C (Junk et al., 1989; McClain et al., 2003). The timing of surface water advancement and contraction over floodplains seems optimize oxidation of this

organic C; concentrations of organic C have been shown to spike immediately following inundation in subtropical, tropical, and Mediterranean floodplains (Burns and Ryder, 2001; Wainright et al., 1992; Vasquez et al., 2015; Zuijdgeest et al., 2016). This suggests that sites inundated the least amount of time would have the greatest aerobic *ER* rates, which is what our study observed.

ER was consistently greater than *GPP*, resulting in net heterotrophy throughout the TSL flood-pulse (Figure 6c). *ER* measured using free water dissolved O_2 methods incorporates both aerobic methanotrophy and R_A, in addition to other aerobic microbial respiration. Methanotrophy was just 0.7 ±0.1 % of *ER* during the high-water stage, consuming 10 ±4 mg C-CH_4 m^{-2} d^{-1} of the 1670 ±4 mg C-CO_2 m^{-2} d^{-1} consumed by *ER* (Figure 6b). *ER* was also two orders of magnitude greater than measured methanotrophy rates during the falling-water stage. The high rates of *ER* relative to methanotrophy and net heterotrophy observed suggest aerobic microbial respiration of floodplain organic matter as the predominant energetic pathway at the base of the TSL food web.

5.4 There is isotopic evidence within multiple fish species for methanogenic support of the food web at higher trophic levels

Compared to primary producers measured by this study and others, invertebrates and fish sampled in TSL were relatively depleted in $^{13}C/^{12}C$. At the lowest trophic levels of the TSL food web, we measured a mean $\delta^{13}C$ of -24.1 ±0.7 ‰ within phytoplankton (Table 5, Figure 7a). In a review of isotopic values for different end members in tropical lakes, Hecky and Hesslein (2001) reported $\delta^{13}C$ values of -8 to -21 ‰ for phytoplankton and -0.5 to -19 ‰ for macrophytes. Terrestrial C^3 vegetation is typically more depleted in $^{13}C/^{12}C$; Boschker and Middleburg reported $\delta^{13}C$ values of -25 to -30 ‰ (2002). Most of our sampled fish species exceeded -30 ‰

(Table 7, Figure 7b), compared with 28.0 ±0.7 ‰ measured within terrestrial C^3 vegetation previously in TSL (Holtgrieve, *unpubl.*) However, we cannot conclusively attribute depletion in $^{13}C/^{12}C$ within our fish biomass to methanogenic support for these members of the TSL food web, given the depletion in $^{13}C/^{12}C$ within terrestrial C_3 vegetation reported elsewhere (up to -30 ‰; Boschker and Middleburg, 2002).

Freshwater shrimp ($\delta^{13}C$=-38 ±1 ‰), *Trichogaster sp.* ($\delta^{13}C$=-35.4 ±0.2 ‰), and some individuals ($\delta^{13}C$ of *Mystus mysticetus* biomass was measured at up to -34.1 ‰) showed unambiguous contributions of methanogenic C to their biomass (Jones and Grey, 2011; Table 6, Figures 6a and 6b). The freshwater shrimp and *Trichogaster sp.* targeted at the edge of TSL using bamboo traps based on their comparatively low mobility and floodplain habitat preferences, where rates of methanogenesis and methanotrophy were expected to be high. *Mystus mysticetus* individuals showing the greatest depletion in $^{13}C/^{12}C$ were caught where methanotrophy was high (Figure 7c). Individuals from other fish species, such as *Cirrhinus lobatus*, showed similar depletion at the edge of TSL (-32 ‰) but comparative enrichment on the floodplain (-27 ‰), suggesting mixed habitat use and diet.

Isotopic C signatures may have been influenced by the turnover rate of the tissue we sampled, dorsal muscle. Muscle tissue has a half-life of approximately 28 days (Tieszen, 1983), or approximately 50 % of two-month high-water stage in TSL. For highly mobile fish species utilizing multiple environments, sampling a tissue with a shorter turnover rate and greater temporal resolution for dietary source may be more appropriate. For example, liver tissue has a half-life of approximately six days (Tieszen, 1983). Analysis of liver tissue rather than muscle may help future studies to further resolve short term use of anaerobic habitat where rates of methanogenesis and methanotrophy are high.

6.0 Conclusion

For the first time that we are aware, we compared aerobic and anaerobic energetic pathways at the base of a tropical flood-pulse lake food web. Methanogenic fixation of C was shown to be a large fraction of *GPP* (up to 1/3) and an important component of ecosystem metabolism. Methanotrophy was less important relative *NPP*, transferring approximately 10 % of C at the base of the TSL food web to higher trophic levels. Even so, this methanogenic C could be detected at the highest trophic levels of a regionally-important fishery (Hortle, 2007; WFP, 2008; McIntyre et al., 2016). The flood-pulse enables partial food web support from anaerobic energetic pathways, and drives aerobic *ER* as a function of inundation time. Collectively, these findings highlight the importance of considering methanogenesis, methanotrophy, and other forms of anaerobic metabolism in estimates of ecosystem metabolism in lakes and other freshwaters.

7.0 Acknowledgements

We gratefully acknowledge the assistance of the Cambodian Inland Fisheries Research and Development Institute staff and the inhabitants of the floating villages on TSL. Their engagement, logistical support, and kindness made this study possible and surpassingly enjoyable. We would like to thank Vittoria Elliott of the Smithsonian Institute and Chey Thavy and David Ford of Royal University of Phnom Penh for further in-country support. Matthew Bonnema guided our application of satellite backscatter data and Hyejoo Ro assisted in stable isotopic analysis of zooplankton, invertebrates, and fish. We would also like to thank Daniel Schindler, Jeffrey Richey, and two anonymous reviewers for helpful comments during the preparation of this manuscript. This research was supported by the National Science Foundation (EAR 1740042) and Margaret A. Cargill Foundation. B.L.M. was additionally supported by a

National Science Foundation Graduate Research Fellowship (DGE 1256260), a National Security Education Boren Fellowship, and a University of Washington School of Aquatic and Fishery Sciences Graduate Fellowship. All data and data products presented in figures and analyses are available by following the link: https://github.com/blm8/Tonle-Sap-Lake-Metabolism.git.

8.0 References

Almeida, R.M., G.N. Nobrega, P.C. Junger, A.V. Figueiredo, A.S. Andrade, C.G.B. de Moura, D. Tonetta, E.S. Oliveira Jr., F. Araujo, F. Rust, J.M. Pineiro-Guerra, J.R. Mendonca Jr., L.R. Medeiros, L. Pinheiro, M. Miranda, M.R.A. Costa, M.L. Melo, R.L.G. Nobre, T. Benevides, F. Roalnd, J. de Klein, N.O. Barros, R. Mendonca, V. Becker, V.L.M. Huszar, and S. Kosten (2016), High primary production contrasts with intense carbon emission in a eutrophic tropical reservoir, *Frontiers in Microbiology*, 7, 717. http://doi.org/10.3389/fmicb.2016.00717

Arias, M.E., T.A. Cochrane, M. Kummu, H. Lauri, G.W. Holtgrieve, J. Koponen, and T. Piman (2014), Impacts of hydropower and climate change on drivers of ecological productivity of Southeast Asia's most important wetland, *Ecological Modelling*, 272, 252-263. http://doi.org/10.1016/j.ecolmodel.2013.10.015

Arias, M.E., T.A. Cochrane, D. Norton, T.J. Killeen, and P. Khon (2013), The flood pulse as the underlying driver of vegetation in the largest wetland and fishery of the Mekong Basin, *AMBIO*, 42(7), 864-876. http://doi.org/10.1007/s13280-013-0424-4

Arias, M.E., T.A. Cochrane, T. Piman, M. Kummu, B.S. Caruso, and T.J. Killeen (2012), Quantifying changes in flooding and habitats in the Tonle Sap Lake (Cambodia) caused by water infrastructure development and climate change in the Mekong Basin, *Journal of Environmental Management*, 112, 53-66. http://doi.org/10.1016/j.jenvman.2012.07.003

Barbosa, P.M., V.F. Farjalla, J.M. Melack, J.H.F. Amaral, J.S. da Silva, and B.R. Forsberg (2018), High rates of methane oxidation in an Amazon floodplain lake, *Biogeochemistry*, 137, 351-365. http://doi.org/10.1007/s10533-018-0425-2

Bastviken, D., J. Ejlertsson, I. Sundh, and L. Tranvik (2003), Methane as a source of carbon and energy for lake pelagic foodwebs, *Ecology*, 84(4), 969-981. http://doi.org/10.1890/0012-9658(2003)084[0969:MAASOC]2.0.CO;2

Bastviken, D., J. Ejlertsson, and L. Tranvik (2002), Measurement of methane oxidation in lakes—A comparison of methods, *Environmental Science and Technology*, 36, 3354-3361. http://doi.org/10.1021/es010311p

Bates, D., M. Maechler, B. Bolker, and S. Walker (2015), Fitting linear mixed effects models using lme4, *Journal of Statistical Software*, 67(1). http://doi.org/10.18637/jss.v067.i07

Bedard, C. and R. Knowles (1991), Hypolimnetic O2 consumption, denitrification, and methanogenesis in a thermally stratified lake, *Canadian Journal of Fisheries and Aquatic Sciences*, 54, 1639-1645. http://10.1139/cjfas-54-7-1639

Berg, I.A. (2011), Ecological aspects of the distribution of the different autotrophic CO2 fixation pathways, *Applied and Environmental Microbiology*, 77(6), 1925-1936. http://doi.org/10.1128/AEM.02473-10

Bleich, M.E., M.T.F. Piedade, A.F. Mortati, and T. Andre (2015), Autochthonous primary production in southern Amazon headwater streams: Novel indicators of altered environmental integrity, *Ecological Indicators*, 53, 154-161. http://doi.org/10.1016/j.ecolind.2015.01.040

Bogard, M.J., P.A. del Giorgio, L. Boutet, M.C. Garcia-Chaves, Y.T. Prairie, A. Merante, and A.M. Derry (2014), Oxic water column methanogenesis as a major component of aquatic CH4 fluxes, *Nature Communications*, 5, 5350. http://doi.org/10.1038/ncomms6350

Boon, P.I. and A. Mitchell (1995), Methanogenesis in the sediments of an Australian freshwater wetland—Comparison with aerobic decay, and factors controlling methanogenesis, *FEMS Microbiology Ecology*, 18(3), 175-190. http://doi.org/10.1016/0168-6496(95)00053-5

Boschker, H.T.S. and J.J. Middleburg (2002), Stable isotopes and biomarkers in microbial ecology, *FEMS Microbiology Ecology*, 40(2), 85-95. http://doi.org/10.1111/j.1574-6941.2002.tb00940.x

Bunn, S.E. and P.I. Boon (1993), What sources of organic carbon drive food webs in billabongs? A study based on stable isotope analysis, *Oecologia*, 96, 85-94. http://doi.org/10.1007/BF00318034

Burnham, K.P. and D.R. Anderson (2004), Multimodel inference—Understanding AIC and BIC in model selection, *Sociological Methods and Research*, 33(2), 261-304. http://doi.org/10.1177/0049124104268644

Burns, A. and D.S. Ryder (2001), Response of bacterial extracellular enzymes to inundation of floodplain sediments, *Freshwater Biology*, 46, 1299–1307. http://doi.org/10.1046/j.1365-2427.2001.00750.x

Carleton, R.G. and R.G. Wetzel (1988), Phosphorus flux from lake sediments—Effect of epipelic algal oxygen production, *Limnology and Oceanography*, 33, 562-570. http://doi.org/10.4319/lo.1988.33.4.0562

Cohen, J. (1988), Statistical power analysis for the behavioral sciences (2nd ed.), Lawrence Earlbaum Associates, Hillsdale, New Jersey, U.S.A.

Cole, J.J. and N.F. Cole (1998), Atmospheric exchange of carbon dioxide in a low wind oligotrophic lake measured by the addition of SF6, *Limnology and Oceanography*, 43(4), 647-656. http://doi.org/10.4319/lo.1998.43.4.0647

Conrad, R., M. Noll, P. Claus, M. Klose, W.R. Bastos, and A. Enrich-Prast (2011), Stable carbon isotope discrimination and microbiology of methane formation in tropical anoxic lake sediments, *Biogeosciences*, 8, 795-814. http://doi.org/10.5194/bg-8-795-2011

Conrad, R., O.C. Chan, P. Claus, and P. Casper (2007), Characterization of methanogenic Archaea and stable isotope fractionation during methane production in the profundal sediment of an oligotrophic lake (Lake Stechlin, Germany), *Limnology and Oceanography*, 52, 1393-1406. http://doi.org/10.4319/lo.2007.52.4.1393

Conrad, R. (2005), Quantification of methanogenic pathways using stable carbon isotopic signatures—A review and a proposal, *Organic Geochemistry*, 36, 739-752. http://doi.org/10.1016/j.orggeochem.2004.09.006

Crawford, J.T., N.R. Lottig, E.H. Stanley, J.F. Walker, P.C. Hanson, J.C. Finlay, and R.G. Streigl (2014), CO2 and CH4 emissions from streams in a lake-rich landscape—Patterns, controls, and regional significance, *Global Biogeochemical Cycles*, 28, 197-210. http://doi.org/10.1002/2013GB004661

Del Sontro, T., D.F. McGinnis, S. Sobek, I. Ostrovsky, and B. Wehrli (2010), Extreme methane emissions from a Swiss hydropower reservoir—Contribution from bubbling sediments, *Environmental Science and Technology*, 44, 2419-2425. http://doi.org/10.1021/es9031369

Deutzmann, J.S., P. Stief, J. Brandes, and B. Schink (2014), Anaerboic methane oxidation coupled to denitrification is the dominant methane sink in a deep lake, *Proceedings of the National Academy of Sciences*, 111(51), 18273-18278. http://doi.org.10.1073/pnas.1411617111

Dilling, W., and H. Cypionka (1990), Aerobic respiration in sulfate-reducing bacteria, *FEMS Microbiology Letters,* 71, 123–127. http://doi.org/10.1016/0378-1097(90)90043-P

Downing, J.A. (2009), Global limnology—Up-scaling aquatic services and processes to planet Earth, *Internationale Vereingigung fur Theorestische und Angewandte Limnologie—Verhandlungen*, 30, 1149-1166. http://doi.org/10.1080/03680770.2009.11923903

Gates, D.M. (1966), Spectral distribution of solar radiation at the earth's surface, *Science*, 151(3710), 523-529. http://doi.org/10.1126/science.151.3710.523

Gorelick, N., M. Hancher, M. Dixon, S. Ilyushchenko, D. Thau, and R. Moore (2017), Google Earth Engine: Planetary-scale geospatial analysis for everyone, *Remote sensing of Environment*, 202, 18-27. http://doi.org/10.1016/j.rse.2017.06.031

Greening, C., A. Biswas, C.R. Carere, C.J. Jackson, M.C. Taylor, M.B. Stott, G.M. Cook, and S.E. Moreles (2016), Genomic and metagenomic surveys of hydrogenase distribution indicate H2 is a widely utilised energy source for microbial growth and survival, *The ISME Journal—Multidisciplinary Journal of Microbial Ecology*, 10, 761-777. http://doi.org/10.1038/ismej.2015.153

Grossart, H., K. Frindte, C. Dziallas, W. Eckert, and K.W. Tang (2011), Microbial methane production in oxygenated water column of an oligotrophic, *Proceedings of the National Academy of Sciences*, 108(49), 19657-19661. http://doi.org/10.1073/pnas.1110716108

Hall Jr., R. and J. Beaulieu (2013), Estimating autotrophic respiration in streams using daily metabolism data, *Freshwater Science*, 32(2), 507-516. http://doi.org/10.1899/12-147.1

Hamilton, S.K., S.J. Sippel, and J.M. Melack (1995), Oxygen depletion and carbon dioxide and methane production in waters of the Pantanal wetland of Brazil, *Biogeochemistry*, 30, 115-141.

Happell, J.D., J.P. Chanton, and W.S. Showers (1994), Influence of methane oxidation on the stable isotopic composition of methane emitted from Florida swamp forests, *Geochimica et Cosmochimica Acta*, 58(20), 4377-4388. http://doi.org/10.1016/0016-7037(94)90341-7

Hecky, R.E. and R.H. Hesslein (2001), Contributions of benthic algae to lake food webs as revealed by stable isotope analysis, *Freshwater Science*, 14(4), 631-653. http://doi.org/10.2307/1467546

Heesen, D. and K. Nygaard (1992), Bacterial transfer of methane and detritus—Implications for the pelagic carbon budget and gaseous release, *Archiv fur Hydrobiologie Beiheft Ergebnisse der Limnologie*, 37, 139-148.

Hortle, K.G. (2007), Consumption and the yield of fish and other aquatic animals from the Lower Mekong Basin (MRC Technical Paper No. 16), Mekong River Commission, Vientiane, Lao PDR.

Holtgrieve, G.W., M.E. Arias, K.N. Irvine, D. Lamberts, E.J. Ward, M. Kummu, J. Koponen, J. Sarkkula, and J.E. Richey, (2013), Patterns of ecosystem metabolism in the Tonle Sap Lake, Cambodia with links to capture fisheries, *PLoS ONE*, 8(8), e71395. http://doi.org/10.1371/journal.pone.0071395

IPCC (2014), Climate change 2014—Synthesis report, Contribution of Working Groups I, II, and III to the Fifth Assessment Report of the Intergovernmental Panel on Climate Change, Core Writing Team, R.K. Pachauri, and L.A. Meyer (eds.), IPCC, Geneva, Switzerland.

IPCC (2007), Climate change 2007—Synthesis report, Contribution of Working Groups I, II, and III to the Fourth Assessment Report of the Intergovernmental Panel on Climate Change, Core Writing Team, R.K. Pachauri, and L.A. Meyer (eds.), IPCC, Geneva, Switzerland.

Jannsch, H.W. (1975), Methane oxidation in Lake Kivua (Central Africa), *Limnology and Oceanography*, 20, 860-862. http://doi.org/10.4319/lo.1975.20.5.0860

Jellison, R. and J.M. Melack (1993), Algal photosynthetic activity and its response to meromixis in hypersaline Mono Lake, California, *Limnology and Oceanography*, 38(4), 818-837. http://doi.org/10.4319/lo.1993.38.4.0818

Jones, R.I. and J. Grey (2011), Biogenic methane in freshwater food webs, *Freshwater Biology*, 56, 213-229. http://doi.org/10.1111/j.1365-2427.2010.02494.x

Jones, R.I., J. Grey, D. Sleep, and L. Arvola (1999), Stable isotope analysis of zooplankton carbon nutrition in humic lakes, *Oikos*, 86, 97-104.

Junk, W.J., P.B. Bayley, and R.E. Sparks (1989), The flood pulse concept in river-floodplain systems, 110-127, *In* D.P. Dodge (ed.), Proceedings of the International Large River Symposium, *Canadian Special Publication of Fisheries and Aquatic Sciences*, 106.

Kankaala, P., S. Taipale, J. Grey, E. Sonninen, L. Arvola, R.I. Jones (2006), Experimental $d^{13}C$ evidence for a contribution of methane to pelagic food webs in lakes, *Limnology and Oceanography*, 51(6), 2821-2827. http://doi.org/10.4319/lo.2006.51.6.2821

Keddy, P.A., L.H. Fraser, A.I. Solomeshch, W.J. Junk, D.R. Campbell, M.T.K. Arroyo, and C.J.R. Alho (2009), Wet and wonderful—The world's largest wetlands are conservation priorities, *BioScience*, 59(1), 39-51. http://doi.org/10.1525/bio.2009.59.1.8

Kellermann, M.Y., G. Wegener, M. Elvert, M.Y. Yoshinaga, Y.S., Lin, T. Holler, X.P. Mollar, K. Knittel, and K.U. Hinrichs (2012), Autotrophy as predominant mode of carbon fixation in thermophilic anaerobic methane-oxidizing microbial communities, *Proceedings of the National Academy of Sciences,* 109, 19321–19326. http://doi.org/10.1073/pnas.1208795109

Kuivila, K.M., J.W. Murray, A.H. Devol, M.E. Lidstrom, and C.E. Reimers (1988), Methane cycling in the sediments of Lake Washington, *Limnology and Oceanography*, 33, 571-581. http://doi.org/10.4319/lo.1988.33.4.0571

Lauri, H., H. de Moel, P.J. Ward, T.A. Rasanen, M. Keskinen, and M. Kummu (2012), Future changes in Mekong River hydrology—Impact of climate change and reservoir operation on discharge, *Hydrology and Earth System Sciences Discussion*, 9, 6569-6614. http://doi.org/10.5194/hessd-9-6569-2012

Li, W., J.E. Dore, A.J. Steigmeyer, Y.J. Cho, O.S. Kim, R.M. Morgan-Kiss, M.L. Skidmore, and

J.C. Priscu (2019), Methane production in the oxygenated water column of a perennially ice-covered Antarctic lake, *Limnology and Oceanography*, 65(1), 143-156. http://doi.org/10.1002/lno.11257

Lungdahl, L.G. (1986), The autotrophic pathway of acetate synthesis in acetogenic bacteria, *Annual Review of Microbiology*, 40, 415-450.

Martinez-Cruz, K., M.C. Lewis, I.C. Herriott, A. Sepulveda-Jauregui, K.W. Anthony, F. Thalasso, M.B. Leigh (2017), Anaerboic oxidation of methane by aerboic methanotrophs in sub-Arctic lake sediments, *Science of the Total Environment*, 607-608, 23-31. http://doi.org/10.1016/j.scitotenv.2017.06.187

Mattson, M.D. and G.E. Likens (1993), Redox reactions of organic matter decomposition in a soft water lake, *Biogeochemistry*, 19, 149-172.

McClain, M. E., E.W. Boyer, C.L. Dent, S.E. Gergel, N.B. Grimm, P.M. Groffman, S.C. Hart, J.W. Harvey, C.A. Johnston, E. Mayorga, W.H. McDowell, and G. Pinay (2003), Biogeochemical Hot Spots and Hot Moments at the Interface of Terrestrial and Aquatic Ecosystems, *Ecosystems*, 6(4), 301–312. http://doi.org/10.1007/s10021-003-0161-9

McIntyre, P.B., C.A. Reidy-Liermann, and C. Revenga (2016), Linking freshwater fishery management to global food security and biodiversity conservation, *Proceedings of the National Academy of Sciences*, 113, 12880-12885. http://doi.org/10.1073/pnas.1521540113

Moreira-Turcq, P., M.P. Bonnet, M. Amorim, M. Bernardes, C. Lagane, L. Maurice, M. Perez, and P. Seyler (2013), Seasonal variability in concentration, composition, age, and fluxes of particulate organic carbon exchanged between the floodplain and Amazon River, *Global Biogeochemical Cycles*, 27(1), 119–130. http://doi.org/10.1002/gbc.20022

MRC (2009), Mekong River Commission Spatial Database, Mekong River Commission, Vientiane, Lao PDR. http://www.mrcmekong.org/spatial/data_catalog.htm

Nelson, G.A. (2019), fishmethods—Fishery Science Methods and Models, R package version 1.11-1, http://CRAN.R-project.org/package=fishmethods.

Patt, T.E., G.C. Cole, J. Bland, and R.S. Hanson (1974), Isolation and characterization of bacteria that grown on methane and organic compounds as sole sources of carbon and energy, *Journal of Bacteriology*, 120(2), 955-964.

Peterson, B.J. and B. Fry (1987), Stable isotopes in ecosystem studies, *Annual Review of Eoclogical Systems*, 18, 293-320.

R Core Team (2019), R—A language and environment for statistical computing, R Foundation for Statistical Computing, Vienna, Austria, http://www.R-project.org/.

Richey, J.E., J.M. Melack, A.K. Aufdenkampe, V.M. Ballester, and L.L. Hess (2002), Outgassing from Amazonian rivers and wetlands as a large tropical source of atmospheric CO2, *Nature*, 416, 617-620. http://doi.org/10.1038/416617a

Roslev, P., N. Iversen, K. Henriksen (1997), Oxidation and assimilation of atmospheric methane by soil methane oxidizers, *Applied and Environmental Microbiology*, 63, 874-880.

Rudd, J.W.M., and R.D. Hamilton (1978), Methane cycling in a eutrophic hield lake and its effects on who lake metabolism, *Limnology and Oceanography*, 23, 337-348. http://doi.org/10.4319/lo.1978.23.2.0337

Sabo, J.L., A. Ruhi, G.W. Holtgrieve, V. Elliot, M.E. Arias, P.B. Ngor, T.A. Rasanen, and S. Nam (2017), Designing river flows to improve food security futures in the Lower Mekong Basin, *Science*, 358(6368), 1-11. http://doi.org/10.1126/science.aao1053

Sanches, L.F., B. Guenet, C.C. Marinho, N. Barros, and F. de Assis Esteves (2019), Global regulation of methane emission from natural lakes, *Scientific Reports*, 9(255), 1-10. http://doi.org/10.1038/s41598-018-3619-5

Sanseverino, A.M., D. Bastviken, I. Sundh, J. Pickova, and A. Enrch-Prast (2013), Methane supports aquatic food webs to the fish level, PLoS ONE, 8(1), e42723. http://doi.org/10.1371/journal.pone.0042723

Shelley, F., J. Grey, and M. Trimmer (2014), Widespread methanogenic primary production in lowland chalk rivers, *Proceedings of the Royal Society—Biology*, 281, 20132854. http://doi.org/10.1098/rspb.2013.2854

St. Louis, V.L., C. Kelly, E. Duchemin, J.W.M. Rudd, and D.M. Rosenberg (2000), Reservoir surfaces as sources of greenhouse gases to the atmosphere—A global estimate, *Bioscience*, 50(9), 766-775. http://doi.org/10.1641/0006-3568(2000)050[0766:RSASOG]2.0.CO;2

Streigl, R.G., M.M. Dornblaser, C.P. McDonald, J.R. Rover, and E.G. Stets (2012), Carbon dioxide and methane emissions from the Yukon River system, *Global Biogeochemical Cycles*, 26, GB0E05. http://doi.org/10.1029/2012GB004306

Su, G., J. opfi, H. Yao, L. Steinle, H. Niemann, and M.F. Lehmann (2019), Manganese/iron-supported sulfate-dependent anaerboic oxidation of methane by archea in lake sediments, *Limnology and Oceanography*, *In press*. http://doi.org/10.1002/lno.11354

Thebrath, B., F. Rothfuss, M.J. Whiticar, and R. Conrad (1993), Methane production in littoral sediment of Lake Constance, *FEMS Microbiology Letters*, 102(3-4), 279-289. http://doi.org/10.1016/0378-1097(93)90210-S

Tieszen, L.L., T. Boutton, K.G. Tesdahl, and N.A. Slade (1983), Fractionation and turnover of stable carbon isotopes in animal tissues—Implications for $d^{13}C$ analysis of diet,

Oecologia, 57(1), 32-37. http://doi.org/10.1007/BF00379558

Torres, R., P. Snoeij, D. Geudtner, D. Bibby, M. Davidson, E. Attema, P. Potin, B. Rommen, N. Floury, M. Brown, I.N. Traver, P. Deghaye, B. Duesmann, B. Rosich N. Miranda, C. Bruno, M. L'Abbate, R. Croci, and F. Rostan (2012), GMES Sentinel-1 mission, *Remote Sensing of Environment*, 120, 9-24. http://doi.org/10.1016/j.rse.2011.05.028

Toth, L.A. (2015), Invasibility drives restoration of a floodplain plant community, *River Research and Applications*, 31, 1319-1327. http://doi.org/10.1002/rra.2836

Trimmer, M., F.C. Shelley, K.J. Purdy, S.T. Maanoja, P.M. Chronopoulou, and J. Grey (2015), Riverbed methanotrophy sustained by high carbon conversion efficiency, *The ISME Journal—Multidisciplinary Journal of Microbial Ecology*, 9, 2304-2314. http://doi.org/10.1038/ismej.215.98

Urmann, K., A. Lazzaro, I. Gandolfi, M.H. Schroth, and J. Zeyer (2009), Response of methanotrophic activity and community structure to temperature changes in a diffusive CH4/O2 counter gradient in an unsaturated porous medium, *FEMS Microbiology Ecology*, 69, 202-212. http://doi.org/10.1111/j.1574-6941.2009.00708.x

Utsumi, M., Y, Nojiri, T. Nakamura, T. Nozawa, A. Otsuki, N. Takamura, M. Watanabe, and H. Seki (1998), Dynamics of dissolved methane and methane oxidation in dimictic Lake Nojiri during winter, *Limnology and Oceanography*, 43, 10-17. http://doi.org/10.4319/lo.1998.43.1.0010

Vasquez, E., E. Ejarque, I. Ylla, A.M. Romaní, and A. Butturini (2015), Impact of drying/rewetting cycles on the bioavailability of dissolved organic matter molecular-weight fractions in a Mediterranean stream, *Freshwater Science*, 34(1), 263–275. http://doi.org/10.1086/679616

Wainright, S.C., C.A. Couch, and J.L. Meyer (1992), Fluxes of bacteria and organic matter into a blackwater river from river sediments and floodplain soils, *Freshwater Biology*, 28(1), 37-48. http://doi.org/10.1111/j.1365-2427.1992.tb00560.x

Wantzen, K.M., W.J. Junk, and K.O. Rothhaupt (2008), An extension of the floodpulse concept (FPC) for lakes, Hydrobiologia, 613, 151-170. http://doi.org/10.1007/s10750-008-9480-3

Whalen, S.C., W.S. Reeburgh, and K.A. Sandbeck (1990), Rapid methan oxidation in a landfill cover soil, *Applied and Environmental Microbiology*, 56, 3405-3411.

Whiticar, M.J. (1999), Carbon and hydrogen isotope systematics of bacterial formation and oxidation of methane, *Chemical Geology*, 161, 291-314. http://doi.org/10.1016/S0009-2541(99)00092-3

Whiticar, M.J. and E. Faber (1986), Methane oxidation in sediment and water column environments—Isotopic evidence, *Organic Geochemistry*, 10(4-6), 759-768.

http://doi.org/10.1016/S0146-6380(86)80013-4

Whittenbury, R., K.C. Phillips, and J.F. Wilkinson (1970), Enrichment, isolation and some properties of methane-utilizing bacteria, *Journal of General Microbiology*, 61, 205-218.

Winfrey, M.R., D.R. Nelson, S.C. Klevickis, and J.G. Zeikus (1977), Association of hydrogen metabolism with methanogenesis in Lake Mendota sediments, *Applied and Environmental Microbiology*, 33, 312-378.

Winslow, L.A., J.A. Zwart, R.D. Batt, H.A. Dugan, R.I. Woolway, J.R. Corman, and J.S. Read (2016), LakeMetabolizer—An R package for estimating lake metabolism from free-water oxygen using diverse statistical models, *Inland Waters*, 6(4), 622-636. http://doi.org/10.1080/IW-6.4.883

Zar, J.H. (2010), Biostatistical Analysis, Pearson, Upper Saddle River, New Jersey, U.S.A.

Zeikus, J.G. and M.R. Winfrey (1976), Temperature limitation of methanogenesis in aquatic sediments, *Applied and Environmental Microbiology*, 31(1), 99-107.

Zuijdgeest, A., S. Baumgartner, and B. Wehrli (2016), Hysteresis effects in organic matter turnover in a tropical floodplain during a flood cycle, *Biogeochemistry*, 131, 49-63. http://10.1007/s10533-016-0263-z

Chapter 4

Magnitudes and drivers of greenhouse gas fluxes in floodplain ponds during drawdown and inundation by the Three Gorges Reservoir

Benjamin L. Miller[1,2]

Huai Chen[1]

Yixin He[1]

Xingzhong Yuan[3]

G. W. Holtgrieve[2]

1. Chinese Academy of Sciences Chengdu Institute of Biology
2. University of Washington School of Aquatic and Fishery Sciences
3. Chongqing University College of Resources and the Environment

1.0 Abstract

Hydropower reservoirs are well-known emitters of greenhouse gases to the atmosphere. This is due in part to seasonal water level fluctuations that transfer terrestrial C and N from floodplains to reservoirs. Partial pressures and fluxes of the greenhouse gases CH_4, CO_2, and N_2O are also a function of *in-situ* biological C and N cycling and overall ecosystem metabolism, which varies on a diel basis within inland waters. Thus, greenhouse gas emissions in hydropower reservoirs likely vary over seasonal and diel timescales with local hydrology and ecosystem metabolism. China's Three Gorges Reservoir is among the largest and newest in the world, with a floodplain that encompasses approximately one third of the reservoir area. We measured diel partial pressures and fluxes of greenhouse gases in ponds on the Three Gorges Floodplain. We repeated these measurements on the submerged floodplain following inundation by the Three Gorges Reservoir. During reservoir drawdown, CH_4 ebullition comprised 60-68 % of emissions from floodplain ponds to the atmosphere. Using linear mixed effects modeling, we show that partial pressures of CH_4 and CO_2 and diffusive CO_2 fluxes in floodplain ponds varied on a diel basis with *in-situ* respiration. Floodplain inundation by the Three Gorges Reservoir significantly moderated areal CH_4 diffusion and ebullition. Diel pCO_2, pCH_4, pN_2O, and diffusive fluxes of CO_2 on the submerged floodplain were also driven by *in-situ* respiration. The drawdown/inundation cycle of the Three Gorges Reservoir therefore changes the magnitudes of aquatic greenhouse gas fluxes on its floodplain.

2.0 Introduction

Impounded rivers are an important component of the global carbon (C) cycle, contributing 4-17 % of C emitted from inland waters to the atmosphere each year (Aufdenkampe et al., 2011; Barros et al., 2011; Deemer et al., 2016). A recent synthesis of hydropower

reservoirs measured globally found that 84% were sources for diffusive carbon dioxide (CO_2) and all were either sources for diffusive methane (CH_4) or CH_4 neutral (Deemer et al., 2016). Hydropower reservoirs occur in larger watersheds than naturally occurring lakes and receive comparatively high nutrient and organic matter (OM) inputs, which influence *in-situ* primary production and respiration (Knoll et al., 2003; Hayes et al., 2017; Mendonca et al., 2017). Reservoirs also receive OM through the flooding of terrestrial landscapes during reservoir formation and subsequent fluctuations in water storage (Jacinthe et al., 2012; Maeck et al., 2014). Growth of terrestrial OM on reservoir floodplains is transferred to reservoirs during often predictable seasonal drawdown/inundation cycles (Junk et al., 1989; Battin et al., 2008; Chen et al., 2009a). Respiration of terrestrial OM proceeds considerably faster in lakes, rivers, and flooded soils (Battin et al. 2008; McNicol and Silver et al., 2014). Riverine OM concentrations have been shown to spike following inundation of subtropical and temperate floodplains (Wainright et al., 1992; Burns and Ryder, 2001; Vasquez et al., 2015). This likely results in concurrent spikes in diffusive CH_4 and CO_2 emissions as OM is respired.

Bubbling or ebullition is another important pathway for CH_4 to the atmosphere in temperate (Del Sontro et al., 2010) and tropical (Del Sontro et al., 2011) reservoirs. Sparingly soluble CH_4 may be produced in anaerobic sediments more quickly than sediment-water diffusion rates and form bubbles (Fendinger et al., 1992; Mattson and Likens, 1990). These bubbles rise to the water's surface, undergoing minimal oxidation (Ostrovsky et al., 2008; Del Sontro et al., 2010). Deemer et al. (2016) estimate that ebullition comprises an average of 65 % of total CH_4 emissions from reservoirs globally. Under low and dynamic hydrostatic pressures on submerged floodplains, ebullition is likely a key component of CH_4 emissions.

There have been fewer measurements of N_2O emissions from hydropower reservoirs. The recent synthesis by Deemer et al. (2016) included flux measurements from 161 reservoirs for CH_4, 229 for CO_2, and just 58 for N_2O. Tropical (Guerin et al., 2008; Naqvi et al., 2018), subtropical (Chen et al., 2009a; Zhao et al., 2013; Zhu et al., 2013; Li et al., 2018), temperate (Tomaszek et al., 2003; Deemer et al., 2011; Beaulieu et al., 2014; Li et al., 2018), and boreal (Huttunen et al., 2002) reservoirs that have been measured indicate that they are also sources for N_2O. N_2O has 298 times the global warming potential of CO_2 on a per molar basis in the atmosphere over a 100-year timescale, making it an important addition to measurements of reservoir greenhouse gas emissions (IPCC, 2001; Myrhe et al., 2013).

CH_4, CO_2, and N_2O within inland waters result from metabolic fixation and respiration of C and nitrogen (N). Most studies of hydropower reservoirs and other aquatic ecosystems concentrate sampling at a single point during the day, despite this association with ecosystem metabolism. H.T. Odum classically showed the metabolic balance of inland waters to be more autotrophic during the day and more heterotrophic during the night using net oxygen (O_2) dynamics (1956). Tobias et al. (2007), Hotchkiss et al. (2014), and Schindler et al. (2017) have since shown that daytime aerobic respiration can be 54-340 % of nighttime respiration in temperate lakes and streams. They attribute this to greater production of labile OM algal exudates (Cole et al., 1982; Kaplan and Blott, 1982; Bains and Pace, 1991) and higher temperatures during the day (Yvon-Durocher et al., 2012). Decoupling of CO_2 partial pressures from O_2 dynamics and correlations to primary production and aerobic respiration have also been shown by others (Peeters et al., 2016; Stets et al., 2017). Thus, metabolic properties such as dissolved O_2 and temperature have the potential to influence net consumption or production of

CO_2 differently over 24 hours. How the partial pressures and fluxes of CH_4 and N_2O vary with ecosystem metabolism on diel timescales is less clear (Hoellein et al., 2013).

Efforts have been made to characterize greenhouse gas emissions from hydropower at other temporal and spatial scales. Hydropower reservoirs less than 10-20 years old tend to emit more CH_4 and CO_2 per unit area than older hydropower reservoirs (St. Louis et al., 2000; Barros et al., 2011). Of these, reservoirs in tropical regions tend to emit more CH_4 and CO_2 per unit area than reservoirs in temperate regions (Galy-Lacaux et al., 1997; Barros et al, 2011). Current rates of hydropower development are greatest in tropical and subtropical regions (Zarfl et al., 2015). Some of the highest rates of impoundment (>100 dams currently planned) are in China's Yangtze River basin (Zarfl et al., 2015), making these newly-constructed, subtropical reservoirs likely greenhouse gas emitters.

The Three Gorges Reservoir on the Yangtze River represents an opportunity for the study of diel greenhouse gas emissions from a comparatively new subtropical hydropower reservoir and its floodplain. Filled in 2010, the Three Gorges Reservoir is among the largest in the world, covering 1,106 km^2 in central China (Zhang et al., 2018). The Three Gorges Floodplain covers 321 km^2 or just under one third of the reservoir's area (Zhang et al., 2018). Studies by Chen et al. (2009a, 2009b), Zhao et al. (2013), Zhu et al. (2013), Li et al. (2013), and Zhou et al. (2017) have quantified diffusive CH_4, CO_2, and N_2O fluxes in the region. However, none have measured diel fluxes and CH_4 ebullition during both reservoir drawdown and inundation on the Three Gorges Floodplain.

The Three Gorges Floodplain is increasingly targeted by displaced farmers for pond aquaculture in attempts to supplement agricultural productivity during reservoir drawdown (Li et al., 2013; Zhou et al., 2017; Zhang et al., 2018). Globally, ponds less than 1,000 m^2 are hotspots

for CH_4 and CO_2 emissions (Holgerson and Raymond, 2016). Although water bodies this size are difficult to detect and delineate from wetlands using satellite imagery, it is thought that ponds comprise approximately 9 % of non-running or lentic inland waters, which include lakes and reservoirs (Holgerson and Raymond, 2016). Holgerson and Raymond (2016) estimate that natural ponds contribute 40% of diffusive CH_4 emissions from lentic inland waters worldwide. Ponds created on the terrestrial landscape for a variety of purposes including stock watering, irrigation, and aquaculture have been also found to emit CH_4 (Ollivier et al., 2018; Peacock et al., 2019). In some cases, these ponds emit CH_4 at higher rates than natural ponds through diffusive and ebullition flux pathways (Grinham et al., 2018), though more comparative data are needed. Natural and aquaculture ponds are among the aquatic environments that remain on the Three Gorges Floodplain during approximately six months of reservoir drawdown, from April to September each year. These expanding environments on the Three Gorges Floodplain are likely emissions hotspots.

In this study, we measured diel greenhouse gas partial pressures and fluxes during both reservoir drawdown and inundation on the Three Gorges Floodplain. During reservoir drawdown, we carried out measurements in a natural pond and a newly-created aquaculture pond. We repeated these measurements on the submerged floodplain following inundation by the Three Gorges Reservoir. We used linear mixed effects modeling to determine relative importance of ecosystem metabolism to observed diel patterns of CH_4, CO_2, and N_2O partial pressures and diffusive fluxes. By conducting field-based measurements of C and N cycling, we account for commonly overlooked contributions of CH_4 emissions from floodplain ponds. We show that greenhouse gas partial pressures and fluxes vary over both seasonal and diel timescales along with drawdown/inundation cycle and ecosystem metabolism.

3.0 Methods

3.1 Study Locations

We conducted this study in the Pengxi River Wetland Reserve on the Three Gorges Floodplain between June 2014 and January 2015 (Figure 1). This region of P.R. China is characterized by a subtropical, humid monsoonal climate, with a mean annual temperature of 18.2 °C and a mean annual precipitation of 1200 mm. The Pengxi River Wetland Reserve occupies 36.9 km^2 at elevations ranging from 160 to 175 m above sea level (a.s.l.). During reservoir drawdown, water levels in the Three Gorges Reservoir are 145 m a.s.l., leaving much of the reserve exposed at pre-impoundment levels (Figure 1b). We sampled one natural pond (31°5'37.74" N, 108°27'45.05" E, 150 m a.s.l., 488 m^2 area, 54 cm mean depth) and one aquaculture pond (31°12'30.26" N, 108°27'0.05" E, 159 m a.s.l., 314 m^2 area, 82 cm mean depth). The aquaculture pond was used to cultivate the emergent macrophyte *Nelumbo nucifera* (lotus). Water storage in the Three Gorges Reservoir increases to 175 m a.s.l. from September to February, submerging most of the reserve (Zhou et al., 2017) (Figure 1c). We repeated sampling at the same study sites on the submerged floodplain following inundation by the Three Gorges Reservoir.

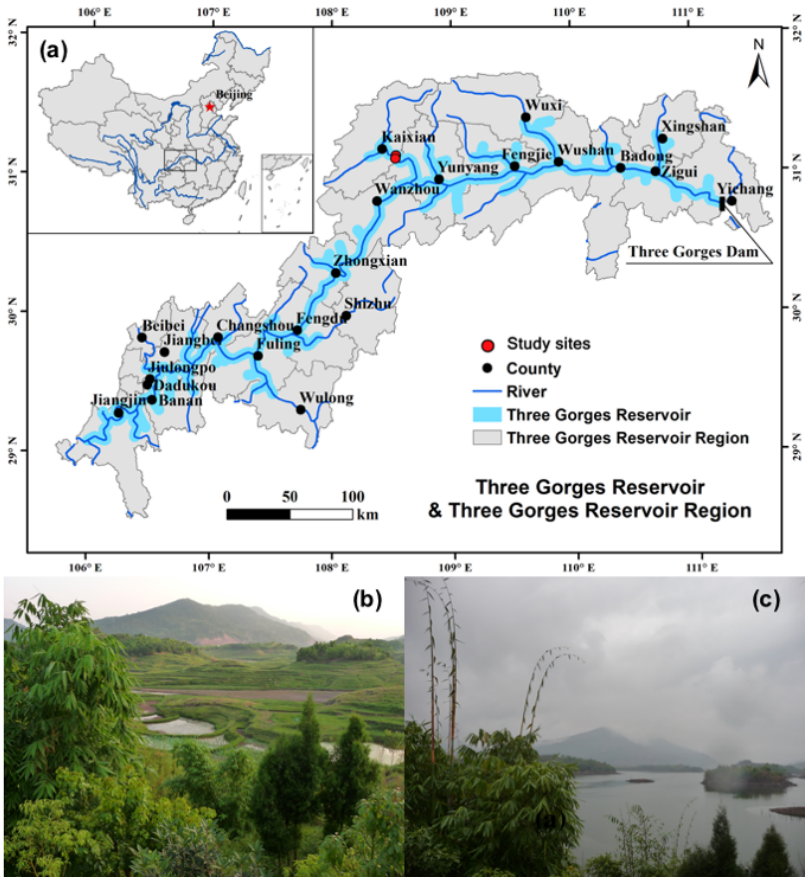

Figure 1. Three Gorges Reservoir on the Yangtze River and its tributaries, with study sites in the Pengxi River Wetland Reserve (a). Blue shading represents the extent of the reservoir during peak floodplain inundation. Study sites were one natural pond and one aquaculture pond on the Three Gorges Floodplain during reservoir drawdown (b), and on the submerged floodplain following inundation by the Three Gorges Reservoir (c).

3.2 Partial Pressures

We sampled three replicate partial pressures of CH_4, CO_2, and N_2O from a water depth of 10 cm in the natural and aquaculture ponds every 12 hours, for 24 hours, on June 28-29, August 9-10 during a rain event (12 mm rain), and August 13-14 after a rain event (reservoir drawdown). We sampled three replicate partial pressures every two hours, for 24 hours, at the same study sites after they were submerged by the Three Gorges Reservoir on January 4-5. Along with each of these partial pressures in water, we sampled three replicate partial pressures in ambient air 1 m above the water's surface. Water samples were equilibrated following Kling et al. (2000).

Equilibrated water samples and ambient air samples were stored in evacuated 5 mL glass vials and analyzed using gas chromatography in the College of Forestry at Northwest Agricultural and Forestry University in Xi'an, P.R. China (PE Clarus 500, PerkinsElmer, Inc., USA equipped with a flame ionizer detector operating at 350 °C and a 2 m Porapak 80-100 Q Column).

3.3 Diffusive Fluxes

We sampled diffusive CH_4, CO_2, and N_2O fluxes in the natural and aquaculture ponds every two hours, for 24 hours, during the June, August, and January sampling events using three replicate floating chambers (Keller and Stallard, 1994). Chambers measured 29.5 cm height above the surface of the water by 31.5 cm width by 31.5 cm depth and were made of heat-insulated propathene plastic. Headspace from each chamber was collected at 0, 5, 10, and 15 minutes following enclosure and stored in evacuated 5 mL glass vials. All samples were analyzed as above. Diffusive fluxes were determined following Frankignoulle (1988) and Alin et al. (2011):

$$F_D = \left(\frac{dP}{dt}\right)\left(\frac{V}{RT_K A}\right) \quad (1)$$

Where F_D is diffusive flux (mg CH_4, CO_2, or N_2O m^2 h^{-1}) (mg m^{-2} d^{-1}) measured directly using floating chambers, P is the partial pressure of CH_4, CO_2, or N_2O (uatm), t is time (min), V is the volume of the floating chamber (L), R is the ideal gas constant (L atm mol^{-1} K^{-1}), T_K is air temperature in degrees Kelvin, and A is the surface area of the floating chamber (m^2) (n=973 total). Each diffusive flux therefore results from a linear regression of four partial pressures that increase or decrease over time. For a positive diffusive flux, the regression is:

$$y_i = \beta_1 x_1 + \beta_2 x_2 + \beta_3 x_3 + \beta_4 x_4 \quad (2)$$

Where y_i is any observed partial pressure of CH_4, CO_2, or N_2O, $\beta_{1\ldots4}$ are the regression coefficients, and $x_{1\ldots4}$ are 0, 5, 10, and 15 minutes. Highly influential data points or outliers in

this linear regression resulting from measurement and experimental errors were identified using the difference between the fitted value and the difference in betas (Kutner et al., 2004). The difference between the fitted value was determined using:

$$DFFIT = \frac{\hat{y}_i - \hat{y}_{i(i)}}{\sqrt{MSE_{(i)} h_{ii}}} \quad (3)$$

Where $DFFIT$ is the difference between the fitted value, $\hat{y}$ is the estimate of y_i using all data points, $y_{i(i)}$ is the estimate of y_i using the regression model with the ith observation omitted, MSE_i is the mean square error for the regression model with the ith observation omitted, and h_{ii} is the ith diagonal term for the hierarchical matrix using all values. The difference between betas was determined using:

$$DFBETAS = \frac{\widehat{\beta}_k - \widehat{\beta}_{k(i)}}{\sqrt{MSE_{(i)} c_{kk}}} \quad (4)$$

Where $DFBETAS$ is the difference between betas, $\hat{\beta}_k$ is the regression coefficient for the kth parameter using all data points, $\hat{\beta}_{k(i)}$ is the regression coefficient for the kth parameter with the ith observation omitted, and c_{kk} is the kth diagonal element in the matrix $(X'X)^{-1}$. Thresholds of $|DFFIT| > 2$ and $|DFBETAS| > 2$ were set for omission of highly influential positive and negative data points in regression models. Such omissions typically moderated diffusive fluxes.

3.4 Ebullition

We estimated CH_4 ebullition (mg m^2 h^{-1}) in shallow water (<2 m) using the distribution and variance in gas transfer velocities among the four replicate floating chambers during the June, August, and January sampling events. Essentially, if one chamber's apparent gas transfer velocity was substantially larger than those measured in adjacent chambers, we assumed that it received ebullition. The apparent gas transfer velocity at ambient temperature in cm h^{-1}, k_T, was calculated following Bastviken et al. (2004, 2010) and Sawakuchi et al. (2014):

$$k_T = \left(\frac{dP}{dt}\right) \frac{V\,(P_w - P_0)}{K_H\,RT_K A} \quad (5)$$

Where P is the partial pressure of CH_4 (uatm), t is time (min), V is the volume of the floating chamber (L), P_w is the partial pressure of CH_4 inside the chamber in equilibrium with P_{aq} (uatm), P_0 is the partial pressure of CH_4 inside the chamber at $t = 0$ (uatm; presumably local atmospheric), K_H is the temperature dependent Henry's constant (mmol L^{-1} atm^{-1}; Figure 3) (Wilhelm et al., 1977), R is the ideal gas constant (L atm mol^{-1} K^{-1}), T_K is water temperature in degrees Kelvin, and A is the surface area of the floating chamber (m^2). The Schmidt number (Sc) for kinematic viscosity and the gas transfer velocity given a Sc of 600, k_{600}, were also calculated following Wanninkhof (1992):

$$Sc = 1897.8 - (114.28\,T_K) + \left(3.2902\,{T_K}^2\right) - \left(0.039061\,{T_K}^3\right) \quad (6)$$

$$k_{600} = k_T \left(\frac{600}{Sc}\right)^{-0.5} \quad (7)$$

Ratios were then created for calculated k_{600}:minimum k_{600} in each of the four replicate floating chambers. Because there were two clear groups in binned ratios for <6.5 and >6.5, chambers with a ratio >6.5 were assumed to have received ebullition (Figure S1). Diffusive CH_4 flux was calculated using the minimum k_{600} from Equations 6 and 7, and CH_4 ebullition was assumed to be the remaining flux.

We also sampled CH_4 ebullition (mg m^2 d^{-1}) in deep water (16-25 m) during the January sampling event using inverted funnels (n=14). Funnels were made of vinyl with minimal seams and no openings along their interior collection surfaces. Funnels channeled CH_4 bubbles from a circular, 0.79 m^2 opening at a water depth of 2 m into a sealed syringe at their terminus (Environnement Illumite, Inc.) (Strayer and Tiedje, 1978; Del Sontro et al., 2010). According to Ostrovsky et al. (2008), CH_4 bubbles collected at this depth in an un-stratified water column

undergo <5 % oxidation before reaching the surface. We assumed that ebullition measured at this depth represented emissions from the water surface. Because ebullition can be a stochastic phenomenon, funnels were deployed continuously over 24 h. Upon retrieval, headspace was sampled using a syringe, stored, and analyzed as described above. Ebullition was determined using:

$$F_E = \frac{(PCH_4 K_H)V}{t_d A_f} \quad (8)$$

Where F_E is CH_4 ebullition (mg m^{-2} d^{-1}) in deep water, PCH_4 is the partial pressure of CH_4 inside of the collected bubbles (uatm), K_H is the temperature dependent Henry's constant (mmol L^{-1} atm^{-1}), V is the bubble volume in the collection syringe (L), t_d is the deployment time (d), and A_f is the cross-sectional area of the sampling funnel (0.79 m^2).

3.5 Water Quality

We measured dissolved O_2 (mg L^{-1}), water temperature (°C), pH, and chlorophyll *a* (ug L^{-1}) from a water depth of 10 cm using a multi-parameter sonde (YSI 6920, YSI, Inc., USA) every two hours, for 24 hours, during each diffusive flux measurement. Dissolved O_2 data were then used to calculate Apparent Oxygen Utilization (AOU) in mg L^{-1}, or the departure from atmospheric equilibrium concentrations of O_2 due to utilization of this dissolved gas by aerobic respiration, following Richey et al. (1988):

$$AOU = PO_{2,eq} K_H - [O_2]_{measured} \quad (9)$$

Where $PO_{2,eq} K_H$ is the equilibrium concentration of O_2 in water according to the temperature dependent Henry's Constant.

3.6 Hypothesis Tests

We assessed normality in the data using quantile-quantile plots and Shapiro-Wilk Tests, and heteroscedasticity in the data using Bartlett Tests for Homogeneity of Variance. CH_4, CO_2,

and N_2O partial pressures and fluxes followed non-normal distributions with unequal variances across sites and months. We compared means of partial pressures and fluxes across sites and months using non-parametric pairwise Wilcoxon signed rank t-tests. We used a Bonferroni correction to an initial critical α-value of 0.05 in order to compensate for loss in statistical power over subsequent comparisons (Zar, 2010). The corrected α for by-site and by-month comparisons was 0.025.

Our methods resulted in large sample sizes for each site (n~36) and month (n~72). To assess whether differences between means were independent of sample size and ecologically as well as statistically significant, we calculated effect sizes following Cohen (1988):

$$d = \frac{\mu_i - \mu_j}{\sqrt{\frac{\sigma_i^2 + \sigma_j^2}{2}}} \quad (10)$$

Where d is a descriptive measure corresponding to a small (0.0-0.4), medium (0.5-0.7), or large (0.8-2.0) effect size, μ is the mean of the sample, and σ is the standard deviation of the sample. Absolute Cohen's d-values for effect size are reported with each α-value.

3.7 Linear Mixed Effects Modeling

We investigated the diel ecosystem drivers of partial pressures and fluxes using linear mixed effects models (Table 1). Linear mixed effects models allowed these heteroscedastic data to vary independently across the random effects of site and month. The slope of each fixed effect relative to each random effect was also allowed to vary independently following Bates et al. (2015):

$$y_i = \beta_{0,i} + \beta_i x_i \ldots + (1 \mid g_i) + (0 + x_i \mid g_i) \ldots + \varepsilon_y \quad (11)$$

Where y_i is the partial pressure or flux, $\beta_{0,i}$ is the intercept of y_i, β_i is the coefficient for each effect, x_i, and g_i is a random effect, such as site or month, and ε_y is the error associated with y_i.

Small sample size-corrected Akaike Information Criterion (AIC_C) was used for model selection following Burham and Anderson (2004). The likelihood of each model in describing partial pressures and diffusive fluxes relative to the other models was expressed in terms of ΔAIC_c and ΔAIC_c weight, w_i, following Burnham and Anderson (2004):

$$\Delta AIC_c = AIC_{c,i} - AIC_{c,min} \quad (12)$$

$$w_i = \frac{e^{-0.5\Delta AIC_{c,i}}}{\sum e^{-0.5\Delta AIC_{c,i}}} \quad (13)$$

Where $AIC_{c,min}$ is the lowest AIC_c value in a group of candidate models. Candidate models for CH_4, CO_2, and N_2O partial pressures, CH_4, CO_2, and N_2O fluxes, and CH_4 ebullition, y_i, were designed according to hypothesized drivers. Model 1 was a null model, which included sampling site and month, only, as random effects with different intercepts.

Table 1. Candidate models and number of model parameters (including $\sigma\varepsilon$) used in AIC_c analyses, grouped by hypothesized drivers of y_i. Here, y_i is the partial pressure of CH_4, CO_2, or N_2O, diffusive flux of CH_4, CO_2, or N_2O, or CH_4 ebullition. The intercept and slope of each fixed effect, x_i, relative to each random effect, g_i, were allowed to vary independently as additional model parameters. Because inundation was measured during only one month, January, this random effect was omitted from the models describing drivers of diel partial pressures and fluxes on the submerged floodplain.

Model Number	Model Name	Model	Number of Model Parameters
1	Null	$y_i = (1 \mid g_i) \ldots + \varepsilon_y$	4
2	Partial *in-situ* production	y_i = *hours since sunrise* + $(1 \mid g_i) + (0 + x_i \mid g_i) \ldots + \varepsilon_y$	7
3	Full *in-situ* production	y_i = *hours since sunrise + water temperature + dissolved* O_2 + *chlorophyll* a + $(1 \mid g_i) + (0 + x_i \mid g_i) \ldots + \varepsilon_y$	16
4	Partial *in-situ* respiration	y_i = *hours since sunset* $(1 \mid g_i) + (0 + x_i \mid g_i) \ldots + \varepsilon_y$	7
5	Full *in-situ* respiration	y_i = *hours since sunset + water temperature + AOU + pH* + $(1 \mid g_i) + (0 + x_i \mid g_i) \ldots + \varepsilon_y$	16

Models 2 and 3 were nested *in-situ* primary production models, which included hours since sunrise, water temperature, dissolved O_2, and chlorophyll *a* as fixed effects. Net primary production is typically greatest during the day (Odum, 1956), when photosynthesis produces dissolved O_2 and the photosynthetic pigment, chlorophyll *a*. Photosynthesis is also a temperature-dependent process (Farquhar et al., 1980). Models 4 and 5 were nested *in-situ* respiration models, which included hours since sunset, water temperature, AOU, and pH as fixed effects. Net respiration is typically greatest at night (Odum, 1956), when dissolved O_2 is consumed and CO_2 is produced in the absence of photosynthesis. Like photosynthesis, respiration is highly temperature-dependent (Yvon-Durocher et al., 2012).

We assessed multicollinearity of fixed effects using Variance Inflation Factors (VIF) and bivariate Pearson Correlation Tests. VIF indicates the magnitude of variance among model coefficients, β_i, when a fixed effect, x_i, is included in a model. Where VIF >5, the

multicollinear fixed effect was tested against all other fixed effects in the model. Where a Pearson coefficient >0.7 (r), the less ecologically relevant fixed effect for the hypothesized driver was omitted. For example, chlorophyll *a* and pH were found to be highly correlated in the full *in-situ* primary production model (r=0.70, df=201, p<0.001), so pH was omitted from this model.

4.0 Results

4.1 Magnitudes of Partial Pressures and Fluxes

4.1.1 Floodplain Ponds During Drawdown

Floodplain ponds were typically oversaturated with greenhouse gases relative to partial pressures sampled in ambient air, leading to diffusive emissions of CH_4, CO_2, and N_2O to the atmosphere (Table 2). There were significant differences in PN_2O and diffusive CH_4 fluxes between natural and newly-created aquaculture ponds on the Three Gorges Floodplain (Table 3). PN_2O was significantly greater in the natural pond in June (p<0.015, d=1.9) and August During Rain (p<0.009, d=1.9). During periods of no rain, diffusive CH_4 fluxes were also significantly greater in the natural pond than in the aquaculture pond (p<0.001, d=0.8 for June; p=0.001, d=0.7 for August After Rain). Effect sizes for these significant differences ranged from medium (d=0.5-0.7), high ($d\geq$0.8), indicating both ecological and statistical significance (Cohen, 1988).

Table 2. Mean diffusive fluxes (mg m^{-2} h^{-1}) ± SE and partial pressures (uatm) ±SE for CH_4, CO_2, and N_2O. Mean ebullition (mg m^{-2} h^{-1}) ±SE is also included.

	n	**CH_4 Flux** (mg m^{-2} h^{-1})	*n*	**Ebullition** (mg m^{-2} h^{-1})	*n*	***P*CH_4** (uatm)	*n*	**CO_2 Flux** (mg m^{-2} h^{-1})	*n*	***P*CO_2** (uatm)	*n*	**N_2O Flux** (mg m^{-2} h^{-1})	*n*	***P*N_2O** (uatm)
June	67	2.2 ±0.4	13	15 ±4	12	50 ±10	62	120 ±20	12	160 ±20	62	0.021 ±0.009	12	0.37 ±0.02
Natural	*34*	3.5 ±0.7	9	18 ±5	6	37 ±9	*30*	80 ±30	*6*	140 ±20	*32*	0.030 ±0.009	*6*	0.41 ±0.01
Aquaculture	*33*	0.8 ±0.3	4	9 ±6	6	60 ±20	*32*	170 ±30	*6*	180 ±40	*30*	0.01 ±0.02	*6*	0.32 ±0.02
August During Rain	65	10 ±1	6	19 ±5	12	130 ±20	65	15 ±10	12	320 ±70	65	0.03 ±0.01	12	0.31 ±0.02
Natural	*32*	12 ±2	6	19 ±5	6	114 ±3	*32*	5 ±18	*6*	250 ±50	*32*	0.03 ±0.01	*6*	0.35 ±0.02
Aquaculture	*33*	8 ±1	0		6	160 ±30	*33*	30 ±10	*6*	400 ±100	*33*	0.03 ±0.01	*6*	0.27 ±0.01
August After Rain	71	2.8 ±0.6	12	6 ±2	12	18 ±2	71	14 ±9	12	150 ±20	71	0.009 ±0.007	12	0.37 ±0.02
Natural	*35*	5 ±1	5	7 ±2	6	18 ±2	*35*	-10 ±10	*6*	170 ±30	*35*	-0.007 ±0.006	*6*	0.37 ±0.04
Aquaculture	*36*	1.0 ±0.2	7	5 ±2	6	18 ±3	*36*	40 ±20	*6*	130 ±10	*36*	0.02 ±0.01	*6*	0.36 ±0.02
January	72	0.13 ±0.05	14	0.09 ±0.05	72	20 ±10	72	28 ±5	72	114 ±8	72	0.004 ±0.019	72	1.30 ±0.03
Natural	*36*	-0.02 ±0.03	1	0.1	36	5.4 ±0.2	*36*	30 ±5	*36*	110 ±10	*36*	0.02 ±0.01	*36*	1.29 ±0.05
Aquaculture	*36*	0.30 ±0.08	13	0.09 ±0.06	36	30 ±20	*36*	26 ±8	*36*	120 ±10	*36*	-0.01 ±0.04	*36*	1.30 ±0.05

Table 3. Statistical comparisons between natural and aquaculture ponds by month. Means that are significantly different according to the Bonferroni-corrected α-value are starred. Absolute Cohen's *d*-values for effect size are also reported. Effect sizes typically ranged from medium (d=0.5-0.7) to high (d>0.8), indicating both ecological and statistical significance. Dissimilar samples sizes were not compared statistically (*NC*).

	CH_4 Flux ($mg\ m^{-2}\ h^{-1}$)	**Ebullition** ($mg\ m^{-2}\ h^{-1}$)	***P*CH_4** (uatm)	**CO_2 Flux** ($mg\ m^{-2}\ h^{-1}$)	***P*CO_2** (uatm)	**N_2O Flux** ($mg\ m^{-2}\ h^{-1}$)	***P*N_2O** (uatm)
June	*** p<0.001 d=0.8	*NC*	p=0.818 d=0.4	p=0.048 d=0.5	p=0.818 d=0.4	p=0.251 d=0.6	*** p=0.015 d=1.9
August During Rain	p=0.778 d=0.3	*NC*	p=0.065 d=0.7	p=0.151 d=0.2	p=0.485 d=0.6	p=0.092 d=0.0	*** p=0.009 d=1.9
August After Rain	*** p=0.001 d=0.7	p=0.149 d=0.4	p=0.240 d=0.1	p=0.03 d=0.6	p=0.484 d=0.6	p=0.050 d=0.6	p=0.589 d=0.2
January	*** p<0.001 d=0.8	*NC*	* p<0.001 d=0.3	p=0.838 d=0.1	p=0.775 d=0.1	p=0.574 d=0.1	p=0.376 d=0.1

*Statistically significant with low effect size, **Statistically significant with medium effect size, ***Statistically significant with large effect size

Precipitation had a significant effect on the partial pressures, diffusive fluxes, and ebullition of CH_4 in floodplain ponds. We observed significantly greater PCH_4 ($p<0.001$, $d=2.0$) and diffusive CH_4 fluxes ($p<0.001$, $d=0.9$) during rain in August than three days later, when the same sites were sampled again under conditions of no rain. Mean ebullition was also greater during rain in August (19 ±5 mg m^{-2} h^{-1}, $n=6$) than after (6 ±2 mg m^{-2} h^{-1}, $n=12$). Partial pressures and diffusive fluxes of CO_2 and N_2O were comparatively unaffected by this rain event.

Monthly and seasonal differences in greenhouse gas emissions measured in floodplain ponds and on the submerged floodplain following inundation by the Three Gorges Reservoir are shown as CO_2-equivalents in Figure 2. CO_2-equivalents were calculated over a 100-year timescale using CO_2 as a reference gas for global warming potential, where CH_4 has a global warming potential 25 times that of CO_2, and nitrous oxide has a global warming potential 298 times that of CO_2 (IPCC, 2001; Myhre et al., 2013). CH_4 diffusion and ebullition increased as a fraction of total CO_2-equivalents emitted by floodplain ponds from June to August, spiking to 98-99% during a rain event. CO_2 diffusion showed the opposite trend, and N_2O diffusion changed little throughout reservoir drawdown.

4.1.2 Submerged Floodplain During Inundation

Areal diffusive CH_4 fluxes were significantly lower on the submerged floodplain following inundation by the Three Gorges Reservoir ($p<0.001$, $d=0.7$) (Figure 2). CH_4 ebullition also decreased significantly from reservoir drawdown to inundation ($p<0.001$, $d=1.4$). Little CH_4 was emitted through either diffusion or ebullition during inundation, when CO_2 and N_2O contributed 57-58 % of total CO_2-equivalents emitted to the atmosphere.

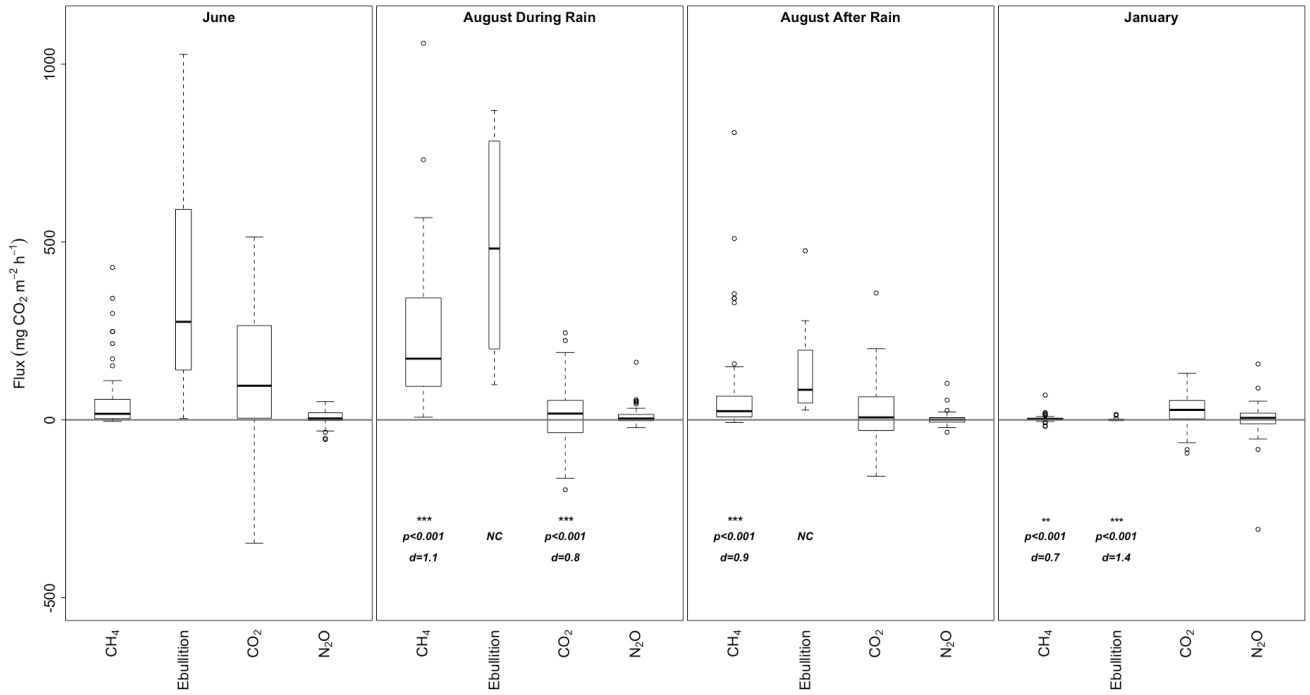

Figure 2. Fluxes of CH_4, CO_2, and N_2O expressed in mg CO_2-equivalents m^{-2} h^{-1} in floodplain ponds during June and August and on the submerged floodplain following inundation by the Three Gorges Reservoir during January. The grey line at y=0 delineates fluxes between these aquatic environments and the atmosphere. Width of boxes reflects relative sample size, which is smaller for ebullition (ranging from n=6 to n=14) than for diffusive fluxes (ranging from *n=62* to *n=72*). Statistical and ecological significance across subsequent months is indicated by α-values and absolute Cohen's d-values for effect size.

4.2 Diel Patterns of Partial Pressures and Diffusive Fluxes

Oversaturation of CO_2 relative to the atmosphere corresponded with undersaturation of O_2 on the floodplain during both reservoir drawdown and inundation, consistent with net heterotrophy (Figure 3). The equimolar consumption of O_2 and production of CO_2 during aerobic respiration can be expressed as a slope of -1 when excess O_2 is regressed with excess CO_2. In both the natural and aquaculture pond, these slopes were approximately -1, indicating *in-situ* respiration as a key driver of PCO_2 (r=-0.13, df=15, p=0.63 for the natural pond and r=-0.60, df=15, p=0.010 for the aquaculture pond). This slope deviated from -1 on the submerged floodplain following inundation by the Three Gorges Reservoir (m=0.4) (r=0.28, df=68,

p=0.021), indicating that other ecosystem processes were affecting PCO_2 (Crawford et al., 2014). Diffusive fluxes of CH_4, CO_2, or N_2O varied throughout the 24 h sampling periods, along with dissolved O_2 and other fixed effects we associate with *in-situ* primary production and *in-situ* respiration (Figure 4; Figure S2). Five linear mixed effects models were used to determine whether *in-situ* primary production and *in-situ* respiration were more likely than a null model to drive observed patterns in greenhouse gas partial pressures and fluxes over diel timescales (Table 1).

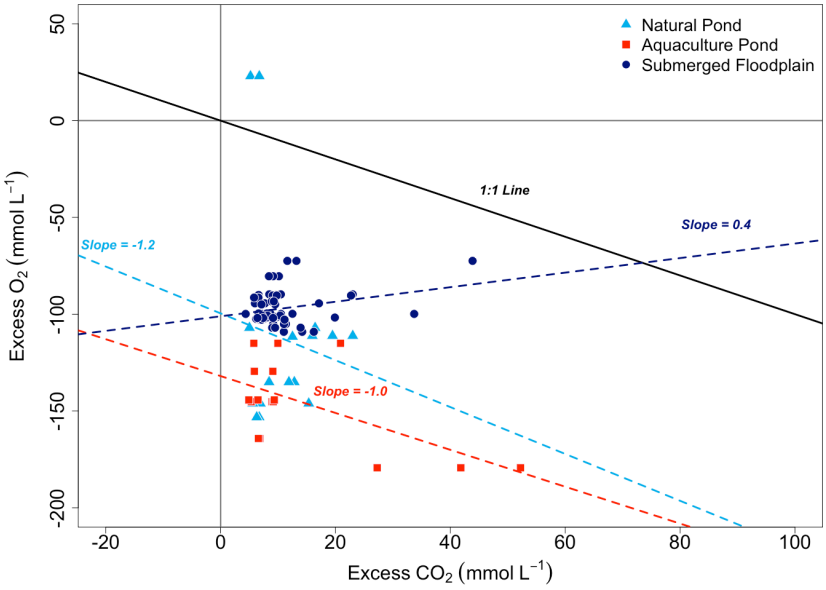

Figure 3. Saturation of O_2 and CO_2 in water relative to atmospheric equilibrium, at the grey lines or 0.0 mmol L^{-1}. The 1:1 line represents the equimolar consumption of O_2 and production of CO_2 during aerobic respiration. Slopes are the changes in excess dissolved O_2 relative to excess dissolved CO_2.

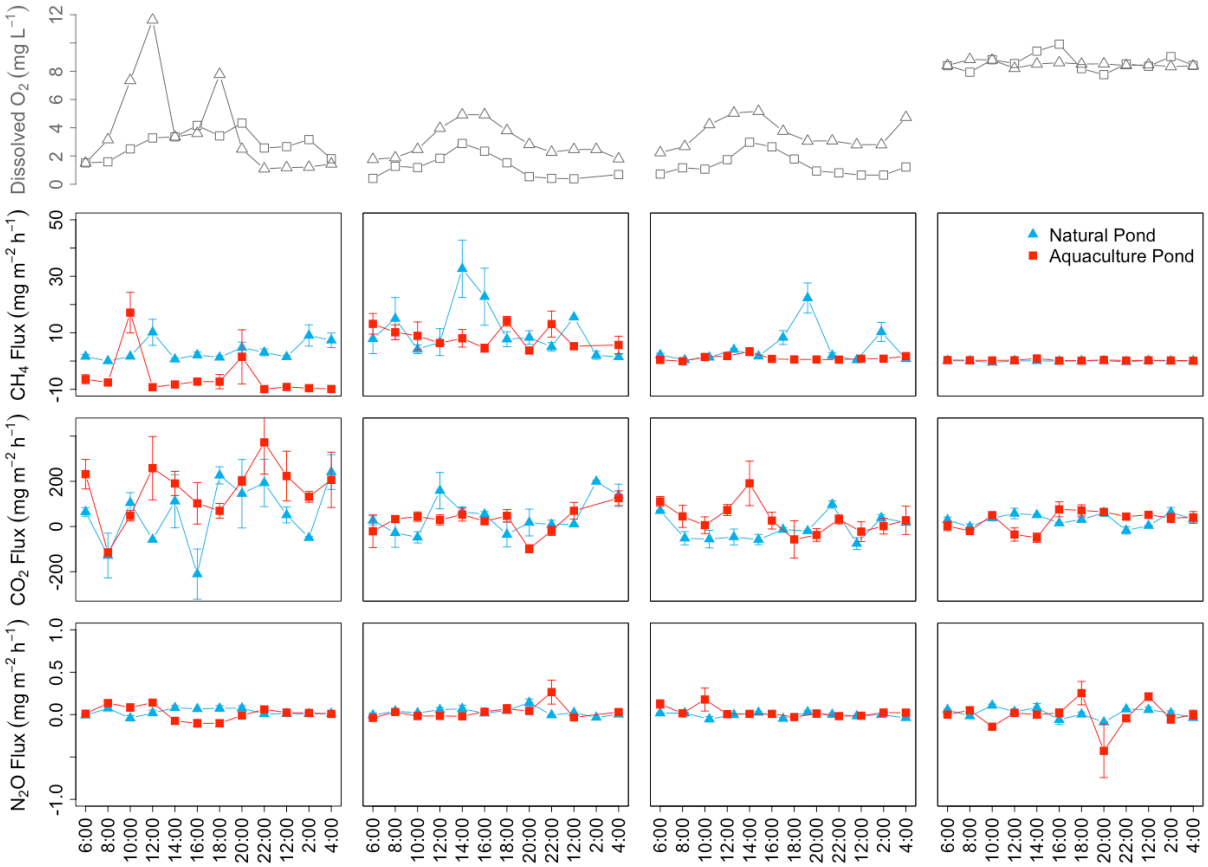

Figure 4. Diel variation in dissolved O_2 in natural and aquaculture ponds during each sampling event, compared with diel variation in diffusive CH_4, CO_2, and N_2O fluxes.

4.3 Drivers of Partial Pressures and Fluxes

4.3.1 Floodplain Ponds During Drawdown

Diel partial pressures of CH_4, CO_2, and N_2O in water showed weak relationships with respective diel diffusive fluxes of CH_4 (r=0.52, df=84, p<0.001), CO_2 (r=0.11, df=84, p=0.310), and N_2O (r=-0.03, df=84, p=0.810). Because diel partial pressures of greenhouse gases in water were weakly related to diffusive fluxes in this study, diel partial pressures were modeled separately from diffusive fluxes. Diel partial pressures were not added as fixed effects in the modeling fluxes of diffusive fluxes.

We found that diel partial pressures of CH_4 and CO_2 in floodplain ponds were strongly supported by our full *in-situ* respiration model, which included hours since sunset, water

temperature, AOU, and pH as fixed effects (Table S1). PN_2O in floodplain ponds was best supported by the null model. Diel CO_2 fluxes in floodplain ponds were also driven by *in-situ* respiration. This model was over 99 % more likely to describe diel diffusive fluxes of CO_2 in floodplain ponds than *in-situ* production or null models (see Weight, Table S2). Model fits for diel diffusive fluxes of CH_4 were inconclusive; relative support of diel CH_4 fluxes was divided between the null model (47 %) and the partial *in-situ* production model (51 %), which included hours since sunrise as a fixed effect. Diffusive fluxes of N_2O in floodplain ponds were best supported by the null model.

4.3.2 Submerged Floodplain During Inundation

The relative importance of *in-situ* respiration to diel partial pressures was consistent following inundation of the floodplain by the Three Gorges Reservoir. During inundation, diel PCH_4 and PCO_2 were still most strongly supported by the full *in-situ* respiration model. However, relative support of PCO_2 by this model decreased from 93 % to 86 % from reservoir drawdown to inundation, consistent with the apparent decoupling of PCO_2 from dissolved O_2 dynamics observed from drawdown to inundation (Figure 3). Diel PN_2O was also most strongly supported by *in-situ* respiration (partial model).

Like diel PCO_2, diel diffusive CO_2 fluxes were strongly supported by the *in-situ* respiration model on the submerged floodplain following inundation by the Three Gorges Reservoir. During inundation, diel diffusive CH_4 and N_2O fluxes were best supported by the null model. Diel CH_4 ebullition was also more likely to be supported by the null model during both reservoir drawdown and inundation.

5.0 Discussion

5.1 PCH_4, PCO_2, and CO_2 fluxes varied on a diel basis with *in-situ* respiration during drawdown

Like other lentic environments on floodplains in Southeast Asia (Holtgrieve et al., 2013), West Africa (Kone et al., 2009), and Australia (Hunt et al., 2012), ponds on the Three Gorges Floodplain were heterotrophic (Figure 3). The accumulation of CH_4 and CO_2 within floodplain ponds varied on a diel basis with *in-situ* respiration according to linear mixed effects modeling, which included hours since sunset, water temperature, AOU, and pH as fixed effects. This model was over 92 % more likely to explain observed diel variations in PCH_4, PCO_2, and diffusive CO_2 fluxes than the null model. Our approach and results are consistent with findings of Tobias et al. (2007), Hotchkiss et al. (2014), and Schindler et al. (2017), who show that respiration rates can vary widely throughout the day. Thus, it may be necessary to measure PCH_4, PCO_2, and diffusive CO_2 fluxes on a diel basis in studies of not only stream and lake metabolism, but also reservoir carbon cycling.

Respiration in the surrounding terrestrial landscape may have also contributed to significant increases in PCH_4 and diffusive CH_4 fluxes during precipitation and transfers of respiratory byproducts from floodplain soils to ponds. During a rain event in August, diffusive CH_4 and ebullition fluxes spiked to 98-99 % CO_2 equivalents emitted to the atmosphere from floodplain ponds. Ponds are intimately connected to the surrounding terrestrial landscape owing to comparatively high surface area-to-volume ratios (Holgerson et al., 2015). Terrestrial-aquatic transfers can enrich surface waters with byproducts of soil respiration, increasing the partial pressures of CH_4 and CO_2 (Kling et al., 1991; Butman et al., 2011; Raymond et al., 2016), or these flows can dilute surface water solute concentrations (Johnson et al., 2010). pCH_4 and diffusive CH_4 fluxes were significantly higher during rain than after rain, suggesting enrichment.

The onset of this rain event corresponded to a decrease in atmospheric pressure from 1016 millibars to 1002 millibars, which may also explain observed significant increases in CH_4 ebullition (Ostrovsky et al., 2008).

5.2 Ebullition was a substantial fraction of total drawdown emissions

CH_4 ebullition comprised 60-68 % of all CO_2-equivalents emitted from floodplain ponds to the atmosphere during reservoir drawdown (Figure 3). This is consistent with findings from the lake and reservoir literatures (Del Sontro et al., 2010; Grinham et al., 2011; Maeck et al., 2014; Deemer et al., 2016). Del Sontro et al. (2016) measured both the magnitude and drivers of ebullition in 10, northern temperate ponds. These ebullitive fluxes averaged 3.1 ±0.7 mg CH_4 m^{-2} h^{-1}, compared with the 15 ±4 mg CH_4 m^{-2} h^{-1}, 19 ±5 mg CH_4 m^{-2} h^{-1}, and 6 ±2 mg CH_4 m^{-2} h^{-1} that we measured in June, August During Rain, and August After Rain, respectively (Table 2). The lower magnitude of ebullitive fluxes in ponds measured by Del Sontro et al. (2016) in northern temperate ponds may be due to the strong temperature dependence of respiration generally (Yvon-Durocher et al., 2012) and methanogenesis particularly in freshwater environments (Schulz and Conrad, 1996; Segers, 1998; Lofton et al., 2014; Yvon-Durocher et al., 2014). Temperatures ranged from 25 °C to 39 °C in our subtropical floodplain ponds and from 28 °C to 35 °C in their sediments, where ebullition originates. Del Sontro et al. (2016) found that sediment temperatures in their ponds rarely exceeded 25 °C, and that ebullition was related to both sediment temperature and trophic status. Diel CH_4 ebullition in in our study was not supported by our *in-situ* production, *in-situ* respiration models, suggesting other biotic and abiotic drivers during reservoir drawdown and inundation, such as atmospheric pressure.

5.3 *P*CH_4 and CH_4 fluxes varied seasonally, from reservoir drawdown to floodplain inundation

Diel PCH_4, PCO_2, and diffusive CO_2 fluxes were also driven by *in-situ* respiration on the submerged floodplain following inundation by the Three Gorges Reservoir. Inundation did change the driver of diel PN_2O from other ecosystem processes during reservoir drawdown (indicated by strong support of the null model) to *in-situ* respiration. Battin et al. (2008) and McNicol and Silver et al. (2014) have each documented respiration of floodplain vegetation following inundation. The only plant species that survive seasonal flooding of the Pengxi River Wetland Reserve are the grasses *Cynodon dactylon* and *Echinochloa crusgali* var. *zelayensis* and the legume *Aeschynomene indica* (Wang et al., 2009). Remaining terrestrial vegetation in the reserve dies following inundation, including the lotus (*Nelumbo nucifera*) cultivated in aquaculture ponds. Seasonal senescence of many aquatic and terrestrial plant species on the Three Gorges Floodplain likely provides ample substrates for *in-situ* respiration following inundation.

Interestingly, the magnitudes of CH_4 emissions alone seemed affected by inundation. Diffusive CH_4 fluxes and CH_4 ebullition decreased significantly from 2.8 ±0.5 and 6 ±2 mg m^{-2} h^{-1}, respectively, during reservoir drawdown to 0.13 ±0.05 and 0.09 ±0.05 mg m^{-2} h^{-1} during inundation. PCO_2, PN_2O, and the diffusive fluxes of CO_2 and N_2O per m^2 were not significantly different from reservoir drawdown to inundation in January. This meant that diffusive CO_2 and N_2O fluxes were proportionately more important to total CO_2-equivalents emitted per unit area during inundation than during reservoir drawdown. The decrease in areal CH_4 emissions during inundation may be due to a combination of lower temperatures and higher O_2 saturation on the submerged floodplain following inundation by the Three Gorges Reservoir. During winter inundation, water temperatures in on the submerged floodplain ranged from 13 °C to 14 °C compared to 25 °C to 39 °C in floodplain ponds during summer reservoir drawdown. Fewer CH_4

bubbles may have been produced in colder submerged floodplain sediments. During inundation, inverted funnels in deeper, colder water (16-25 m) also captured much smaller magnitudes of ebullition than floating chambers in shallower water (<2 m) (p<0.001, d=1.4), which is consistent with other studies (Deshmukh et al., 2014; Del Sontro et al., 2016). Furthermore, dissolved O_2 on the submerged floodplain was significantly greater than during drawdown in floodplain ponds (p<0.001, d=2.0; Figure 4), sometimes approaching 98 % saturation. Dissolved CH_4 may have been oxidized within this more oxic water column (Guerin and Abril, 2007). Therefore, both inundation and the season in which it occurs likely contributed to our observed decreases in diffusive CH_4 fluxes and CH_4 ebullition.

No other studies in the Three Gorges Reservoir have measured ebullition, meaning that spatial coverage is limited to our study, 14 inverted funnels, a small area of the submerged floodplain, and one January sampling event over two days thus far. Wik et al. (2016) estimated that 11 inverted funnels and 39 days of sampling were required in northern temperate lakes encompassing 0.02-0.17 km^2 in order to accurately (±20 %) measure ebullition captured by 17 funnels over 62 days. Lower spatial and temporal coverage most often results in underestimates of ebullition (Wik et al., 2016). This makes greater coverage and more accurate ebullition estimates for the Three Gorges Reservoir a priority for future studies.

5.5 Partial pressures were weakly related to diffusive fluxes

The modeled diffusive flux of any gas between water and the atmosphere is a function of its concentration gradient between water and the atmosphere and the gas transfer velocity. Yet, partial pressures of CH_4, CO_2, and N_2O in water were weakly related to our measured diffusive fluxes. This indicates the importance of the gas transfer velocity, which depends largely on turbulence at the interface between water and the atmosphere (Banjeree and MacIntyre, 2004;

McGillis et al., 2004). Turbulence can result from convection or wind speed, which are positively correlated to diffusive flux (MacIntyre et al., 2010). Diffusive CH_4 fluxes measured by this study were slightly more related to the gas transfer velocity (r=0.60, df=84, p=0.016) than to partial pressures of CH_4 (r=0.52, df=84, p<0.001). This was not true for diffusive CO_2 and N_2O fluxes. It is generally assumed and, in some cases, empirically shown (Natchimuthu et al., 2017) that partial pressures are highly correlated to diffusive fluxes. Other studies by Shilder et al. (2013) in lakes and Crawford et al. (2015) in streams have shown weak relationships between partial pressures and diffusive fluxes and stronger relationships between diffusive fluxes and the gas transfer velocity. Our results and others suggest that synoptic observations of partial pressures do not always predict the magnitudes of diffusive fluxes. Further comparisons between partial pressures of CH_4, CO_2, and N_2O in water and the diffusive fluxes measured by floating chambers are needed, particularly when partial pressures are widely used to model diffusive fluxes when not directly measured by chambers.

5.6 Ponds on the Three Gorges floodplain were sizeable CH_4 emitters

We used the Institute for Scientific Information Web of Science to review other studies reporting diffusive CH_4, CO_2, and N_2O fluxes from aquatic and terrestrial environments on the Three Gorges Floodplain and in the Three Gorges Reservoir. During reservoir drawdown, these environments included ponds, wetlands, the Yangtze River, its tributaries, grasslands, forests, and agricultural lands. During inundation, these environments included the mainstem Three Gorges Reservoir and its submerged floodplain. Fluxes were converted to mg CO_2-equivalents m^{-2} d^{-1} ±SE for comparison across environments (Tables 4 and 5). The surface areas occupied by each environment during reservoir drawdown and inundation are presented in Table 6 (Chen

et al., 2009b; Zhang et al., 2018). Studies that did not specify sampling month or environment were omitted.

Table 4. Mean diffusive CH_4, CO_2, and N_2O fluxes, in mg CO_2 equivalents ±SE, reported by other studies in aquatic and terrestrial environments on the Three Gorges Floodplain, Yangtze River, and its tributaries during reservoir drawdown.

Ecosystem Type	Month	CH_4 Flux (mg CO_2 m^{-2} h^{-1})	CO_2 Flux (mg CO_2 m^{-2} h^{-1})	N_2O Flux (mg CO_2 m^{-2} h^{-1})	Source
Three Gorges Floodplain					
S. triqueter wetland	July-September	373 ±273		15 ±18	Chen et al., 2009a,b
J. amuricus wetland	July-September	6 ±16		6 ±15	Chen et al., 2009a,b
T. augustifolia wetland	July-September	16 ±28		6 ±6	Chen et al., 2009a,b
P. distichum wetland	July-September	170 ±125		9 ±12	Chen et al., 2009a,b
O. sativa wetland	June	122 ±58			Lu et al., 2011
Aquaculture pond	June	4 ±1			Zhou et al., 2017
Aquaculture pond	June	20 ±8	168 ±29	3 ±6	*This study*
Natural pond	June	35 ±13		3 ±12	Zhou et al., 2017
Natural pond	June	88 ±18	78 ±32	9 ±3	*This study*
Aquaculture pond	August	113 ±20	38 ±14	3 ±3	*This study*
Natural pond	August	175 ±25	6 ±15	6 ±3	*This study*
Grasslands	July-September	7 ±2			Chen et al., 2009a,b
Grasslands	June	-1 ±1			Yang et al., 2012
Grasslands	June	18 ±8		21 ±9	Zhou et al., 2017
Forests	June	0.3 ±0.9			Yang et al., 2012
Forests	June	13 ±8			Zhou et al., 2017
Agricultural lands	June	-0.3 ±0.8			Yang et al., 2012
Agricultural lands	June	150 ±50			Zhou et al., 2017
	April	2 ±2			Xiao et al., 2013
Yangtze River & Tributaries					
Yangtze River					
Yangtze River	June	8 ±23			Lu et al., 2011
Yangtze River	July	13 ±13			Yang et al., 2013
Yangtze River	August	1.5 ±0.5			Xiao et al., 2013
Tributary	April	8 ±2			Xiao et al., 2013
Tributary	June		-47 ±22		Zhao et al., 2013
Tributary	July	6 ±2			Chen et al. 2009
Tributary	July		-90 ±18		Zhao et al., 2013
Tributary	August	2.3 ±0.5			Xiao et al., 2013

Table 5. Mean diffusive CH_4, CO_2, and N_2O fluxes, in mg CO_2 equivalents ±SE, reported in the mainstem Three Gorges Reservoir and its submerged floodplain during inundation.

Ecosystem Type	Month	CH_4 Flux (mg CO_2 m^{-2} h^{-1})	CO_2 Flux (mg CO_2 m^{-2} h^{-1})	N_2O Flux (mg CO_2 m^{-2} h^{-1})	Source
Three Gorges Reservoir					
Mainstem reservoir	January	5 ±3			Yang et al., 2013
Mainstem reservoir	February	0.5 ±0.3			Xiao et al., 2013
Mainstem reservoir	October	1.0 ±0.8			Xiao et al., 2013
	January-April	8 ±10			Chen et al., 2011
Submerged Floodplain					
Submerged wetlands					
Submerged aquaculture pond	January	8 ±2	30 ±9	-3 ±9	*This study*
Submerged natural pond	January	-1 ±1			Zhou et al., 2017
Submerged natural pond	January	0.5 ±0.8	33 ±5	6 ±3	*This study*
Submerged grasslands	November	5 ±8			Yang et al., 2012
Submerged grasslands	January	-1 ±2			Zhou et al., 2017
Submerged forests	November	5 ±5			Yang et al., 2012
Submerged agricultural lands	November	10 ±10			Yang et al., 2012
Submerged agricultural lands	January	13 ±8			Zhou et al., 2017
Submerged tributary	January-April		111 ±11		Li et al., 2014
Submerged tributary	January-April	5 ±10			Chen et al., 2011
Submerged tributary	March		-13 ±4		Zhao et al., 2013
Submerged tributary	October	2.0 ±0.5			Xiao et al., 2013

Table 6. Surface areas of aquatic and terrestrial environments in the Three Gorges region, in km^2. Surface areas during reservoir drawdown (Three Gorges Floodplain, Yangtze River, and Tributaries) total 1,053.3 km^2, not including 52.9 km^2 of urban and suburban areas (Zhang et al., 2018). Surface areas during inundation (Three Gorges Reservoir and Submerged Floodplain) total 1,602.1 km^2.

Environment	Surface Area *(km^2)*	Source
Reservoir Drawdown		
Ponds		*unavailable*
Wetlands	100.0	Chen et al., 2009b
Yangtze River & tributaries	784.8	Chen et al., 2009b; Zhang et al., 2018
Grasslands	15.1	Zhang et al., 2018
Forests	63.8	Zhang et al., 2018
Agricultural lands	89.6	Zhang et al., 2018
Building lands	52.9	Zhang et al., 2018
Inundation		
Mainstem reservoir	784.8	Chen et al., 2009b; Zhang et al., 2018
Submerged floodplain	321.4	Chen et al., 2009b; Zhang et al., 2018

We found that most studies measure diffusive CH_4 fluxes, only. Ponds and wetlands have the highest diffusive CH_4 emissions per m^2 on the Three Gorges Floodplain during reservoir drawdown (Table 6), meaning that recent expansion of ponds for aquaculture on the Three Gorges Floodplain is likely increasing diffusive CH_4 emissions (Li et al., 2013; Zhou et al., 2017; Zhang et al., 2018). Grasslands, forests, and agricultural lands measured by other studies on the Three Gorges Floodplain were also sources for diffusive CH_4 to the atmosphere. Globally, terrestrial soils are typically CH_4 sinks (Smith et al., 2000). However, CH_4 oxidation rates in terrestrial soils are diminished by porewater content and landscape disturbances like agriculture (Smith et al., 2000). Both high porewater content and landscape disturbances can be expected on a humid, monsoonal, and historically densely populated Three Gorges Floodplain now undergoing seasonal inundation. Published diffusive CH_4 fluxes for the Yangtze River and its tributaries during reservoir drawdown show that these environments are essentially CH_4 neutral.

Aquatic and terrestrial floodplain environments during reservoir drawdown (comprising a total surface area of 1,053.3 km^2) tend to have higher diffusive CH_4 fluxes per m^2 than the surface of both the mainstem Three Gorges Reservoir and submerged floodplain during inundation (1,106.2 km^2) (Tables 6, 7, and 8). Diffusive CH_4 fluxes range from -1 ±1 mg CO_2-equivalents m^{-2} d^{-1} in grasslands to 373 ±273 mg CO_2-equivalents m^{-2} d^{-1} in wetlands during drawdown. These fluxes range from -1 ±1 mg CO_2-equivalents m^{-2} d^{-1} in submerged grasslands to 13 ±8 mg CO_2-equivalents m^{-2} d^{-1} in submerged agricultural lands during inundation.

Comparisons of diffusive CH_4 emissions from aquatic and terrestrial floodplain environments during reservoir drawdown and from the mainstem reservoir and submerged floodplain during inundation come with two important caveats. The first is that data from the literature include few measurements of diffusive CO_2 fluxes and no estimates of terrestrial primary production in grasslands, forests, and agricultural lands during reservoir drawdown. Each of these ecosystems is likely to sequester considerable quantities of CO_2. Based on the negative diffusive CO_2 fluxes reported in the literature, tributaries are also net autotrophic. In a study by Zhao et al. (2013), for example, it was found that the Yangtze River and its tributaries have the potential to sequester up to 90 ±18 mg CO_2 m^{-2} h^{-1} during reservoir drawdown. During late summer (August), we also found that natural floodplain ponds also have the potential to sequester comparatively small amounts (-10 ±10 to 5 ±18 mg m^{-2} h^{-1}) of CO_2, perhaps due to primary production. Indeed, chlorophyll *a* was significantly higher in the natural pond than in the aquaculture pond ($p<0.001$, $d=2.0$). More diffusive CO_2 flux measurements are needed in both aquatic and terrestrial floodplain environments during reservoir drawdown and inundation to adequately assess the complete C balance of the region under its new and dynamic hydrologic regime.

Secondly, the fate of CH_4 stored in the large water volumes of the mainstem Three Gorges Reservoir and its submerged floodplain is unknown. Though diffusive CH_4 emissions are comparatively low from the surface of the reservoir during inundation, total water volumes increase from 17.2 km^3 during drawdown to 39.9 km^3 during this period (Wang et al., 2013). CH_4 can be stored at higher concentrations in the anoxic layer of vertically stratified lakes and reservoirs, and then released via diffusion during periods of overturn and mixing (Michmerhuizen et al., 1996; Riera et al., 1999; Beaulieu et al., 2014). We sampled dissolved CH_4 from the surfaces of the Three Gorges Reservoir, only. Using these mean concentrations, the water level-water volume relationship reported by Wang et al. (2013) for the Three Gorges region, and assuming that the water column is uniformly mixed, we can extrapolate that the Three Gorges Reservoir stores 8 ±1 kg CH_4 during the winter, when PCH_4 and diffusive CH_4 emissions are comparatively low. By comparison, the Three Gorges Floodplain, Yangtze River, and its tributaries may store up to 3.6 ±0.7 kg CH_4 during reservoir drawdown in August, when diffusive emissions are comparatively high, using CH_4 concentrations measured in floodplain ponds and a local tributary (Pengxi River). The fate of the larger quantities of dissolved CH_4 in the Three Gorges Reservoir during reservoir overturn and downstream export is unclear. Drops in hydrostatic pressure during the transition from peak inundation to reservoir drawdown may also result in bubble release from reservoir sediments and additional CH_4 emissions (Harrison et al., 2017; Beaulieu et al., 2018). Reservoir overturn, downstream export, and drops in hydrostatic pressure each constitute "hot moments" for CH_4 emissions, which are important to reservoir C balances though difficult to capture via synoptic field sampling (Deemer et al., 2016). Irrespective of ultimate atmospheric CH_4 contributions by the Three Gorges Reservoir,

our study and other studies show that ponds and wetlands on the Three Gorges Floodplain during reservoir drawdown are also sizeable sources for diffusive CH_4 to the atmosphere.

6.0 Conclusion

Our study shows that it is critical to consider how drawdown and inundation tie C and N cycling in hydropower reservoirs to their floodplains. Greenhouse gas emissions resulting from this C and N cycling are temporally dynamic. This is due not just to the association of greenhouse gas production with diel ecosystem metabolism, but also with the seasonal disturbance regime of inundation. The Three Gorges Dam is one case study in a global hydropower boom (Zarfl et al., 2015) that is altering the hydrologic regime, frequency and scale of inundation, and balance of autotrophic and heterotrophic processes within river basins. We show that the drawdown/inundation cycle on the Three Gorges Floodplain changes the magnitudes of greenhouse gas fluxes from one of the world's largest reservoirs to the atmosphere, and that certain environments on reservoir floodplains during drawdown can be nontrivial sources for CH_4.

7.0 Acknowledgements

This work was partially supported by the National Science Foundation Grant No. 1310724, the National Science Foundation Graduate Research Fellowship Grant No. DGE1256260, the 100 Talents of the Chinese Academy of Sciences, and the Chinese Science and Technology Exchange Council. Evan V. Arntzen provided critical support during field sampling. We also thank Matthew J. Bogard and four anonymous reviewers for helpful comments during the preparation of this manuscript. All data and data products presented in figures and analyses are available by following the link: https://github.com/blm8/Three-Gorges-Floodplain.git.

8.0 References

Alin, S.R., M. de Fatima F.L. Rasera, C.I. Salimon, J.E. Richey, G.W. Holtgrieve, A.V. Krusche, and A. Snidvongs (2011), Physical controls on carbon dioxide transfer velocity and flux in low-gradient river systems and implications for regional carbon budgets, *Journal of Geophysical Research*, 116, G01009. doi:10.1029/2010JG001398.

Aufdenkampe, A.K., E. Mayorga, P.A. Raymond, J.M. Melack, S.C. Doney, S.R. Alin, R.E. Aalto, and K. Yoo (2011), Riverine coupling of biogeochemical cycles between land, oceans, and atmosphere, *Frontiers In Ecology and the Environment*, 9(1), 53-60. doi:10.1890/100014.

Bains, S.B. and M.L. Pace (1991), The production of dissolved organic matter by phytoplankton and its importance to bacteria: Patterns across marine and freshwater systems. *Limnology and Oceanography*, 36, 1078-1090. doi:10.4319/lo.1991.36.6.1078.

Banerjee, S. and S. MacIntyre (2004), The air-water interface—Turbulence and scalar exchange, *In* Advances in Coastal and Ocean Engineering, 9, eds. J. Grue et al., 181-237, World Scientific Publishing, Hackensack, N.J.

Barros, N., J.J. Cole, L.J. Tranvik, Y.T. Prairie, D. Bastviken, V.L.M. Huszar, P. del Giorgio, and F. Roland (2011), Carbon emission from hydroelectric reservoirs linked to reservoir age and latitude, *Nature Geoscience*, 4, 1-4. doi:10.1038/NGEO1211.

Bastviken, D., A.L. Santoro, H. Marotta, L.Q. Pinho, D.F. Calheiros, P. Crill, A. Enrich-Prast (2010), Methane emissions from Pantanal, South America, during the low water season: Toward more comprehensive sampling, *Environmental Science and Technology*, 44, 5450-5455. doi:10.1021/es1005048.

Bastviken, D., J. Cole, M. Pace, L. Tranvik (2004), Methane emissions from lakes—Dependence of lake characteristics, two regional assessments, and a global estimate, *Global Biogeochemical Cycles*, 18, GB4009. doi:10.1029/2004GB002238.

Battin, T.J., L.A. Kaplan, S. Findlay, C.S. Hopkinson, E. Marti, A.I. Packman, J.D. Newbold, and F. Sabater (2009), Biophysical controls on organic carbon fluxes in fluvial networks, *Nature Geoscience*, 1, 95-100. doi:10.1038/ngeo101.

Bates, D., M. Maechler, B. Bolker, and S. Walker (2015), Fitting linear mixed effects models using lme4, *Journal of Statistical Software*, 67(1). doi:10.18637/jss.v067.i07.

Beaulieu, J.J., D.A. Balz, M.K. Birchfield, J.A. Harrison, C.T. Nietch, M.C. Platz, W.C. Squier, S. Waldo, J.T. Walker, K.M. White, and J. L. Young (2018), Effects of an experimental water-level drawdown on methane emissions from a eutrophic reservoir, *Ecosystems*, 21(4), 657-674. doi:10.1007/s10021-017-0176-2.

Beaulieu, J.J., R.L. Smolenski, C.T. Nietch, A. Townsend-Small, M.S. Elovitz, and J.P. Schubauer-Berigan (2014), Denitrification alternates between a source and sink of nitrous oxide in the hypolimnion of a thermally stratified reservoir, *Limnology and Oceanography*, 59(2), 495-506. doi:10.4319/lo.2014.59.2.0495.

Burnham, K.P. and D.R. Anderson (2004), Multimodel inference—Understanding AIC and BIC in model selection, *Sociological Methods and Research*, 33(2), 261-304. doi:10.1177/0049124104268644.

Burns, A. and D.S. Ryder (2001), Response of bacterial extracellular enzymes to inundation of floodplain sediments, *Freshwater Biology*, 46, 1299–1307. doi:10.46/j.1365-2427.2001.00750.x.

Butman, D. and P.A. Raymond (2011), Significant efflux of carbon dioxide from streams and rivers in the United States, *Nature Geoscience*, 4, 839-842. doi:10.1038/ngeo1294.

Chen, H, X. Yuan, Y. Gao, N. Wu, D. Zhu, and J. Wang (2009a), Nitrous oxide emissions from newly created littoral marshes in the drawdown area of the Three Gorges Reservoir, China, *Water, Air, and Soil Pollution*, 211, 25-33. doi:10.1007/s11270-009-0277-4.

Chen, H., Y. Wu, X. Yuan, Y. Gao, N. Wu, and D. Zhu (2009b), Methane emissions from newly created marshes in the drawdown area of the Three Gorges Reservoir, *Journal of Geophysical Research*, 114, D18301. doi:10.1029/2009JD012410.

Cohen, J. (1988), Statistical Power Analysis for the Behavioral Sciences (2nd ed.), Lawrence Earlbaum Associates, Hillsdale, New Jersey.

Cole, J.J., G.E. Likens, and D.L. Strayer (1982), Photosynthetically produced dissolved organic carbon: An important source for planktonic bacteria, *Limnology and Oceanography*, 43, 647-656. doi:10.4319/lo.1982.27.6.1080.

Crawford, J.T., M.M. Dornblaser, E.H. Stanley, D.W. Clow, and R.G. Striegl (2015), Source limitation of carbon gas emissions in high-elevation mountain streams and lakes, *Journal of Geophysical Research—Biogeosciences*, 120, 952-964. doi:10.1002/2014JG002861.

Crawford, J.T., N.R. Lottig, E.H. Stanley, J.F. Walker, P.C. Hanson, J.C. Finlay, and R.G. Striegl (2014), CO2 and CH4 emissions from streams in a lake-rich landscape—Patterns, controls, and regional significance, *Global Biogeochemical Cycles*, 197-210. doi:10.1002/2013GB004661.

Deemer, B., J.A. Harrison, S. Li, J.J. Beaulieu, T. DelSontro, N. Barros, J.F. Bezerra-Neto, S.M. Powers, M.A. dos Santos, and J.A. Vonk (2016), Greenhouse gas emissions from reservoir water surfaces: A new global synthesis, *BioScience*, 66(11), 949-964. doi:10.1093/biosci/biw117.

Deemer, B.R., J.A. Harrison, and E.W. Whitling (2011), Microbial dinitrogen and nitrous oxide

production in a small eutrophic reservoir: An in situ approach to quantifying hypolimnetic process rates, *Limnology and Oceanography*, 56(4), 1189-1199. doi:10.4319/lo.2011.56.4.1189.

Del Sontro, T., L. Boutet, A. St. Pierre, P.A. del Giorgio, and Y.T. Prairie (2016), Methane ebullition and diffusion from northern ponds and lakes regulated by the interaction between temperature and system productivity, *Limnology and Oceanography*, 61(S1), S62-S77. doi:10.1002/lno.10335.

Del Sontro, T., M.J. Kunz, T. Kempter, A. Wuest, B. Wehrli, and D.B. Senn (2011), Spatial heterogeneity of methane ebullition in a large tropical reservoir, *Environmental Science and Technology*, 45, 9866-9873. doi:10.1021/es205545.

Del Sontro, T., D.F. McGinnia, S. Sobek, I. Ostrovsky, and B. Wehrli (2010), Extreme methane emissions from a Swiss hydropower reservoir: Contribution from bubbling sediments, *Environmental Science and Technology*, 44, 2419-2425. doi:1021/es9031369.

Deshmukh, C., D. Serca, C. Delon, R. Tardiff, M. Demarty, C. Jarnot, Y. Meyerfeld, V. Chanudet, P. Guedant, W. Rode, S. Descloux, and F. Guerin (2014), Physical controls on CH4 emissions from a newly flooded subtropical freshwater hydroelectric reservoir—Nam Theun 2, *Biogeosciences*, 11, 4251-4269. doi:10.5194/bg-11-4251-2014.

Farquhar, G.D., S. von Caemmerer, and J.A. Berry (1980), A biochemical model of photosynthetic CO2 assimilation in leaves of C3 plants, *Planta*, 149, 78-90.

Fendinger, N.J., D.D. Adams, and D.E. Glotfelty (1992), The role of gas ebullition in the transport of organic contaminants from sediments, *Science of the Total Environment*, 112, 189-201. doi:10.1016/0048-9697(92)90187-W.

Frankignoulle, M. (1988), Field measurements of air-sea CO2 exchange, *Limnology and Oceanography*, 33, 313-322. doi:10.4319/lo.1988.33.3.0313.

Hayes, N.M., B.R. Deemer, J.R. Corman, N. Roxanna Razavi, and K.E. Strock (2017), Key differences between lakes and reservoirs modify climate signals—A case for a new conceptual model, *Limnology and Oceanography—Letters*, 2(2), 47-62. doi:10.1002/lol2.10036.

Harrison, J.A., B.R. Deemer, M.K. Birchfield, and M.T. O'Malley (2017), Rservoir water-level drawdowns accelerate and amplify methane emission, *Environmental Science and Technology*, 51(3), 1267-1277. doi:10.1021/acs.est.6b03185.

Hoellein, T.J., D.A. Bruesewitz, and D.C. Richardson (2013), Revisiting Odum (1956): A synthesis of aquatic ecosystem metabolism, *Limnology and Oceanography*, 58(6), 2089-2100. doi:10.4319/lo.2013.58.6.2089.

Holgerson, M.A. and P.A. Raymond (2016), Large contribution to inland water CO2 and CH4

emissions from very small ponds (2016), *Nature Geoscience*, 9, 22-226. doi:10.1038/ngeo2654.

Holgerson, M.A. (2015), Drivers of carbon dioxide and methane supersaturation in small, temporary ponds, *Biogeochemistry*, 124(1-3), 305-318. doi:10.1007/s10533-015-0099-y.

Holtgrieve, G.W., M.E. Arias, K.N. Irvine, D. Lamberts, E.J. Ward, M. Kummua, J. Koponen, J. Sarkkula, and J.E. Richey (2013), Patterns of ecosystem metabolism in the Tonle Sap Lake, Cambodia with links to capture fisheries, *PLOS ONE*, 8(8), e71395. doi:10.1371/journal.pone.0071395.g001.

Hotchkiss, E.R. and R.O. Hall, Jr. (2014), High rates of daytime respiration in three streams: Use of d^{18}O-O2 and O2 to model diel ecosystem metabolism, *Limnology and Oceanography*, 59(3), 798-810. doi:10.4319/lo.2014.59.3.0798.

Hunt, R.J., T.D. Jardine, S.K. Hamilton, and S.E. Bunn (2012), Temporal and sptial variation in ecosystem metabolism food web carbon transfer in a wet-dry tropical river, *Freshwater Biology*, 57, 435-450. doi:10.1111/j.1365-2427.2011.02708.x.

Huttunen, J.T., T.S. Vaisanen, S.K. Hellsten, M. Heikkinen, H. Nykanen, H. Jungner, A. Niskanen, M.O. Virtanen, O.V. Lindqvist, O.S. Nenonen, and P.J. Martikainen (2002), Fluxes of CH4, CO2, and N2O in hydroelectric reservoirs Lokka and Porttipahta in the northern boreal zone in Finland, *Global Biogeochemical Cycles*, 16(1), 1003-1020. doi:10.1029/2000GB001316.

IPCC (2001), Climate Change 2001: The Scientific Basis. Intergovernmental Panel on Climate Change, Cambridge University Press, Cambridge, UK.

Jacinthe, P.A., G.M. Filippelli, L.P. Tedesco, and R. Raftis (2012), Carbon storage and greenhouse gases emission from a fluvial reservoir in an agricultural landscape, *Catena*, 94, 53-63. doi:10.1016/j.catena.2011.03.012.

Johnson, M.S., M.F. Billet, K.J. Dinsmore, M. Walling, K.E. Dyson, and R.S. Jassal (2010), Direct and continuous measurement of dissolved carbon dioxide in freshwater aquatic systems—Method and applications, *Ecohydrology*, 3, 68-78. doi:10.1002/eco.95.

Junk, W.J., P.B. Bayley, and R.E. Sparks (1989), The flood pulse concept in river-floodplain systems, *Canadian Special Publication of Fisheries and Aquatic Sciences*, 106, 110-127.

Kaplan, L.A. and T.L. Blott (1982), Diel fluctuations of DOC generated by algae in a piedmont stream, *Limnology and Oceanography*, 27, 1091-110. doi:10.4319/lo.1982.27.6.1091.

Keller, M. and R.F. Stallard (2012), Methane emission by bubbling from Gatun Lake, Panama, *Journal of Geophysical Research—Atmospheres*, 99(D4), 8307-8319. doi:10.1029/92JD02170.

Knoll, L.B., M.J. Vanni, and W.H. Renwick (2003), Phytoplankton primary production and photosynthetic parameters in reservoirs along a gradient of watershed land use, *Limnology and Oceanography*, 48(2), 608-617. doi:/10.4319/lo.2003.48.2.0608.

Kling, G.W., G.W. Kipphut, M.M. Miller, and W.J. O'Brien (2000), Integration of lakes and streams in a landscape perspective: The importance of material processing on spatial patterms and temporal coherence, *Freshwater Biology*, 43, 477-497. doi:10.1046/j.1365-2427.2000.00515.x.

Kling, G.W., G.W. Kipphut, M.C. Miller (1991), Arctic lakes and streams as gas conduits to the atmosphere: Implications for tundra carbon budgets, *Science*, 251(4991), 298-301. doi:10.1126/science.251.4991.298.

Kone, Y.J.M., G. Abril, K.N. Kouadio, B. Delille, and A.V. Borges (2009), Seasonal variability of carbon dioxide in the rivers and lagoons of Ivory Coast (West Africa), *Estuaries and Coasts*, 32, 246-260. doi:10.1007/s12237-008-9121-0.

Kuehn, K.A. and K. Suberkropp (1998), Diel fluctuations in rates of CO2 evolution from standing dead leaf litter of the emergent macrophyte *Juncus effuses*, *Aquatic Microbial Ecology*, 14, 171-182. doi:10.3354/ame014171.

Kutner, M.H., C.J. Nachtsheim, and J. Neter (2004), Applied Linear Regression Models, McGraw-Hill Irwin, Boston, Massachusetts.

Galy-Lacaux, C., R. Delmas, and C. Jambert (1997), Gaseous emissions and oxygen consumption in hydroelectric dams: A case study in French Guyana, *Global Biogeochemical Cycles*, 11(4), 471-483, doi:10.1029/97GB01625.

Giles, J. (2006), Methane quashes green credentials of hydropower, *Nature*, 444, 524-525. doi:10.1028/444524a.

Grinham, A., M. Dunbabin, D. Gale, and J. Udy (2011), Quantification of ebullitive and diffusive methane release to atmosphere from a water storage, *Atmospheric Environment*, 45, 7166-7173. doi:10.1016/j.atmosenv.2011.09.011.

Guerin, F., G. Abril, A. Tremblay, and R. Delmas (2008), Nitrous oxide emissions from tropical hydropower reservoirs, *Geophysical Research Letters*, 35, L06404. doi:10.1029/2007GL033057.

Guerin, F. and G. Abril (2007), Significance of pelagic aerobic methane oxidation in the methane and carbon budget of a tropical reservoir, *Journal of Geophysical Research—Biogeosciences*, 112, G03006. doi:10.1029/2006JG000393.

Li, S., R.T. Bush, I.R. Santos, Q. Zhang, K. Song, R. Mao, Z. Wen, and X.X. Lu (2018), Large greenhouse gas emissions from China's lakes and reservoirs, *Water Research*, 147, 13-24. doi:10.1016/j.watres.2018.09.053.

Li, B., H. Xiao, X. Yuan, J.H.M. Wilson, H. Liu, Z. Chen, Y. Zhang, W. Deng, and J. Yue (2013), Analysis of ecological and commercial benefits of a dike-pond project in the drawdown one of the Three Gorges Reservoir, *Ecological Engineering*, 61, 1-11. doi:10.1016/j.ecoleng.2013.09.033.

Lofton, D.D., S.C. Whalen, and A.E. Hershey (2014), Effect of temperature on methane dynamics and evaluation of methane oxidation kinetics in shallow Arctic Alaskan lakes, *Hydrobiologia*, 721, 209-22. doi:10.1007/s10750-013-1663-x.

Maeck, A., H. Hofmann, and A. Lorke (2014), Pumping of methane out of aquatic sediments—Ebullition forcing mechanisms in an impounded river, *Biogeosciences*, 11, 2925-2938. doi:10.5194/bg-11-2925-2014.

MacIntyre, S., A. Jonsson, M. Jansson, J. Aberg, D. E. Turney, and S.D. Miller (2010), Buoyancy flux, turbulence, and the gas transfer coefficient in a stratified lake, *Geophysical Research Letters*, 37, L24604. doi:10.1029/2010GL044164.

Mattson, M.D. and G.E. Likens (1990), Air pressure and methane fluxes, *Nature*, 347, 718-719.

McGillis, W.R., J.B. Edson, C.J. Zappa, J.D. Ware, S.P. McKenna, E.A. Terray, J.E. Hare, C.W. Fairall, W. Drennan, M. Donelan, M.D. DeGrandpre, R. Wanninkhof, and R.A. Freely (2004), Air-sea CO2 exchange in the equatorial Pacific, *Journal of Geophysical Research—Oceans*, 109, C08S02. doi:10.1029/2003JC002256.

McNicol, G. and W.L. Silver (2014), Separate effects of flooding and anaerobiosis on soil greenhouse gas emissions and redox sensitive biogeochemistry, *Journal of Geophysical Research—Biogeosciences*, 119, 557-566. doi:10.1002/2013JG002433.

Mendonca, R., R.A. Mueller, D. Clow, C. Verpooter, P. Raymond, L.J. Tranvik, and S. Sobek (2017), Organic carbon burial in global lakes and reservoirs, *Nature Communications*, 8, 1694. doi:10.1038/s41467-017-01789-6.

Mengis, M., R. Gaechter, and B. Wehrli (1997), Sources and sinks of nitrous oxide (N2O) in deep lakes, *Biogeochemistry*, 38, 281-301, 38(3), 281-301. doi:10.1023/A:10058114020322.

Michmerhuizen, C.M., R.G. Streigl, and M.E. McDonald (1996), Potential methane emission from north-temperate lakes following ice melt, *Limnology and Oceanography*, 41, 985-991. doi:10.4319/lo.1996.41.5.0985.

Moran, M.A. and R.G. Zepp (1997), Role of photoreactions in the formation of biologically labile compounds from dissolved organic matter, *Limnology and Oceanography*, 42, 1307-1316. doi:10.4319/lo.1997.42.6.1307.

Myhre, G., D. Shindell, F.-M. Bréon, W. Collins, J. Fuglestvedt, J. Huang, D. Koch, J.F. Lamarque, D. Lee, B. Mendoza, T. Nakajima, A. Robock, G. Stephens, T. Takemura, and H. Zhang (2013), Anthropogenic and natural radiative forcing, *In* Climate Change 2013: The Physical Science Basis. Contribution of Working Group I to the Fifth Assessment Report of the Intergovernmental Panel on Climate Change, eds. T. F. Stocker et al., 659–740, Cambridge University Press, Cambridge, U. K., and New York.

Natchimuthu, S., I. Sundgren, M. Galfalk, L. Klemedtsson, and D. Bastviken (2017), Spatiotemporal variability of lake pCO2 and CO2 fluxes in a hemiboreal catchment, *Journal of Geophysical Research—Biogeosciences*, 122, 30-49. doi:10.1002/2016JG003449.

Naqvi, S.W.A., P. Lam, G. Narvenkar, A. Sarkar, H. Naik, A. Pratihary, D.M. Shenoy, M. Gauns, S. Kurian, S. Damare, M. Duret, G. Lavik, and M.M.M. Kuypers (2018), Methane stimulates massive nitrogen loss from freshwater reservoirs in India, *Nature Communications*, 9, 1265. doi:10.1038/s41467-018-03607-z.

Odum, H.T. (1956), Primary production in flowing waters, *Limnology and Oceanography*, 1(2), 102-117. doi:10.4319/lo.1956.1.2.0102.

Ostrovsky, I., D.F. McGinnis, L. Lapidus, and W. Eckert (2008), Quantifying gas ebullition with echosounder—The role of methane transport by bubbles in a medium-sized lake, *Limnology and Oceanography—Methods*, 6, 105-118. doi:10.4319/lom.2008.6.105.

Peeters, F., D. Atamanchuk, A. Tengberg, J. Encinas-Fernandez, and H. Hofmann (2016), Lake metabolism—Comparison of lake metabolic rates estimated from a diel CO2 and the common diel O2 technique, *PLOS ONE*, e0168393. doi:10.1371/journal.pone.0168393.

Raymond, P.A., J.E. Saiers, and W.V. Sobczak (2016), Hydrological and biogeochemical controls on watershed dissolved organic matter transport—Pulse-shunt concept, *Ecology*, 97(1), 5-16. doi:10.1890/14-1684.1.

Richey, J.E., A.H. Devol, S.C. Wofsy, R. Victoria, and M.N.G. Riberio (1988), Biogenic gases and the oxidation and reduction of carbon in Amazon River and floodplain waters, *Limnology and Oceanography*, 33(4.1), 551-561. doi:10.4319/lo.1988.33.4.0551.

Riera, J.L., J.E. Schindler, and T.K. Kratz (1999), Seasonal dynamics of carbon dioxide and methane in two clear-water lakes and two bog lakes in northern Wisconsin, U.S.A., *Canadian Journal of Fisheries and Aquatic Sciences*, 56, 265-274. doi:10.1139/f98-182.

Rudd, J.W.M., R. Harris, C.A. Kelly, and R.E. Hecky (1993), Are hydroelectric reservoirs significant sources of greenhouse gases?, *Ambio*, 22, 246-248.

Sasaki, Y., K. Koba, M. Yamamoto, A. Makabe, Y. Ueno, M. Nakagawa, S. Toyoda, N, Yoshida, and M. Yoh (2011), Biogeochemistry of nitrous oxide in Lak Kizaki, Japan, elucidated by nitrous oxide isotopomer analysis, *Journal of Geophysical Research—*

Biogeosciences, 116(G4), G04030. doi:10.1029/2010JG001589.

Sawakuchi, H.O., D. Bastviken, A.O. Sawakuchi, A.V. Krusche, M.V.R. Ballester, and J.E. Richey (2014), Methane emissions from Amazonian Rivers and their contribution to the global methane budget, *Global Change Biology*, 20, 2829-2840. doi:10.1111/gcb.12646.

Schilder, J.D., D. Bastviken, M. van Hardenbroek, P. Kankaala, P. Rinta, T. Stotter, and O. Heiri (2013), Spatial heterogeneity and lake morphology affect diffusive greenhouse gas emission estimates of lakes, *Geophysical Research Letters*, 40, 5752-5756. doi:10.1002/2013GL057669.

Schindler, D.E., K.J. Jankowski, Z.T. A'Mar, and G.W. Holtgrieve (2017), Two-stage metabolism inferred from diel oxygen dynamics in aquatic ecosystems, *Ecosphere*, 8(6), e01867. doi:10.1002/ecs2.1867.

Schultz, S. and R. Conrad (1996), Influence of temperature on pathways to methane production in the permanently cold profundal sediment of Lake Constance, *FEMS Microbiology Ecology*, 20(1), 1-14. doi:10.1016/0168-6496(96)00009-8.

Segers, R. (1998), Methane production and methane consumption—A review of processes underlying wetland methane fluxes, *Biogeochemistry*, 41, 23-51. doi:10.1023/A:1005929032764.

Smith, K.A., K.E. Dobbie, B.C. Ball, L.R. Bakken, B.K. Sitaula, S. Hansen, R. Brumme, W. Borken, S. Christensen, A. Prieme, D. Fowler, J.A. MacDonald, U. Skiba, L. Klemedtsson, A. Kasimir-Klemedtsson, A. Degorska, and P. Orlanski (2000), Oxidation of atmospheric methane in Northern European soils, comparison with other ecosystems, and uncertainties in the global terrestrial sink, *Global Change Biology*, 6(7), 791-803. doi:10.1046/j.1365-2486.2000.00356.x.

Stets, E.G., D. Butman, C.P. McDonald, S.M. Stackpoole, M.D. DeGrandpre, and R.G. Striegl (2017), Carbonate buffering and metabolic controls on carbon dioxide in rivers, *Global Biogeochemical Cycles*, 31(4), 663-677. doi:10.1002/2016GB005578.

St. Louis, V.L., C.A. Kelly, E. Duchemin, J.W.M. Rudd, and D.M. Rosenberg (2000), Reservoir surface as sources of greenhouse gases to the atmosphere: A global estimate, *BioScience*, 50(9), 766-775. doi: 10.1641/0006-3568(2000)050[0766:RSASOG]2.0.CO;2

Strayer, R.F. and J.M. Tiedje (1978), In situ methane production in a small, hypereutrophic hard-water lake: Loss of methane from sediments by vertical diffusion and ebullition, *Limnology and Oceanography*, 23(6), 1201-1206.

Tobias, C.R., J.K. Bohlke, and J.W. Harvey (2007), The oxygen-18 isotope approach for measuring aquatic metabolism in high productivity waters. *Limnology and Oceanography—Methods*, 5, 145-155. doi:10.4319/lo.2007.52.4.1439.

Tomaszek, J.A. and E. Czerwieniec (2003), Denitrification and oxygen consumption in bottom sediments: Factors influencing rates of the processes, *Hydrobiologia*, 504, 59-65. doi:10.1023/BB:HYDR.0000008508.81690.10.

Vasquez, E., E. Ejarque, I. Ylla, A.M. Romaní, and A. Butturini (2015), Impact of drying/rewetting cycles on the bioavailability of dissolved organic matter molecular-weight fractions in a Mediterranean stream, *Freshwater Science*, 34(1), 263–275. doi:10.1086/679616.

Wainright, S.C., C.A. Couch, and J.L. Meyer (1992), Fluxes of bacteria and organic matter into a blackwater river from river sediments and floodplain soils, *Freshwater Biology*, 28(1), 37-48. doi:10.1111/j.1365-2427.1992.tb00560.x.

Wang, Q., H. Liu, X. Yuan, R. Sun, and J. Wang (2009), Pattern and biodiversity of plant community in water-level-fluctuation zone of Pengxi River after impoundment of the Three Gorges Reservoir, *Journal of Chongqing Normal University—Natural Sciences*, 26, 48-54.

Wik, M., B.F. Thorton, D. Bastviken, J. Uhlbaeck, and P.M. Crill (2016), Biased sampling of methane release from northern lakes—A problem for extrapolation, *Geophysical Research Letters*, 43(3), 1256-1262. doi:10.1002/2015GL066501.

Wilhelm, E., R. Battino, and R.J. Wilcock (1977), Low-pressure solubility of gases in liquid water, *Chemical Reviews*, 77(2), 219-262. doi:10.1021/cr60306a003.

Winfrey, M.R. an J.G. Zeikus (1979), Microbial methanogenesis and acetate metabolism in a meromictic lake, *Applied and Environmental Microbiology*, 37(2), 213-221.

Xiao, S., D. Liu, Y. Wang, Z. Yang, and W. Chen (2013), Temporal variation of methane flux from Xiangxi Bay of the Three Gorges Reservoir, *Scientific Reports*, 3, 1-8. doi:10.1038/srep02500.

Yvon-Durocher, G., A.P. Allen, D. Bastviken, R. Conrad, C. Gudasz, A. St-Pierre, N. Thanh-Duc, P.A. del Giorgio (2014), Methane fluxes show consistent temperature dependence across microbial to ecosystem scales, *Nature*, 507, 488-491. doi:10.1038/nature13164.

Yvon-Durocher, G., J.M. Caffrey, A. Cescatti, M. Dossena, P. del Giorgio, J.M. Gasol, J.M. Montoya, J. Pumpanen, P.A. Staehr, M. Trimmer, G. Woodward, and A.P. Allen (2012), Reconciling the temperature dependence of respiration across timescales and ecosystem types, *Nature*, 487, 472-476. doi:10.1038/nature11205.

Zar, J.H. (2010), Biostatistical Analysis, Pearson, Upper Saddle River, New Jersey.

Zarfl, C., A.E. Lumsdon, J. Berlekamp, L. Tydecks, K. Tockner (2015), A global boom in hydropower dam construction, *Aquatic Sciences*, 77(1), 161-170. doi:10.1007/s00027-014-0377-0.

Zhang, J., S. Li., R. Dong, and C. Jiang (2018), Physical evolution of the Three Gorges Reservoir using advanced SVM on Landsat images and SRTM DEM data, *Environmental Science and Pollution Research*, 25(15), 14911-14918. doi:10.1007/s11356-018-1696-9.

Zhao, Y., B.F. Wu, and Y. Zeng (2013), Spatial and temporal patterns of greenhouse gas emissions from Three Gorges Reservoir of China, *Biogeosciences*, 10, 1291-1230. doi:10.5194/bg-10-1219-2013.

Zhou, S., Y. He, X. Yuan, S. Peng, and J. Yue (2017), Greenhouse gas emissions from different land-use areas in the littoral zone of the Three Gorges reservoir, China, *Ecological Engineering*, 100, 316-324. doi:10.1016/jecoleng.2017.01.003.

Zhu, D., H. Chen, X. Yuan, N. Wu, Y. Gao, Y. Wu, Y. Zhang, C. Peng, Q. Zhu, G. Yang, and J. Wu (2013), Nitrous oxide emissions from the surface of the Three Gorges Reservoir, *Ecological Engineering*, 60, 150-154. doi:10.1016/j.ecoleng.2013.07.049.